AUTOMATED DETECTION OF PREHISTORIC CONICAL BURIAL MOUNDS FROM LIDAR BARE-EARTH DIGITAL ELEVATION MODELS

A THESIS PRESENTED TO
THE DEPARTMENT OF GEOLOGY AND GEOGRAPHY
IN CANDIDACY FOR THE DEGREE OF
MASTER OF SCIENCE

By
MELANIE A. RILEY

NORTHWEST MISSOURI STATE UNIVERSITY
MARYVILLE, MISSOURI
APRIL 2009

AUTOMATED DETECTION OF PREHISTORIC BURIAL MOUNDS

Automated Detection of Prehistoric Conical Burial Mounds From LIDAR Bare-Earth Digital Elevation Models

Melanie A. Riley

Northwest Missouri State University

THESIS APPROVED

Thesis Advisor	Dr. Ming-Chih Hung	Date
	Dr. Yi-Hwa Wu	
	Dr. Gregory Haddock	
Dean of Graduate School		Date

Automated Detection of Prehistoric Conical Burial Mounds

From LIDAR Bare-Earth Digital Elevation Models

Abstract

The Iowa Department of Natural Resources (IDNR) and partnering agencies are conducting a statewide LiDAR data collection project. A 1 m shaded relief image from an early collection clearly displayed a recorded, prehistoric mound group on IDNR property, except for a set of three mounds overshadowed from a nearby hill. Prehistoric burial mounds are protected from disturbance through several federal and state laws. Unfortunately, the State Archaeologist and State Historic Preservation Offices do not have the resources to conduct mound surveys throughout the state for the sake of knowing what areas should be protected from future development. LiDAR introduces the possibility that large-area mound prospection is feasible.

There are challenges to image interpretation that can make such a task time-consuming with potentially mixed results. Conical mounds visible on shaded relief images are as small as 5 m diameter and 30 cm high. Interpretation over large areas can become tedious and may affect the quality and consistency of the interpretation over time. The interpreter's experience and ability to detect subtle changes in shading also impact interpretation quality. The early relief image demonstrated that more than one image with different settings will be necessary to interpret areas that are overshadowed.

A conical mound detection model was developed in the ArcGIS 9.2 ModelBuilder environment using Spatial Analyst tools. The model works as an interpretation aid by marking features that fit the metrics of the most common mound type. ArcGIS is the prevalent GIS software used by archaeologist in the state and the model, stored as a .tbx file, is easily distributable. The base of the model relies on three variables derived from the BE DEM – height, slope and aspect variety. An additional segment of the model is for clean-up and conversion from the raster data model to vector.

The model was tested in five areas representing three physiographic regions; it detected 90% of mounds that were interpretable from shaded relief images and have been recently field-verified, including other mound types. The model reduced the area to be checked to 0.15% - 0.4% of the area of interest. Natural and man-made features that triggered false positives were consistent; future work will be directed towards reducing the occurrences.

The model can expedite prospection of counties with high mound densities to the point where the time required for such a project would fit a modest budget. The results of the interpretation can be disseminated through an Internet Map Service (IMS) already established for professional archaeologists. County planners and local governments could get the results to the quarter section through an IMS currently in development, giving them warning that a potential prehistoric burial may be in a planned project area.

TABLE OF CONTENTS

LIST OF FIGURES

LIST OF TABLES

ACKNOWLEDGEMENTS

Many thanks are in order to the Iowa Department of Natural Resources and its partners for undertaking such an initiative and conducting a program of outreach and education early in the process. A special thanks goes to Chris Kahle from the Iowa Geological Survey who has been very accommodating in providing the data and answering any questions that I may have had with alacrity. Dr. Ramanathan Sugumaran led a workshop through University of Northern Iowa's GeoTREE Center that helped removed the mystique behind the mass points. The Office of the State Archaeologist provided many images, access to the gray literature and electronic site data.

The greatest depth of gratitude goes to my daughter Hannah and husband Wade for all their support, patience, encouragement and understanding not only during this project, but all through graduate school.

LIST OF ABBREVIATIONS

AOI	Area of Interest
ASTER	Advanced Spaceborne Thermal Emission and Reflection Radiometer
BE DEM	Bare-Earth Digital Elevation Model
DOD	Department of Defense
DSM	Digital Surface Model
FEMA	Federal Emergency Management Agency
GPR	Ground Penetrating Radar
IDNR	Iowa Department of Natural Resources
IDOT	Iowa Department of Transportation
IGS	Iowa Geological Survey
LiDAR	Light Detection and Ranging
NAGPRA	Native American Graves Protection and Repatriation Act
NASA	National Aeronautics and Space Administration
NDVI	Normalized Difference Vegetation Index
NHPA	National Historic Preservation Act
NIR	Near Infrared
NPS	National Park Service
NRCS	Natural Resources Conservation Service
TIMS	Thermal Infrared Multispectral Scanner
TM	Thematic Mapper
TMS	Thematic Mapper Simulator
UI-OSA	University of Iowa Office of the State Archaeologist
USDA	United States Department of Agriculture
USGS	United States Geological Survey

CHAPTER 1: INTRODUCTION

Archaeology has a long history of using remotely sensed data to gain a unique perspective of large sites. An aerial photo of Stonehenge taken from a hot air balloon in 1906 is attributed as the first time remote sensing was used for archaeology in the United Kingdom (Bewley 2003). One hundred years later archaeologists in the United Kingdom and The Netherlands are taking advantage of a remote sensing technology that has only recently become affordable for large-area data collection. Light Detection and Ranging (LiDAR) data collected in the two countries under national initiatives have led to a rise in the number of journal articles and conference presentations within the last five years on the utility of LiDAR in archaeology. While the articles brandish many impressive images, most sites are large relative to Midwestern United States prehistoric sites. Description of the data is scarce in many articles as well as the metrics of small archaeological features detected.

Even more inauspicious is the absence of professional journal articles on the use of LiDAR for archaeological prospection in the United States. Perhaps archaeologists in this country are waiting for the windfall of publicly available data that their colleagues across the Atlantic enjoy. Fortunately initiatives for statewide LiDAR data collection are currently in various stages of completion in a few states.

1.1 Research Background

Large-area or statewide LiDAR data acquisition programs are currently underway in

Iowa, Ohio, Pennsylvania, Louisiana, Florida, Oregon and Minnesota (Cunningham *et al.* 2004, Pennsylvania Department of Conservation and Natural Resource 2006, Florida State Emergency Response Team 2007, Iowa Department of Natural Resources 2007, Ohio Office of Information Technology 2007, Oregon Lidar Consortium 2008, Minnesota Department of Natural Resources 2009). Wyoming is in the planning stages of a similar initiative and North Carolina has completed their collection (United States Department of Agriculture-Natural Resource Conservation Service Wyoming 2005, North Carolina Flood Mapping Program 2007). A review of the LiDAR specifications for all of these states revealed that the data is going to be similar in terms of accuracy and point cloud density. This is largely due to the states following the Federal Emergency Management Agency's (FEMA) "Guidelines and Specifications for Flood Hazard Mapping Partners" in the collection of LiDAR. Results and observations using Iowa's LiDAR data are applicable to these other states which can produce Bare-Earth Digital Elevation Models (BE DEM) of the same resolution used in this research.

Data collection in Iowa began spring 2007 with 55% of the land area collected or partially collected as of January 2009 (Iowa Department of Natural Resources 2009). The LiDAR project is being lead by the Iowa Department of Natural Resources (IDNR) and, in the agency's interest, an area managed by the IDNR was collected early where a conservation project was underway. Remote sensing specialists at the Iowa Geological Survey (IGS) of the IDNR created a 1 m BE DEM of the managed area and notified the University of Iowa Office of the State Archaeologist (UI-OSA) of the clear appearance of the Slinde Mound Group in the shaded relief image of the BE DEM (Figure 1). The

mounds visible in the image are as small as 5 m diameter with a height as low as 30 cm.

Despite being located in a heavily wooded area, LiDAR was able to obtain enough last-return points of the ground to produce a shaded relief image of these micro topographic features (Figure 1). It is not an overreach to state that the ability to remotely sense small burial mounds, moreover in heavily forested areas, will alter the quintessence of archaeological prospection in the United States as more LiDAR data will become publicly available in the near future.

1.2 Burial Mounds Defined

Burial mounds in the United States are most common in the eastern half of the country with the distribution extending westward to the Missouri River in the north and eastern Kansas, Oklahoma and Texas in the south (Figure 2). The New England states, coastal regions of the Mid-Atlantic states and areas around Lake Superior are exceptions to this distribution where mounds are scarce or nonexistent (Anfinson 1984). In Iowa, mounds more often are located in the uplands on areas with low slope gradients and close proximity to a river valley, but there are mounds located within valleys on stable terraces and near large lakes.

The archaeological feature type that is the focus of this research is conical mounds. *Conical* is the descriptor for mounds that resemble the top half of an oblate spheroid with varying diameters and slope angles (Figure 3). All of the mounds in the Slinde Mound Group are conical mounds. Conical mounds were constructed by heaping basketfuls

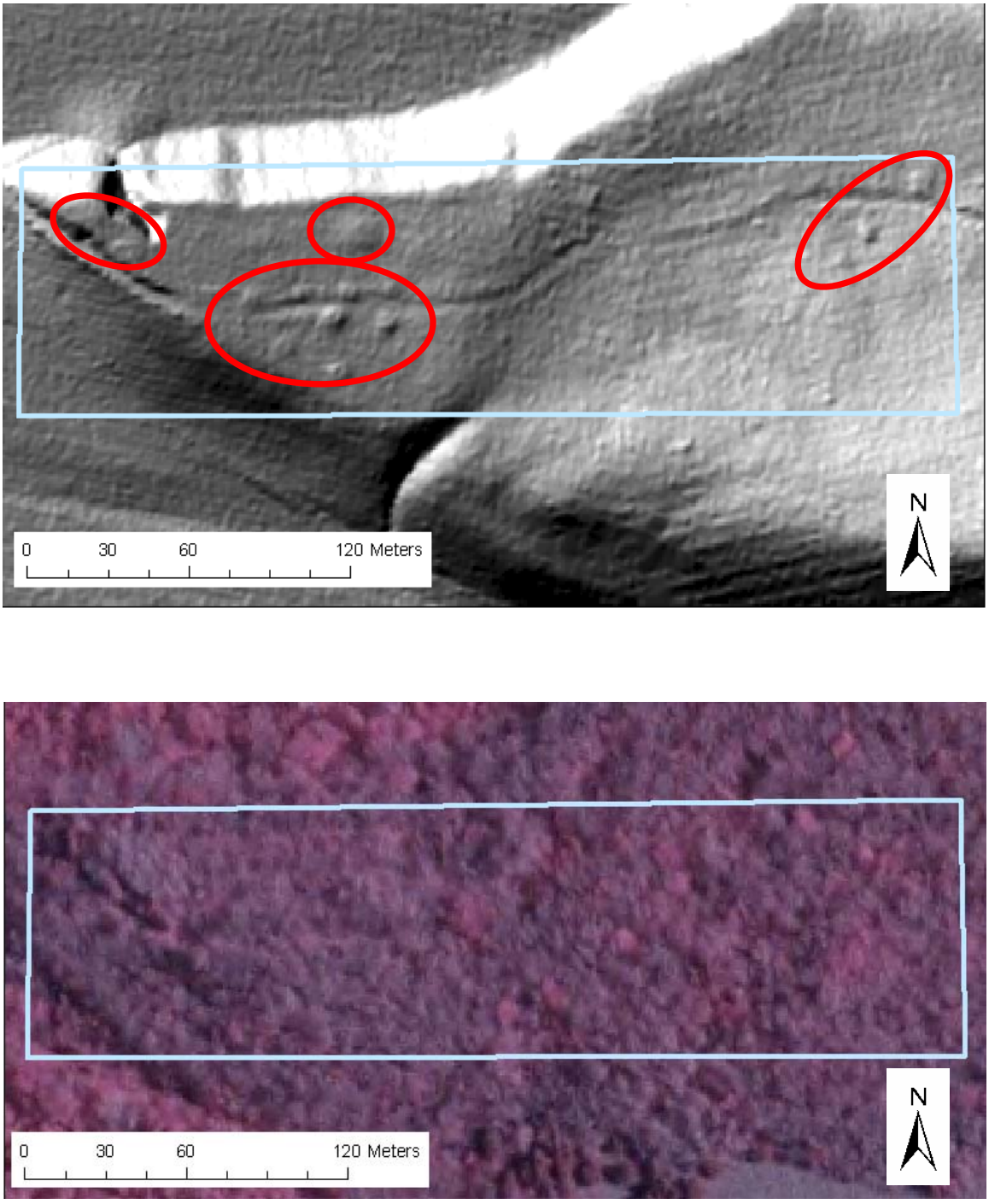

Figure 1. Top: LiDAR-derived 1- meter shaded relief of the Slinde Mound Group, Allamakee County, Iowa. Mounds are circled in red. Bottom: Same area from a 2002 color-infrared orthophoto displaying heavy tree cover (CIR photo: Iowa Department of Natural Resources 2002, used with permission).

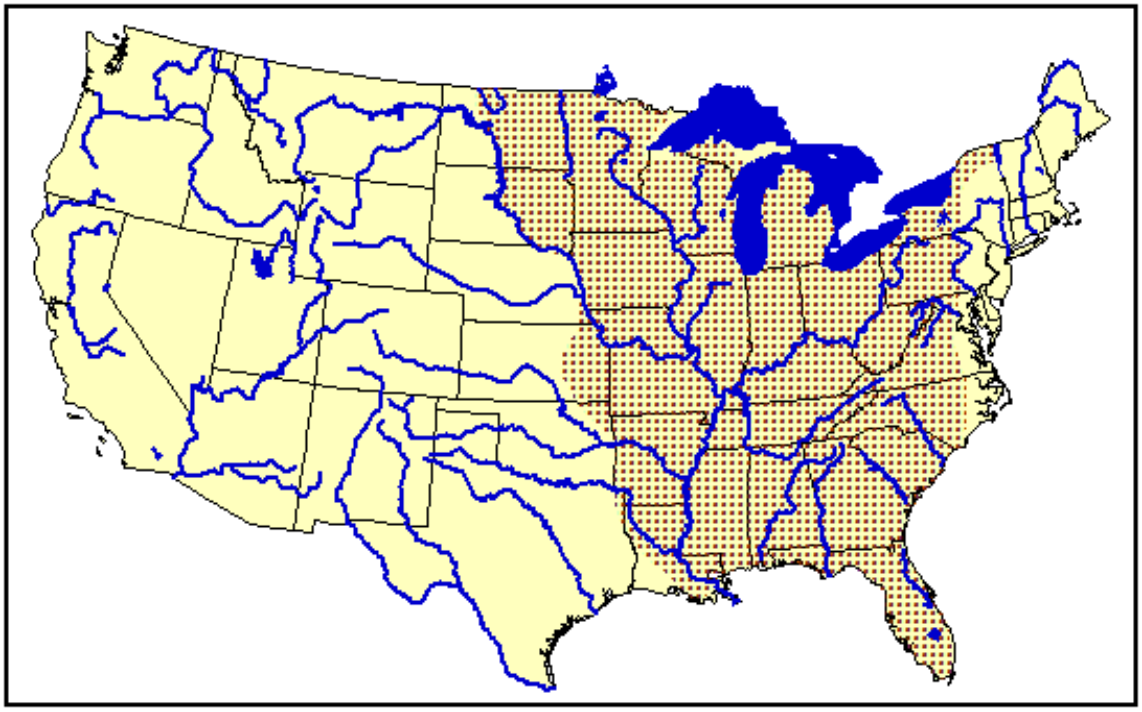

Figure 2. Shaded area is general distribution of burial mounds in the United States (map adapted from Anfinson 1984).

of soil creating a gradually-rounded summit in the center and moderate slopes radiating outward from the center forming a circular or oval footprint on the landscape. The method of internal mound construction and burial customs vary throughout prehistory, but externally the general shape is consistent. Conical mounds are the most common type in Iowa; they can exist as one isolated mound or in groups and can be mixed or conjoined with other mound types.

Effigy mounds are in the shape of animals such as birds, bears and turtles and are rare with only 50 known to exist in Iowa in the northeast corner of the state along the Mississippi, Turkey and Yellow River valleys (Figure 4). Effigy mound building occurred A.D. 600 – 1100 in parts of Iowa, Wisconsin, Illinois and Minnesota with the

Figure 3. An exceptional example of conical mounds, located at Effigy Mounds National Monument, Allamakee County, Iowa. (photo: University of Iowa Office of the State Archaeologist, used with permission).

epicenter of effigy mound building in southern Wisconsin (Alex 2000). *Linear* mounds are long and narrow with rounded ends and are located across the state (Figure 5). Many linear mound groups in eastern Iowa are contemporary with the effigy mounds (Alex 2000). Both effigy and linear mound types were constructed with the soil heaped highest towards the center of the form and gradually sloping outward. A few known sites are *compound mounds* where conical and linear mounds alternate and are linked or set closely in a line.

Most mounds are burial sites built from 1000 B.C. - A.D. 1600 with prolific conical mound building attributed to the Middle Woodland period 200 B.C. – A.D. 400; however

groups of mounds without burials do exist, especially linear mounds (Alex 2000, O'Bright 1989). Precise locations of archaeological sites used in this research will not be disclosed pursuant to Iowa State Code 305A.10.

Figure 4. Marching Bear Mound Group at Effigy Mounds National Monument, Allamakee County, Iowa. The figures of a bird and bears are outlined in lime to enhance visibility of the mound shapes (photo: National Park Service, used with permission).

Figure 5. Linear mounds at Sny Magill Mound Group, Clayton County, Iowa (photo: National Park Service, used with permission).

1.3 Impetus for research

While the initial shaded relief image of the Slinde Mound Group made a great impression on archaeologists at the UI-OSA, there are a few challenges that threaten the full utilization of LiDAR for archaeological prospection of prehistoric mounds. Among these challenges are limitations of using a single shaded relief image, restricted resources and a dearth of personnel in archaeology well-versed in raster data manipulation with GIS software and familiarity with LiDAR data.

1.3.1 Limitations of shaded relief image

The first shaded relief image provided to the UI-OSA by the IDNR displayed clearly the Slinde Mound Group on the west side, but the three small mounds to the east were hidden in the "shadows" of the ridge (Figure 1). The three mounds not visible in the initial shaded relief were only known after viewing a paper map drawn from a field visit in 1987 and comparing the map to the shaded relief image. After requesting the BE DEM of the area, a second shaded relief was created using slightly different illumination and display parameters which made the three mounds to the east visible. Only one shaded relief image will be available for download to the public. It has already been demonstrated through the Slinde Mounds image and other preliminary viewing of shaded relief images around known mound sites that one shaded relief image of the study area alone will not be sufficient for remote prospection of all mounds.

Figure 6 demonstrates how landscape features such as high river terraces where mounds are known to exist can be overshadowed by the bluffs above. Site 13AM116 is located on

a river terrace where the image is so dark it is difficult to determine whether or not mounds are located there; north and east of the site boundary the terrace is not "illuminated" at all. In the same image on top of the bluff along a ridge, site 13AM149 mounds are clearly visible.

Figure 7 is the same area using a different stretch rendering method for the shaded relief symbology, but the same BE DEM data. The high terrace is now visible and site 13AM116 is illuminated. Inside the site boundary, it looks as though the mounds have been destroyed. Checking site records confirmed that three of the mounds were excavated

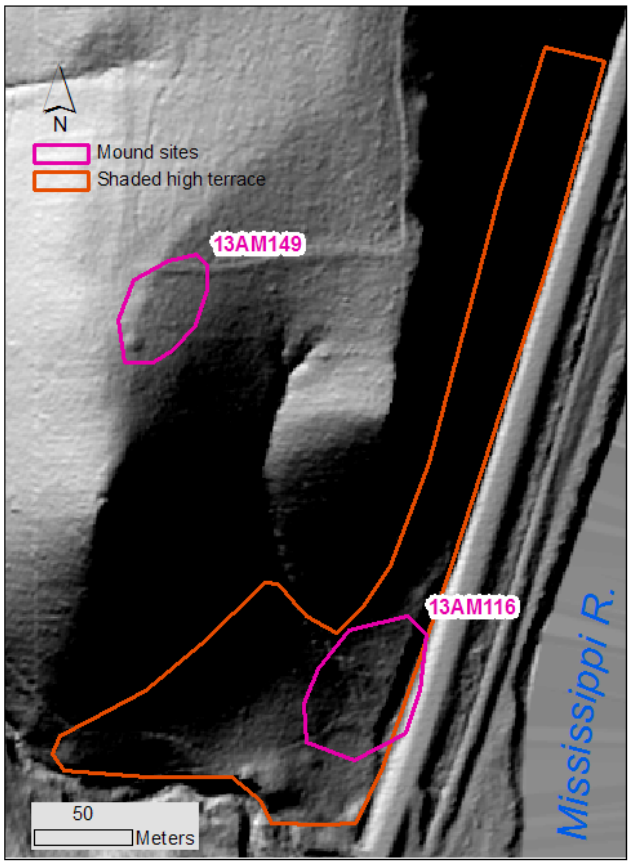

Figure 6. River terrace outlined in orange is overshadowed in this shaded relief image by the bluff above making thorough mound prospection impossible from this image alone.

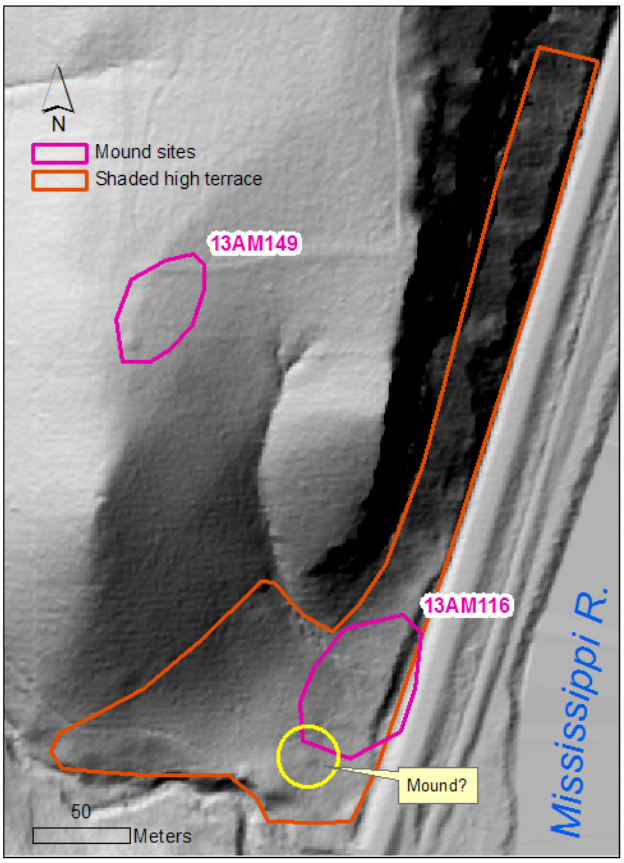

Figure 7. Same river terrace is now visible after applying a different stretch rendering to the shaded relief image. Other areas still in black may need an adjustment to illumination source for the shaded relief algorithm.

over 70 years ago and two others were destroyed by road construction. However, just southeast of the site boundary a feature that resembles a conical mound is visible. It is plausible this is a mound that has been missed because the area is heavily forested and it cannot be viewed from the road; or, it was simply part of 13AM116 and the site boundaries are incorrect.

A second limitation of using the shaded relief image for archaeological prospection is that the mounds that have been plowed down, trampled by livestock or eroded naturally have very little relief. The Slinde Mound Group image shows that the mounds only 30 or

40 cm in height have very little or no shading, reflecting how low and gradual the mounds' footprints are on the surface in relation to surrounding topography (Figure 8). Without the luxury of having site boundaries in a shapefile or accurate field maps within reach, many of these known mound sites would be very difficult or impossible to visually detect.

1.3.2 Restricted resources

Contrary to misconceptions from the public, state historic preservation officers and state archaeologists do not go out everyday and hunt for sites that need to be preserved or saved from all development; they do not have the time or money to do so. These positions are to enforce compliance to state and federal laws involving historic

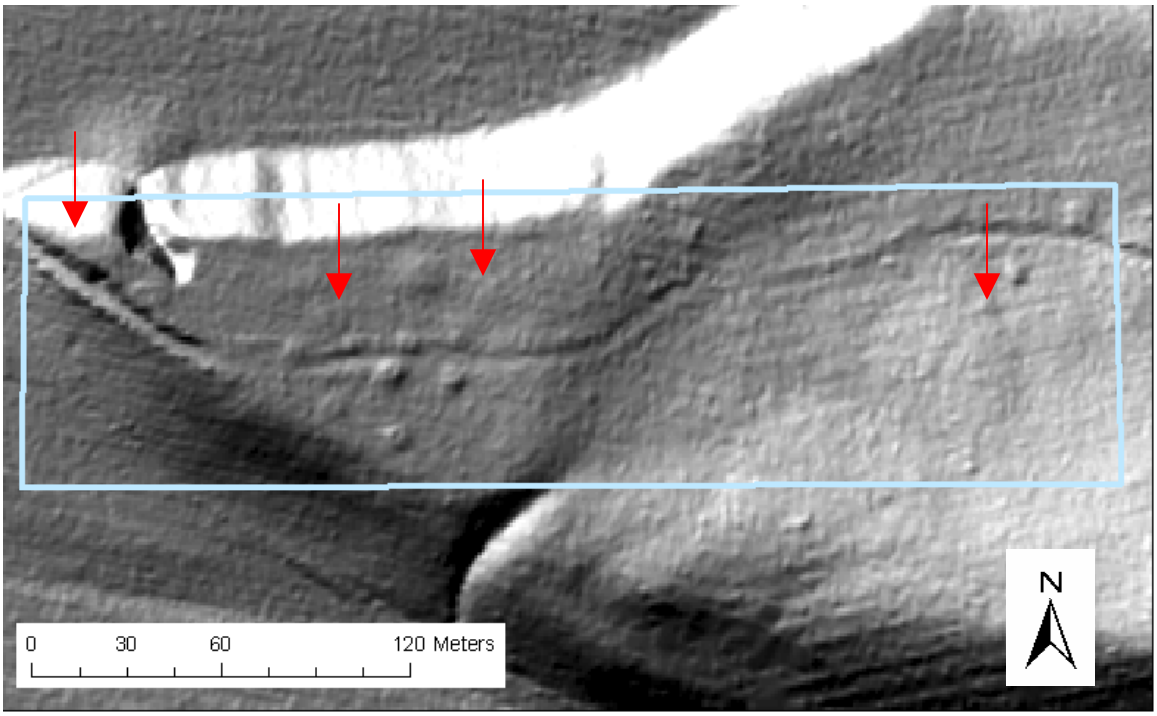

Figure 8. Small mounds with low relief, marked with red arrows, are difficult to discern from a shaded relief image without the aid of accurate site boundaries and field maps drawn to scale.

preservation, cultural resource management and prehistoric and pioneer burials. Federal historic preservation law requires archaeological survey only when development uses federal funds or is directly regulated by a federal agency. Iowa's ancient burials law makes the looting or destruction of prehistoric or pioneer burials illegal regardless of how a development project is funded. This law also prohibits landowners from looting or knowingly destroying burials on their own land.

Many mound sites were documented from the late 1850's through the 1940's as a result of initiatives taken by people not trained in archaeology (O'Bright 1989). The early mound surveys were primarily in northeastern Iowa; however, a federally funded survey during the Great Depression resulted in the documentation of mound sites by Charles Keyes and Ellison Orr in other parts of the state. While the Keyes/Orr field notes are an important resource for modern archaeologists, some of the mound locations in the notes are incorrect and can be off by miles (R. Lillie personal communication, 2008). Although Ellison Orr (Orr 1944 cited in O'Bright 1989) claimed in his autobiography that he "located and surveyed all the known village sites, burial places and mound groups in Allamakee County and down along the Mississippi River in Clayton County", the first glimpse of the LiDAR-derived shaded relief raster north of the Slinde Group revealed that one of the linear mound sites Orr surveyed and documented in Allamakee County has a plausible, undocumented conical mound less than 50 meters away (Figure 9).

Orr cannot be faulted for this omission because mounds with low-relief in heavily wooded areas are hard to see from a short distance (Figure 10). The terrain where many

well-preserved mounds exist is rugged with heavy vegetation making pedestrian survey slow, laborious and at times dangerous. The money and time required to conduct a thorough survey in an area the size of a watershed is prohibitive for such a task to come to fruition and does not guarantee that every mound is recorded. In addition, some landowners will not allow archaeologists on their land to conduct a survey, even for academic purposes.

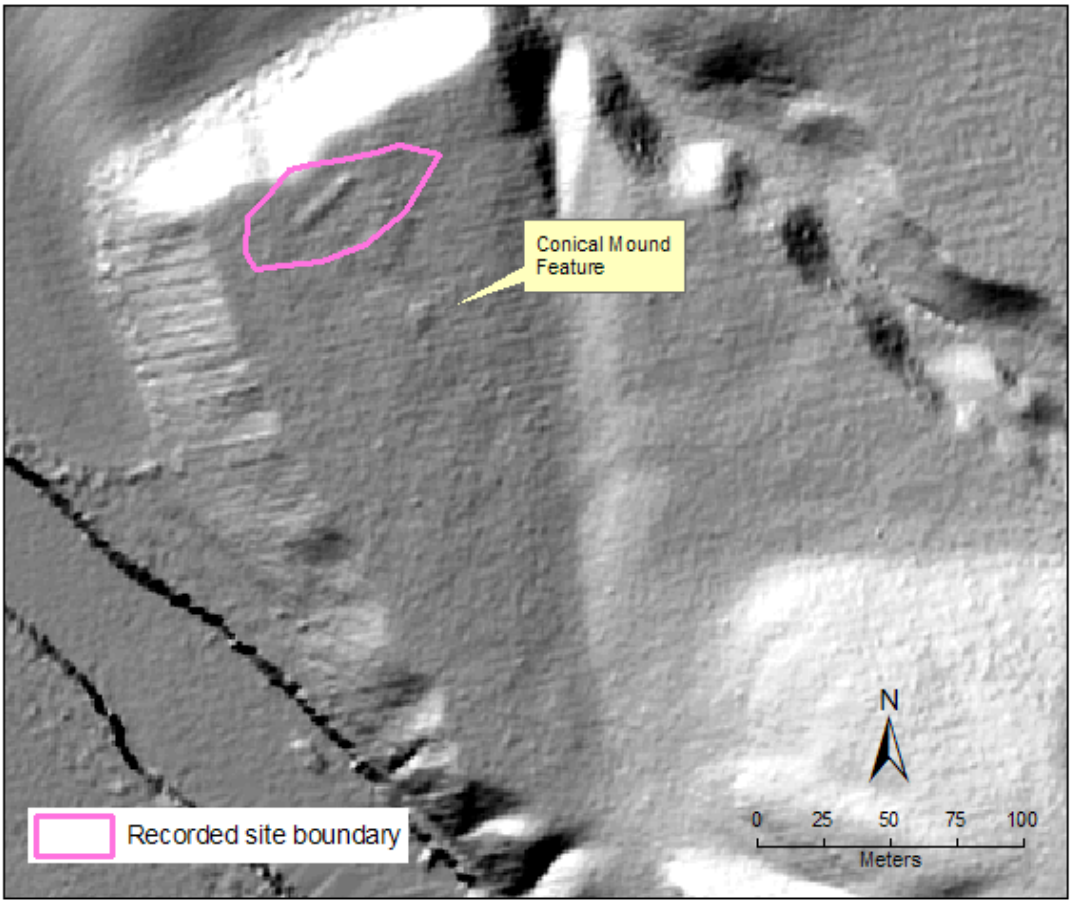

Figure 9. LiDAR-derived 1 m shaded relief image of a linear mound site recorded by Ellison Orr and a nearby, possible undocumented conical mound.

Figure 10. Top: Background depicts typical vegetation cover in northeast Iowa. Bottom: Conical mound circled in red (photos: University of Iowa Office of the State Archaeologist, used with permission).

This introduces a significant conundrum – how can archaeologists, state historic preservation officers and local officials enforce the Iowa burials law when archaeological survey is not required if no one knows a prehistoric burial exists in the area of potential effect? Even among "known" mound sites, according to the Iowa Site File 37% of mound site locations are noted as having uncertain boundaries or locations. A preliminary review of mound sites with "definite" boundaries revealed that not all those boundaries truly mark or encompass their sites when viewed with a BE DEM.

1.3.3 Varying levels of expertise

A simplistic solution would be to have someone canvass the LiDAR BE DEMs and mark all the features that resemble a mound. But when the image interpreter has to look over several different shaded relief images, zoomed in, with different illumination sources or stretch renderings the task quickly becomes time consuming and, in turn, costly. Sometimes the smaller features are questionable and additional tools and analysis would be required before it would be designated as 'maybe a mound'. This may require the interpreter to have some working knowledge of extensions such as ArcGIS 3D Analyst or Spatial Analyst. Unfortunately, limited budgets have a deleterious effect on the amount of GIS training that is available for archaeologists outside of map making and simple feature plotting.

Jensen (2007) emphasizes the point that image interpretation is not only a science but an art. Not all interpreters will have the same proficiency at visually detecting features from an image due to a combination of factors including but not limited to life experience on

the ground, years of experience with the technology/subject matter and physical abilities. If there are several people using the LiDAR data, there is a good chance that the success of detecting mound-like features will not be consistent.

1.4 Research Objectives

The purpose of this study is to create a feature detection tool for conical, and perhaps, linear and effigy mounds. Conical mounds are the primary focus of the research because they are the most common mound type, many times exist with other mound types and there is a resemblance of the conical's morphology in the other mound types.

This detection tool addresses the issues discussed above. First, the model needs to be easy to distribute and functional for any archaeologist with access to ESRI ArcGIS 9.1 or higher and the Spatial Analyst extension, the most common GIS software used in Iowa archaeology. Little knowledge of raster data manipulation is necessary to run the tool which will simplify training other archaeologists to use publicly-available LiDAR BE DEMs for automated feature detection of mounds. Second, the model's results will decrease the time required for image interpretation by minimizing the amount of area that the interpreter would have to look over and apply additional visualization and analysis techniques. The model itself could be run over large areas overnight without anyone present. Third, because the model works from a group of set parameters, what is flagged as detected conical mounds should be consistent no matter who is running the model. The model results will not vary due to differing life experiences, fatigue, boredom or the ability to see subtle features on a shaded relief image.

CHAPTER 2: LITERATURE REVIEW

2.1 History of Mound Prospection in Iowa

Although there had been a Euro-American presence in Iowa since 1660 starting with illegal French fur traders or *coureurs des bois*, observation of mounds in Iowa were not documented until much later. One of the first reports of mounds in northeast Iowa was by Jonathan Carver in 1766, a surveyor who was travelling with a group of fur traders from Wisconsin and wintered over in Iowa's Yellow River valley. There are many effigy mounds in this region, but Carver did not specifically mention this type. Peter Pond, a fur trader who also (albeit illegally) camped on the west side of the Mississippi River documented the existence of mounds in 1773 with no elaboration or maps (O'Bright 1989).

In 1840 an antiquarian named William Pidgeon carried out the first documented survey that was exclusively for the purpose of studying earthworks, mounds and burial tumuli in Iowa and surrounding states bordering the upper Mississippi River (Pidgeon 1852). Pidgeon's book provides many illustrations of mounds and earthworks, but without a specific geographic reference. He also notes that some of the works found in Iowa were already being destroyed due to cultivation practices. Unfortunately, the text is not a true example of archaeology but rather an historical documentation of ignorance and racist views at the time that dominated the study of ancient history in the Americas. Much of the mound exploration and excavation during this period was driven by the belief that a once-great civilization occupied the Americas and built all of the grand earthworks. The

reasoning was that the indigenous peoples, regarded as uncivilized, red savages, were not capable of building such great works and they must have conquered and exterminated the culture that really built the earthworks. Pidgeon (1852, p.15) perpetuated the moundbuilder myth by comparing the ancient, extinct race to the Romans and the Native Americans to:

> the Goths and Vandals, who overran the Roman Empire, destroying their accounts of discoveries, and history of antiquities, and casting over the regions they subdued, the gloom of barbarous ignorance, congenial with the shades of the forest, whence they originated.

This observation conveniently explains why there was no writing left to be found from the advanced, ancient society.

Mounds were the focus of many excavations in Iowa during the 1870's through the 1890's. Unfortunately, the purpose of the excavations were not to understand or describe the internal arrangement of the mounds, how they were built, or to try to link them to the ancestors of the Native Americans. These endeavors were better described as the destruction and looting of burial mounds in order to find exotic antiquities (Alex 2000). Meanwhile, in the early 1880's more-systematic mound survey work was being conducted in the eastern United States and the moundbuilder myth was becoming discredited.

Theodore Lewis and Alfred Hill partnered in 1881 to conduct archaeological survey in Iowa and many other nearby states and the province of Manitoba. The fifteen-year initiative, named the Northwestern Archaeological Survey, was privately funded by Hill while Lewis conducted the actual surveys (Dobbs 1999). Their work is considered the

first true archaeological survey in Iowa. Many publications came out of the surveys which include good maps of mound groups in Iowa. While the Northwestern Archaeological Survey was coming to an end, a few people in Iowa were employing more systematic methods in the excavation of mounds. Archaeology in the late nineteenth century and early twentieth century was still primarily focused on mound sites, but the excavations produced field maps of the mounds' stratigraphy and artifact collections were well-documented (Alex 2000).

By the 1920's other site types were gaining attention in Iowa. Most notable was the work of Charles Keyes, often called the "Father of Iowa Archaeology", and Ellison Orr. Keyes, a German language professor, devoted much of his time to documenting artifact collections and conducting interviews with the public for information on known sites in every county. After years of collecting information and reviewing all the literature in Iowa archaeology up to that time, Keyes began piecing together prehistoric cultural groups. In 1934 as the Director of the State Archaeological Survey, he partnered with Orr to conduct several projects funded by the Federal Emergency Relief Administration and Works Project Administration which lasted through 1939 (Alex 2000). The field notes from these surveys and Keyes other work are still important resource for modern archaeologists and contain exceptional notes and maps of many mound groups across the state. Efforts have been made by archaeologists in the last forty years to assign these sites formal site numbers, enter them into the Iowa Site File and plot them on 7.5' United States Geological Survey (USGS) topographic maps. However, locations of some of these sites cannot be pinpointed accurately because locations may reference distances to

man-made features that no longer exist or there are location errors in the mapping.

The National Historic Preservation Act of 1966 (NHPA) has provided much-needed financial support in modern archaeology (Alex 2000). The Act mandates that any project undertaken by a federal agency or involving federal funds and permits must undergo an assessment of how the project will impact any historic or prehistoric sites. While the law does not provide funding for archaeologists to conduct studies where ever they want, it still has had a significant, positive impact on archaeology in Iowa. The NHPA, however, does not protect prehistoric burials from excavation and Iowa law at the time only protected historic cemeteries from disturbance. In 1979 Iowa passed legislation making illegal the excavation of any burial over 150 years old without authorization (Alex 2000). The culturally-sensitive treatment of prehistoric burials gained additional attention and support in 1990 through the Native American Graves Protection and Repatriation Act (NAGPRA). NAGPRA required federal agencies and museums to catalog all human remains and artifacts associated with burials and make an attempt to give them back to the affiliated tribes.

Facilitating the use of LiDAR data to detect mounds fits with the current shift towards archaeological practices and laws that respect the Native American culture which regards these places as sacred. A more-comprehensive site file on the accurate locations of these sacred sites will help planners in the private and public sectors avoid these areas in development projects. Areas marked as mound-like features by the detection tool will aid archaeologists in formulating a more effective survey and for large surveys, would save

time and money by minimizing the effort required for image interpretation.

2.2 Remote Sensing Utilization in Archaeology

Modern archaeology utilizes many other disciplines such as osteology, palynology, zoology, paleontology, geology and geographic information science in order to reconstruct the past from the fragments that remain. Finding evidence from the past in certain locales or specific time periods can be a difficult endeavor. Once sites are found, some may fall under protection laws of the state, provenance or country. Often these laws require monitoring of the sites' conditions - to check for looting, erosion, encroachment from development or changes in vegetation that may be damaging to the site. Known for their multidisciplinary resourcefulness, it would be intuitive that archaeologists use remote sensing technology to aid in site prospection and monitoring.

2.2.1 Satellite imagery

Landsat satellites have provided continuous images of the earth's surface since 1972 (Jensen 2007). The option of obtaining multiple images of the same area over a long period of time allows for change detection studies that can be applied to archaeological site monitoring. In North Norway cultural heritage officers are facing the challenge of monitoring a large area that contains Iron Age burial cairns. Changes in the climate and the decline in agriculture and grazing over the last twenty years in North Norway have affected the vegetation and land cover in that region. Spread of vegetation and reforestation threatens to damage or destroy the burial cairns. To determine which parts of North Norway were increasing in vegetation a Normalized Difference Vegetation

Index (NDVI) was calculated from multispectral images collected fifteen years apart. Image differencing was then used to find where the rapid change in vegetation was taking place (Barlindhaug et al. 2007). This technique provided change detection information over a large area rather quickly.

A study in the U.K. (Fowler 2002) found that Landsat TM for small site detection can be useful with the near infrared (NIR) band due to variations in vegetation, but visible light bands could not detect sites the size of hillforts. Roman roads carved into the chalk substrate show in the visible light bands due to the high contrast with their surroundings. SPOT panchromatic images with 6 m spatial resolution (compared to Landsat's 28.5 m) surprisingly did not do much better than the Landsat images at detecting sites (Figure 11). Only one hillfort was sharper, and another was not detected at all but was detected on the Landsat NIR. Roman roads were as distinct on the SPOT images as the Landsat images. The Russian KVR-1000 images at spatial resolution of 1.5 m can detect sites without any prior knowledge of the sites existing, small sites and sites that have been plowed over (Figure 12). Overall, the Landsat and SPOT images are useful for base mapping, but for archaeological prospection and monitoring at a medium-scale the KVR-1000 can provide the necessary detail.

Corona images from the 60's and 70's were released to the public by presidential executive order in the mid 1990's (Jensen 2007) and have proven to be an effective tool for archaeologists. A study in northern Iraq demonstrates that Corona KH-4B images are

Figure 11. Comparison between Landsat TM Multispectral and SPOT panchromatic images. Center of each image is the Iron Age hillfort and later medieval site at Old Sarum, Wiltshire, U.K. A) Landsat TM visible bands 1-3, B) Landsat TM near-infrared band 4, C) SPOT panchromatic image (image adapted from Fowler 2002, used with permission ©Wiley InterScience).

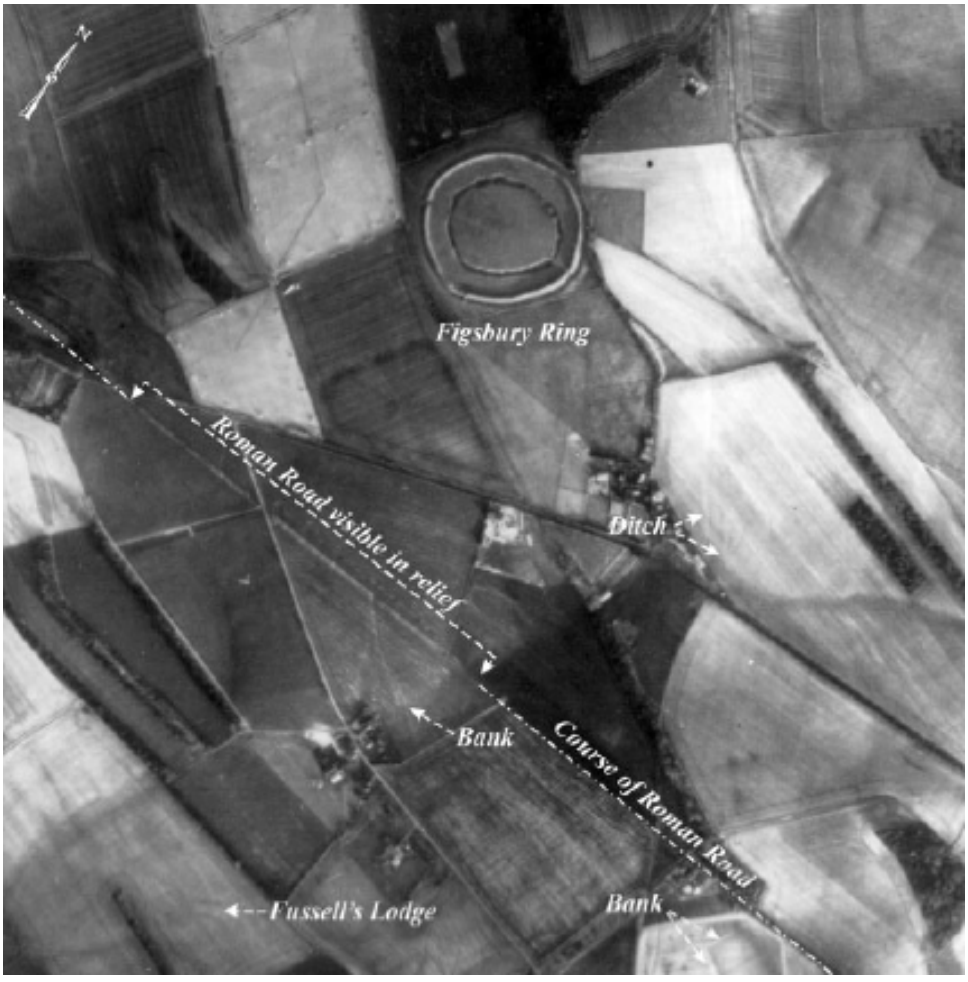

Figure 12. A KVR-1000 image of a Roman road and an Iron Age hillfort at Figsbury Ring, Wiltshire, U.K. (image: Fowler 2002, used with permission ©Wiley InterScience).

useful in detecting ancient footpaths (called hallow ways), canals and tells (Altaweel 2005). Altaweel has found that the spatial resolution of Corona data is satisfactory for finding such sites. Contrasting soil moisture regimes between the canal or hallow way and their surroundings aided the detection of these features in the Corona images. However the author found that if the area was in drought or the shadows were not at an effective angle, then features would be missed or interpreted incorrectly (Altaweel 2005).

In Syria, Corona KH-4B images have been used to remotely survey smaller site types that have largely been overlooked in favor of tells – large mounds of ruins created by hundreds of years of settlement and layers of subsequent settlements rebuilt in the same place. Corona's spatial resolution of nearly 2 m has allowed for the detection of 51 new sites in the Homs Region, Syria (Wilkinson et al. 2006). The sites typically show up as high light reflectance and rarely high absorption due to the difference in soil texture caused by the disintegration of mud brick or building stones acting as a lag deposit. IKONOS images were compared with the Corona images with similar results. Wilkinson et al. (2006) conclude that besides habitation areas that used mud brick or stone, other features such as canals and roads can be successfully spotted using Corona or IKONOS images. During the field survey they discovered that the images did not detect smaller cultural features such as a stone-carved olive press or short-term occupation scatters. Both the Wilkinson *et al.* (2006) and Altaweel (2005) articles emphasize that this technology cannot replace a field survey but it is a helpful tool for prospection and monitoring, especially in areas that aerial photography at present is nearly impossible to obtain.

As a supplement to the Corona images Altaweel (2005) used Advanced Spaceborne Thermal Emission and Reflection Radiometer (ASTER) multispectral data from the VNIR subsystem for its ability to detect minor variations in soil moisture regimes and vegetation. The ASTER system was preferred by Altaweel over the older Landsat satellite data because of its finer spatial and spectral resolutions. ASTER data proved to be helpful in differentiating between hallow ways and smaller canals as well as elucidating soil signatures for archaeological sites. One disadvantage was that the spatial resolution was too coarse to detect sites less than 1 hectare.

ASTER data has also been utilized for geoarchaeological studies in the Eastern Sahara region west of the Nile River (Bubenzer and Riemer 2007). ASTER provided stereoscopic images that were used to create a digital elevation model (DEM) at 1:50000 scale. The area of study seems to belie common sense because it is west of the Nile River Valley in the desert. However, with analysis of the DEM in a GIS and utilization of hydro-modeling software the authors were able to find areas of specific relief expression that indicated surface storage of surplus water during the Holocene humid wet phase. Bubenzer and Riemer (2007) state that these areas would be conducive for hunter-gatherer occupation. Past and current on-going field studies find that concentrations of hunter-gatherer campsites from the wet phase (ca. 9500 – 6300 B.P.) do correlate with the landforms identified by the authors as seasonal pools in the desert.

2.2.2 Suborbital remote sensing

Archaeology has utilized aerial photography for the last 100 years for reconnaissance.

Aerial photography is still a cheaper alternative to satellite imagery and can provide a much finer spatial resolution or larger scale; often the desired spatial resolution in archaeology is around 0.2 meters (Fowler 2002). The success of identifying new archaeological sites from aerial photography has compelled the English Heritage Aerial Survey team to map all archaeological sites viewable from aerial photography at a 1:10000 scale nationally. One of the challenges is to be able to identify the site type or age from the photos. Many times this can only be done through field investigations (Bewley 2003).

Large-scale aerial photography is used to record significant individual sites (Figure 13). By creating multiple photos of the site at scales around 1:1500 or larger, orthophotographs can be produced to create high-resolution DEMs. The orthophotos can then be draped over the site to create 3-D images. Photography at this scale has been known to detect rabbit holes and disturbances from looting (Bewley 2003). Aside from spatial resolution, aerial photography has an advantage over satellite imagery in that archaeologists have more temporal control of image acquisition. Often satellite images of an area of interest are not usable due to cloud cover or the image angle is too vertical. With aerial photography several oblique angles can be flown at specific times of the day over the same area to create various shadows which aid in the detection of archaeological features on the landscape (Fowler 2002).

A weakness of aerial photography is that the majority of aerial photos is black/white or true color that can only detect light in the visible spectrum, but signatures of buried sites

Figure 13. Digital orthophotograph of Roman Camps at Cawthorn, U.K. created from 15 vertical aerial photos (image: Bewley 2003, used with permission ©Wiley InterScience).

may be only present in near-infrared or longer wavelengths. Early satellite imagery in the 1970's and 80's had multispectral data, but was not used in archaeology because the spatial resolution was too coarse and using the images required too much technical expertise (de Sherbinin *et al.* 2002). Instead, airborne multispectral sensors were the first method of remote sensing used in archaeology after aerial photography. A mid-1970's National Park Service (NPS) survey of Chaco Canyon, New Mexico is regarded as the first archaeological study where remote sensing was the sole method for data collection and analysis (de Sherbinin *et al.* 2002). In 1982 Thomas Sever, an archaeologist for the National Aeronautics and Space Administration (NASA), partnered with the NPS to conduct a broader survey of the Chaco Canyon area using NASA's airborne scanner

technology which had been untested in the field of archaeology. The performance of the Thematic Mapper Simulator (TMS) and Thermal Infrared Multispectral Scanner (TIMS) at 10 m and 5 m resolution were compared. TIMS images by far sensed more features than the color-infrared images from TMS. The TIMS sensor could detect prehistoric surface and buried features such as walls, buildings, agricultural fields and roadways dating to AD 1020 – 1220; many were not detectable on the ground (Sever and Wagner 1991).

2.2.3 Remote sensing on the ground

Not all sites can be preserved due to unavoidable development such as road construction. The site is usually excavated and artifacts curated at a cultural resource management facility, research agency or museum. The site is destroyed forever; but there are methods to try to preserve the orientation of the feature's components, maybe even to reconstruct the feature somewhere else. Close-range photogrammetry is used for individual features at a site or a whole site excavation. It involves a simple digital camera taking several overlapping pictures around the feature. The overlap creates stereo pairs from which accurate metrics can be extracted. RMS error of object's measurements created from control point measurements is as little as 4-6 mm for X, Y and Z. Highly-detailed digital drawings can be created from these metrics as well as a 3-D rendition of the feature or excavation layer by layer (Figure 14). Realistic textures can be added to the feature's 3-D rendition from the actual photographs (Pollefeys et al. 2000, Lorenzo and Arias 2005).

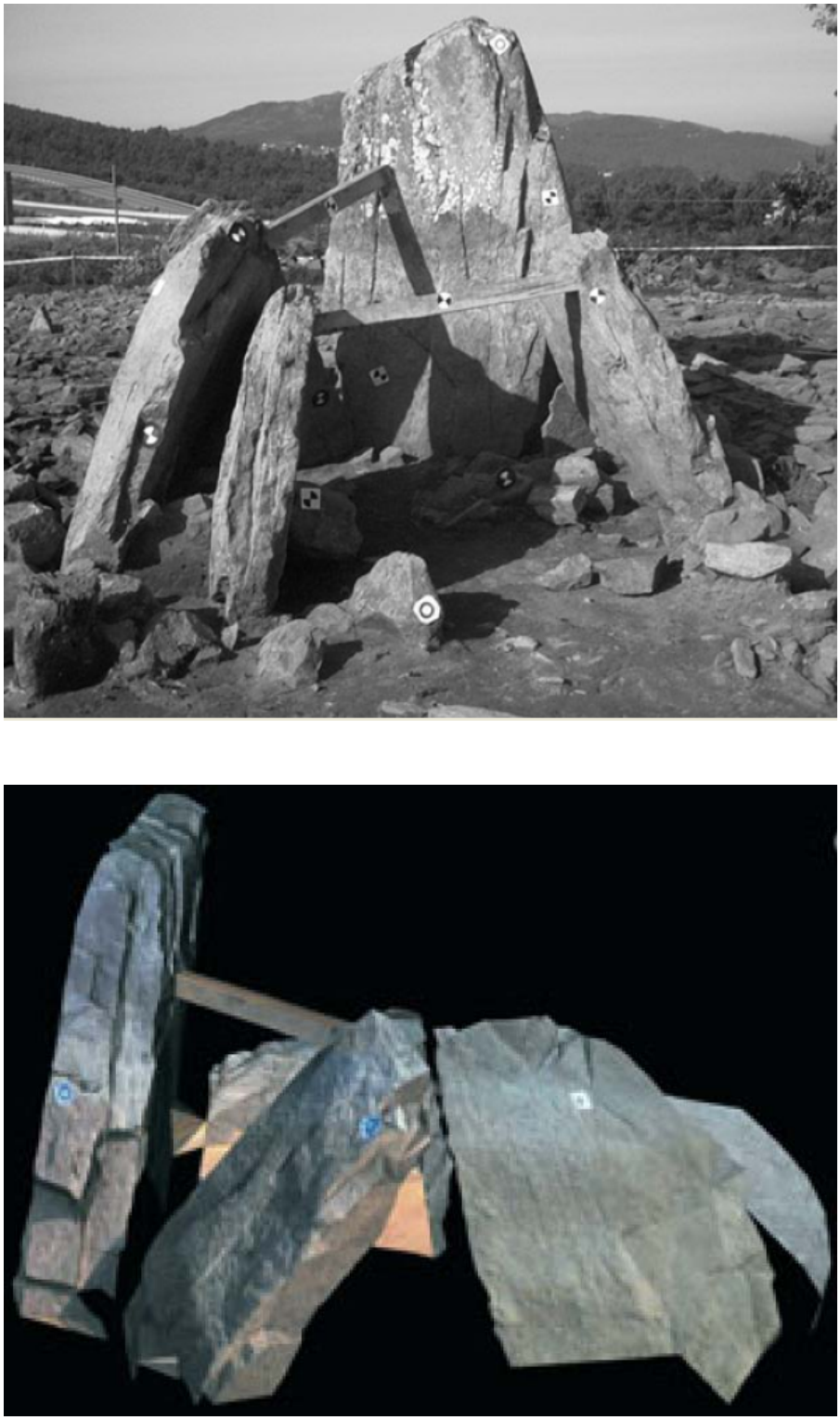

Figure 14. Above: Photograph of gravestone chamber at Vigo, Spain. Below: A 3-D virtual image of the same feature using metrics obtained from close-range photogrammetry (image: Lorenzo and Arias 2005, used with permission ©Wiley InterScience).

Many current journal articles are being published about the use of ground penetrating radar (GPR) for buried site prospection. The common theme among most of those articles is that GPR used for archaeological prospection is still in an early experimental phase and there are as many challenges as success stories. A survey of a Roman cemetery in Greece used GPR to find graves or tombs that had not been disturbed by looting. Before the GPR was used, a survey of the site area using electromagnetic susceptibility and conductivity was conducted and anomalies were isolated. The GPR was used over the anomalous areas with controlled scans over two known tombs. The measurements from the GPR matched closely with the measurements of the tombs. GPR scans were able to detect small looting pits, linear feature of a later medieval foundation and two other Roman tombs and several cist graves (Sarris et al. 2007).

Another GPR survey at three mound sites in the U.S. was carried out to see if soils that were placed by humans would express a different GPR signature than natural soils, for many natural features resemble mounds. They found that GPR worked with varying success depending on the depth of the disturbed soils and the natural stratigraphy of the area. GPR did not work well in alluvial settings where the stratigraphy can be very complex and change over small areas. Additional geophysical methods were used and it was concluded that there were no standard signatures for mounds - it is site specific; and different methods work for different sites (Dalan and Bevan 2002).

In the review of the literature it is clear that archaeology has embraced remote sensing technology using a great diversity of sensors. Most of the literature has a common theme

throughout – that there is no one method that is the best and more than one technology may need to be employed. The method(s) to use largely depend on the size and accessibility of the study area, the size of the features to be studied, money and time available, and the nature of the research question. The size of the sites where remote sensing technology was employed is large compared to most mounds in Iowa. The literature that described "small" sites were generally 250 m^2 or larger; conical mounds are generally 5 – 12 m in diameter. However, Iowa archaeologists have successfully detected conical mounds on the larger end of the spectrum on 1930's aerial photography before cultivation practices had worn them down. The sites in the reviewed literature were also not obscured by wooded areas. Using LiDAR, mounds located in heavily wooded areas can be detected as demonstrated in Figure 1 with the Slinde Mound Group.

2.3 Traditional Uses of LiDAR

The purpose of LiDAR is to quickly collect relatively-accurate elevation data over large areas. Basically, any field that uses elevation data and derivatives of that data should find utility in LiDAR. It is not hard to find evidence supporting this hypothesis as it seems LiDAR use has grown exponentially over the last ten years as the price of data collection has decreased.

2.3.1 LiDAR in the natural environment

Forestry was one of the first fields to commercially use LiDAR (Fowler *et al*. 2007). Radar and satellite imaging cannot map the ground under the tree canopy and the tree height at the same time, but LiDAR can. This enables those in forestry and natural

resource management to quickly obtain tree heights from the BE DEMs and Digital Surface Models (DSM) derived from the LiDAR data (Fowler *et al.* 2007). The heights give an idea of how much area is in a particular stage of growth, i.e. shrub, young, mature or old growth (Renslow *et al.* 2000). Wildfire management studies are increasingly using LiDAR data because of its fine spatial resolution, accuracy and the many height levels in a forest that can be extracted such as ground to crown. Fire spread modeling also uses variables of slope, density of vegetation, aspect and elevation which are all derived from LiDAR data. Mutlu *et al.* (2008) found that using LiDAR data improved fuel mapping accuracy by 13%.

The last twenty years has seen a shift in federal and state laws towards greater protection and conversion of coastal and inland wetlands. Section 404 of the Clean Water Act allows for the federal government to review potential deleterious effects of projects on extant wetlands (Votteler and Muir 1999). In some places, the boundaries or even definite existence of a wetland is not so obvious due to partial or complete draining in the past. The advent of LiDAR has spurred studies in how well the technology can detect the very subtle drainage patterns demarcating a wetland. In 1999 the USGS underwent a LiDAR topographic mapping project in the Florida Everglades after a wildfire burned off the vegetation with great success. However, another wetland project in Florida proved that in normal vegetation conditions, the vegetation was too thick for the light to penetrate the true ground surface (Maune 2007). Since then, there have been a few studies on how different wetland vegetation types have an affect on LiDAR ground elevation and vegetation height data (Hopkinson *et al.* 2004, Henry and Gonzalez 2005). Overall

consensus with researchers and agencies is that LiDAR is an important tool for wetland delineation (United States Army Corps of Engineers 1999, Henry and Gonzalez 2005, Gritzner 2006).

2.3.2 LiDAR in the built environment

Applications of LiDAR in the built environment have received as much, if not more, attention than natural environment applications. Mapping linear corridors such as power lines, gas pipelines and highways has created market niches in the remote sensing industry over the last ten years. Mapping power lines has become an important market because information such as sag, ground clearance and vegetation encroachment can be mapped quickly over large areas (Figure 15). A survey that would once take months, now only require a few hours with airborne LiDAR (Fowler *et al.* 2007).

Many pipelines carry volatile products such as natural gas. Breaks in the line due to geological shifts and third parties accidentally rupturing the line can cause catastrophic damage and fatalities. Because the pipeline corridor fits within a single swath width of a LiDAR scanner, collecting data on topography and encroaching vegetation is quick and relatively cheap. The BE DEM clearly shows the anomalous surface where the pipeline is buried allowing for the creation of alignment sheets – the record of pipeline location. A safety risk assessment can be carried out using derivatives from BE DEMs such as slope. Pipeline segments along steep slopes may be subject to landslides; even gradual shifts of the land can cause stress cracks in the pipe. Aspects that face prevailing winds and are covered with dense vegetation carry a fire risk. Altogether a risk rating can be applied

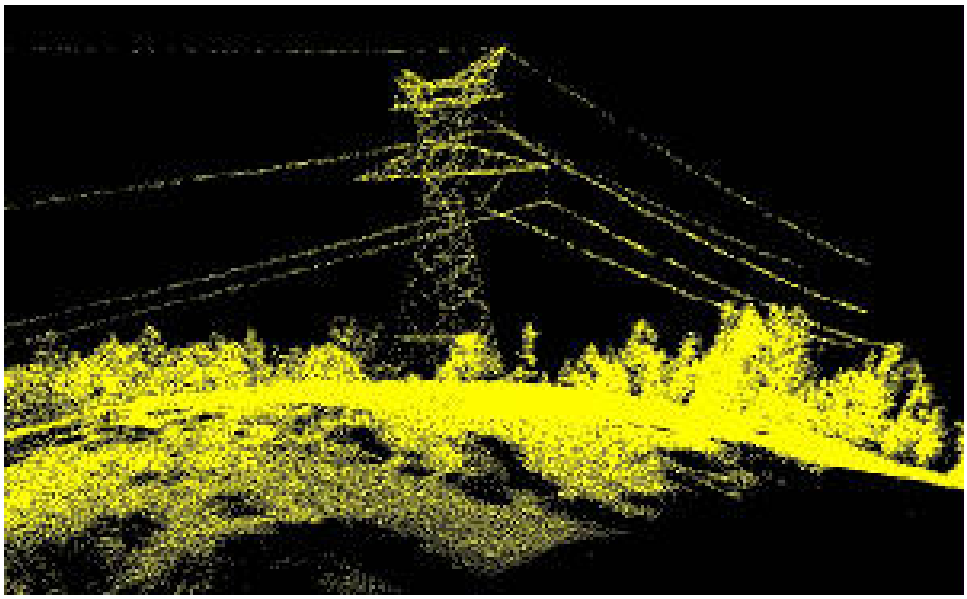

Figure 15. LiDAR point cloud of power line corridor (image: Spatial Resources 2009, used with permission).

along the pipeline based on slope, aspect and biomass (Tao and Hu 2002).

For the transportation industry, LiDAR surveys are reliable enough that some applications can be applied without field surveys. Aside from the usual applications of mapping and 3D visualization, other applications related to siting, safety and emergency management have been developed for transportation. Flooding models based from a LiDAR-derived DEM can determine if any part of a transportation network would be inundated under different flood levels. For driver safety, line of sight tools are used to study driver sight distances and stopping sight distances. Modeling surface runoff and drainage of water may identify driving hazards and high-risk areas for landslides (Applied Imagery 2009).

Modeling applications in the urban landscape using LiDAR data are used for

telecommunications, wireless communications, storm water management, micro climate studies and law enforcement (Fowler *et al.* 2007). Perhaps the most prevalent topic is the extraction of building footprints from LiDAR and building 3D models of urban centers. Articles for at least 14 years have presented a variety of methods for the semi- or full automation of extracting building footprints to create vector files and 3D renderings (Weidner and Förstner 1995, Mass and Vosselman 1999, Hewett 2005, Opitz *et al.* 2006). The methods have changed generally due to the increase in software capabilities, computing power and availability of higher resolution LiDAR data.

In 2005 commercial-off-the-shelf software called LIDAR Analyst was released by Visual Learning Systems, Inc., now Overwatch Geospatial, as an extension that worked with ESRI ArcGIS and later ERDAS Imagine (Figure 16). Development of the product was in response to growing demand in the private and public sector to be able to quickly and accurately classify features from LiDAR data and extract them into clean 3D shapefiles – with very little training required.

Traditionally such feature extraction endeavors were expensive due to the large amount of man-hours required plus it required a lot of specific expertise. Opitz *et al.* (2006) claimed that in testing their product 11,000 buildings were extracted in 9 minutes with 97% accuracy – including complex rooflines. The tree extraction functionality of the software can extract over 100,000 trees in 6 minutes. Unfortunately the price of the software may be prohibitive for small agencies and municipalities; special government pricing is over $10,000 per license and $2000 per year for maintenance fees.

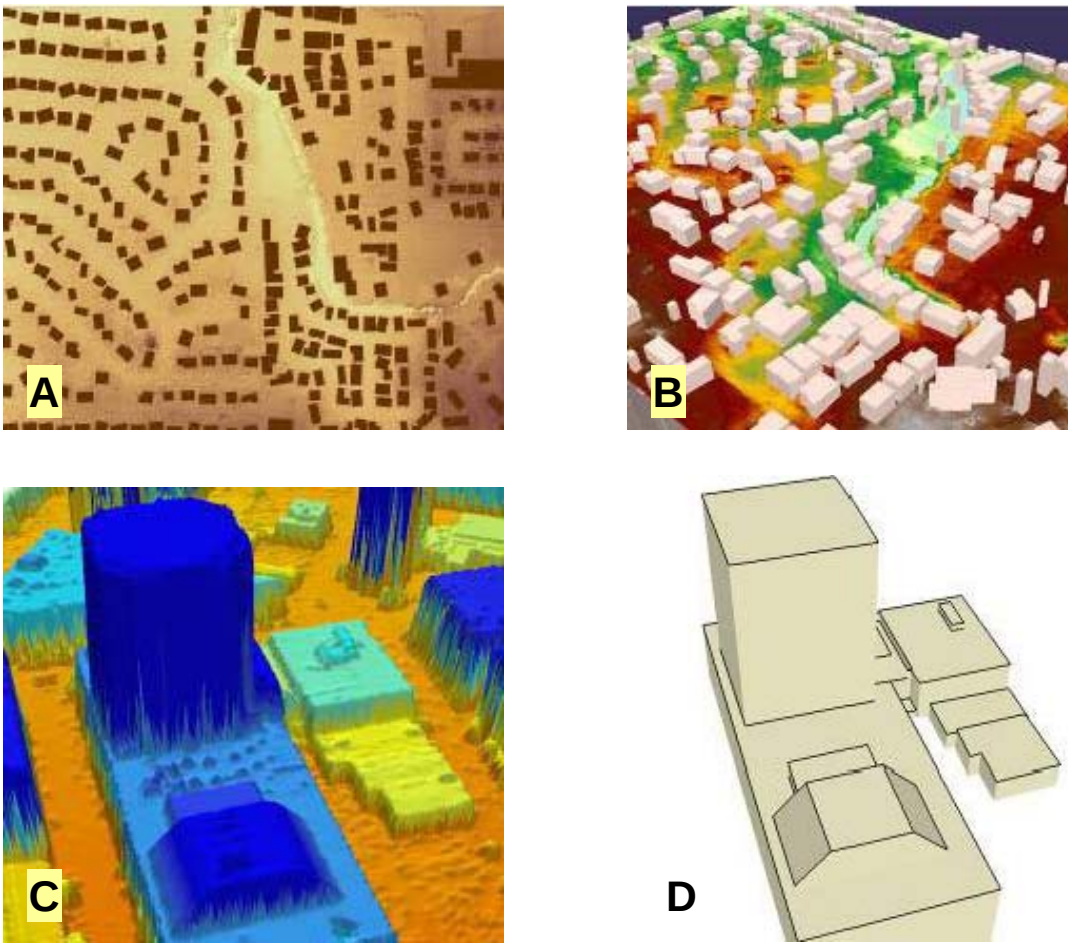

Figure 16. Images from LIDAR Analyst. A) building footprints automatically extracted from DEM, B) 3D buildings on a terrain model, C) complex building in a LiDAR DEM, D) 3D extraction using Overwatch Geospatial's proprietary algorithm (images: Visual Learning Systems, Inc. 2005, used with permission ©Overwatch Geospatial. All rights reserved).

Hewett (2005) demonstrated an economical, automated feature extraction solution in ArcGIS for features like buildings, treed areas and rural dams using tools available with the Spatial Analyst extension and ModelBuilder. The general methodology follows what was envisioned for this research. Each of Hewett's extraction models adheres to a few general steps:

Assess the data – first return, last return, intensity, bare earth
Identify – figure out what is unique about your feature that you want to extract
Convert data to useable form – i.e. ASCII .xyzi to point file

Enhance the data - separate what you want from the rest using mathematical calculations and Spatial Analyst tools
Simplify the data – get it ready to convert to line or polygon file
Extract – send it to shapefile
Clean-up – these can be automated or manual procedures to get rid of extra polygons, for example.

Hewett (2005) also included ModelBuilder diagrams used for each extracted feature type to supplement his instructions. There is no programming of complicated algorithms involved, only using the algorithms already available in the software and implementing simple map algebra. The final products are 2D shapefiles demarcating ponds, wooded areas and buildings. The building edges are not crisp as with LIDAR Analyst, but the general outline of the building footprint is there.

LiDAR has been recognized in many industries as a technology that can save time and money by reducing labor hours for field surveys. The elevation data and its derivatives are used in various combinations to suit many different applications. For example, large digitization projects of buildings and vegetation are now more financially and temporally feasible with automated feature extraction techniques and software. A mound detection model using BE DEM derivatives would facilitate image interpretation and save labor hours. Like LIDAR Analyst, the process will be automated so relatively little training will be required. However, the word “extraction” has been avoided and “detection” used instead for this research in light of what actual commercial feature extraction software can do (i.e. sharp clean lines, 3D rendering of the polygons, highly accurate classification). Opitz *et al.* (2006) received much financial support from the U.S. Department of Defense (DOD) and NASA to develop software with such capabilities and

the DOD continues to support the developers' efforts to this day. The technology is proprietary, but Opitz *et al.* (2006) has credited the success of LIDAR Analyst to machine learning technology – something that far surpasses the scope of this research. Considering that for over ten years researchers have spent millions of dollars finding reliable full or semi-automated building extraction techniques, the idea that the mound model will actually "extract" precise shapes with attributes is chimerical.

2.4 Utilization of LiDAR in Archaeology

The Netherlands collected LiDAR data nationwide between 1996 and 2004 with at least a 4 m post in leaf-off conditions. Elevation data derived from LiDAR first became available in 2001 (van Zijverden & Laan 2003). The United Kingdom Environment Agency began LiDAR collection in 1996 and is still collecting data today. Approximately two-thirds of the U.K. now has data with a minimum 2 m posting (Environment Agency 2007). Although the data have thinner postings than Iowa's, researchers have still been able to use it for archaeological prospection.

In the United Kingdom, known sites such as a medieval settlement, Roman sites, hillforts as shown in Figure 17 and Stonehenge have been used to check the efficacy of LiDAR for archaeological prospection (Barnes 2003, Bewley 2003, Devereux *et al.* 2005, Challis 2006). Most results of these surveys were positive; however the size of these features is measured in the hectares, which is a stark contrast to a 5 m diameter burial mound. The amount of topographic relief of these features was not a focus for discussion. Devereux *et al.* (2005) conducted a study of a hillfort site largely concealed by forest using LiDAR-

derived bare earth surfaces of .25 m and 1 m resolution. The images also revealed a possible Bronze Age field system and smaller features that had not been mapped in prior ground surveys. The topographic relief of the "smaller" features were not discussed nor the dimensions.

In the Netherlands, sites such as burial mounds, Bronze Age villages and 2500-year-old Celtic fields are detectable using the 4-meter posting data (van Zijverden & Laan 2003, Humme *et al.* 2006). Only the topographic relief of the Celtic field feature (10 cm) is given, which was successfully expressed in a BE DEM created by a kriging interpolation method; however the authors mention that some of the points used for the BE DEM were seeded by the researchers with no specifics on the points (Humme *et al.* 2006). The utility

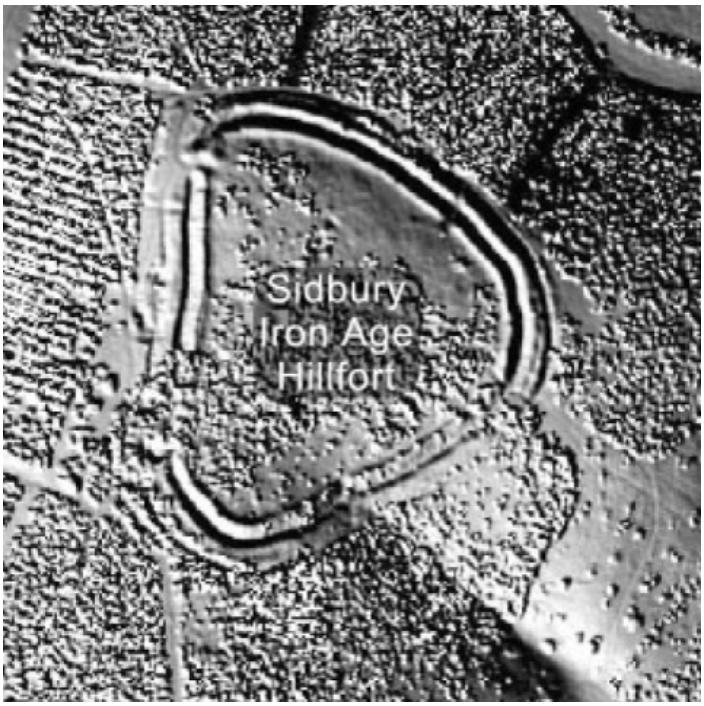

Figure 17. LiDAR DSM of an Iron Age hillfort on the eastern side of Salisbury Plain, United Kingdom (image: Barnes 2003, used with permission ©Wiley InterScience).

of LiDAR for finding such microtopographic features is dubious without a description of how many points were added, their assigned elevations or where they were placed.

Very little information exists on archaeological prospection using airborne LiDAR in the United States. Harmon *et al.* (2006) assessed the utility of 1 m resolution LiDAR images for studying historic landscaping of two eighteenth-century plantation sites in Maryland. These landscapes are so large that subtleties such as abandoned garden terraces are impossible to see as a whole from the ground. Comparing 1m resolution LiDAR data to Maryland Department of Natural Resource's 2 m resolution data, the coarser resolution did pick up the terraces and other major features but was too coarse for some other important features the 1 m resolution image revealed. Relief visually detected from the images was as subtle as 15 cm.

Gallagher and Josephs (2008) acknowledge woodland areas are difficult to survey and as a result many woodland areas have no archaeological record. To test the efficacy of LiDAR in heavy woodland areas, the authors did a presurvey review of a shaded relief image from a 2 m BE DEM from the Isle Royale National Park, Michigan. Thirty-two potential archaeological features were interpreted from the imagery; 18 were previously recorded. A pedestrian survey was able to locate 25 of the 32 features – all 18 previously recorded sites and seven newly discovered sites. Seven other sites that were detected on the LiDAR imagery could not be found in the field survey; this was largely attributed to heavy undergrowth vegetation and fallen trees.

The authors cite over-smoothing of the BE DEM for hydrological modeling (the original intent of the data's use) and their own inexperience in using the technology as making image interpretation difficult. They also laud the benefits of having free LiDAR data available for presurvey planning; including being able to identify potentially dangerous situations like old mining pits and deep trenches that may be obscured on the ground by vegetation. Gallagher and Josephs (2008) conclude that using LiDAR for presurvey planning makes the survey more effective and saves time and money; their observations were supported by empirical data.

Archaeologists in Ohio used LiDAR to locate a 2000-year-old road that was mapped several times in the 1800's and was subsequently destroyed by urbanization or cultivation. The remaining segment of road was preserved in a wooded area with 30 cm embankments rising above either side of the path. Several profiles taken along the road showed that its morphology matched another prehistoric road segment in a different part of the state. The researchers were impressed with how much information they were able to collect without doing an actual field survey and look forward to more LiDAR work in the future (Romain and Burks 2008).

Studies in the United States demonstrate that subtle features are detectable by ordinary visual interpretation of a shaded relief image when the features form patterns over a substantial area. LiDAR use in archaeology in both Europe and the U.S. primarily relies on shaded relief image interpretation without much manipulation of the data to enhance visibility of archaeological features. Romain and Burks (2008) was the only study

encountered that used tools to analyze the site, in this case a profile tool. There were no articles where an attempt was made to detect features through an automated method. The closest was Humme *et al.* (2006) where a kriging interpolation method and seeded points were used to make a BE DEM that expressed a Celtic field system.

CHAPTER 3: METHODOLOGY

3.1 Description of Data

The BE DEMs created from Iowa's statewide LiDAR project are the foundation dataset for the mound detection model. The collection initiative is a partnership of the IDNR with the Iowa Department of Transportation (IDOT), Iowa Department of Agriculture and Land Stewardship, Iowa office of the U.S. Department of Agriculture Natural Resources Conservation Service (USDA-NRCS), Rock Island District of the U.S. Army Corps of Engineers and USGS (Iowa Department of Natural Resources 2007). The vendor, Sanborn Map Company, is to adhere to the following contract specifications:

- GPS baseline every 40 km, every 20 km for FEMA spec areas
- 1.4 m sample density
- Vertical accuracy:
    - bare earth - 18.5 cm RMSE
    - heavy vegetation - 37cm RMSE
- Horizontal accuracy 50 cm RMSE
- 90% of collected data leaf-off. (Young 2007)

Mass point data stored in 2 x 2 km tiles are classified by several vendors subcontracted by Sanborn. The IDNR-IGS receives first and last return data in approximately 350 mi^2 blocks of tiles to produce the 1-meter BE DEMs, Digital Surface Models (DSM) and shaded relief rasters using QCoherent LP360 software. Eventually, the agency will create other derivative files from the BE DEMs and all data, including the point data in .las and ASCII format, will be available for download to the public.

Archaeological site locations are available in a shapefile stored at the UI-OSA. This file is updated by the Site Records Manager as new sites or modifications to site boundaries

come in. Site locations in the site file are coded by: whether a boundary and location is known; location is known but boundaries are uncertain; or, boundary and location are uncertain. Mounds were a popular site type for study in the late 1800's and early 1900's, so a large percentage of mound sites were reported a long time ago and have not been field visited/verified since. Site locations from historic field notes can be tenuous because many reference locations are based on features that do not exist anymore such as large trees, fence corners and outbuildings on farms. Mound site locations also used landowners' names as reference, but in the last 80 – 100 years the property has changed many owners and may have been divided into smaller parcels. For these reasons, 37% of the mound sites have uncertain boundaries and location.

Site locations are only required to be reported by drawing the boundary on a USGS 7.5' topographic map and reporting the legal location to the quarter quarter (QQ) section; although most report to the QQQ or QQQQ section. Archaeologists pace out or use a tape measure from a reference point in the field to record the site location. More reports within the last 20 years generally will have a large-scale map in addition to the topographic map of the site boundary. Location data from earlier archaeological surveys in the 1950s – 1980s are many times available only by the topographic map. Site boundaries reported to the UI-OSA that had been determined by GPS coordinates is still unusual, but has increased in the last few years. It was expected in this course of study that sites with "definite" boundaries may be off and not encompass a mound in a single-mound site or all the mounds in a mound group.

A Microsoft Access database called the Iowa Site File stores a digital record of attributes for each site in Iowa. This too is maintained and stored by the UI-OSA and is updated daily. The database includes information on when the site was reported, if it has been revisited and how the location of the site was derived (i.e. pacing, tape measure, GPS) as well as descriptive information such as site type, cultural affiliation and artifacts recovered.

Other datasets were used in post-processing and interpretation of the mound model results. When available, field maps were used for interpreting whether the model detected low-relief mounds that are not easily visible on a shaded relief image. Individual mounds in mound groups are mapped using relative measurements from other mounds in the group or from other features such as fencelines; this is as true for a recent 1987 field map as a 1935 field map. Distances of mounds visible on the shaded relief to those not visible were obtained from the field maps and applied to the shaded relief image in order to locate the low-relief mounds.

Road files used for clean-up are countywide shapefiles of road centerlines with its origins from the 2006 IDOT Geographic Information Management System. “Incorporated Cities of Iowa, 2000” is a polygon dataset created by the IDNR used to eliminate false positives due to residual building footprints. Other ancillary data were loaded into the map documents via the Iowa Geographic Map Server, a Web Map Service (WMS) maintained by Iowa State University Geographic Information System Support and Research Facility.

The datasets used were:

- 2004-2008 USDA National Agriculture Imagery Program (NAIP) 2-meter resolution true color orthophotos.
- 2002 digital 1-meter color-infrared county orthophoto mosaics created by IDNR-IGS.
- Seamless mosaic of 1-meter resolution panchromatic Iowa digital orthophoto quads from 1990-1999, originated by USDA-NRCS.
- Iowa 1:24,000-scale seamless digital raster graphics from 7.5' USGS topographic maps developed by USDA-NRCS.
- 1930's Iowa USDA panchromatic 1-meter digital orthophotos originally photographed at 1:20,000 scale. Countywide mosaics were developed by IDNR.

3.2 Study Area

Areas used for developing the model were based on where the BE DEMs have already been created by IGS, where well-documented mound sites are still extant and physiographic region. Although 55% of the land area in Iowa has been collected, only a few blocks have been processed into DEMs by the IGS due to a time lag between collection, point processing, quality checking and delivery to the IGS. Additional checks by the IGS after processing DEMs and shaded relief images revealed that all the blocks in northwest and northcentral Iowa contained errantly processed point clouds at the tile boundaries. The data for those areas were rejected and the vendor was required to reprocess the data; the corrected regions were not available at the time of this research.

The Iowa Site File database was sorted for all mound sites; this table was subsequently joined to the site boundary shapefile creating a mound site shapefile. Mound sites for the training area were then selected based on the designation of site location confidence and whether there were BE DEMs already processed by IGS. The initial area chosen for developing the model is located in the Paleozoic Plateau physiographic region where

many well-documented mound groups exist including the Slinde Mound Group and sites in Effigy Mounds National Monument (Figure 18). The Paleozoic Plateau is known for its high bluffs, bedrock outcrops, deeply entrenched streams, sinkholes and generally rough topography (Prior 1991). The areas where it is too steep for agriculture are primarily forested with deciduous trees. This region was expected to be the most difficult to detect small conical mounds on LiDAR BE DEMs because of the precarious nature of how BE DEM extraction algorithms handle heavily-vegetated and high-relief landscapes (Sithole & Vosselman 2004).

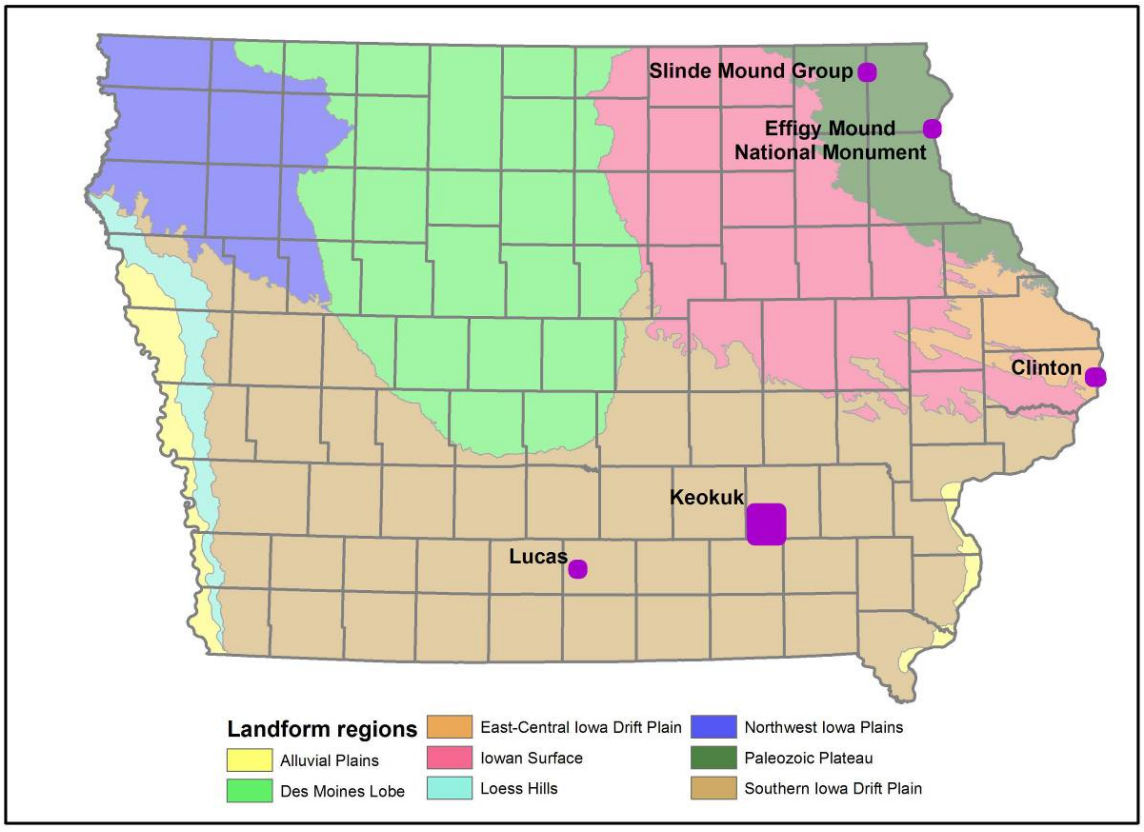

Figure 18. Landform regions and locations of model test areas.

The bumpy “features” anticipated with BE DEMs in northeast Iowa made the region top priority for developing the model. If the model works well in this region, then it should work well in physiographic regions of low, gradual relief where much of the land will have sparse vegetation during leaf-off conditions. The initial training area selected for the model is the Slinde Mound Group. This mound group has been subject to several levels of disturbance, from archaeological excavation and backfilling, looters’ “pot holes”, livestock trampling to undisturbed. Aside from the challenging terrain, if the model can detect mounds that do not fit the ideal morphology then it should be functional in detecting imperfect mounds across the state.

Additional areas for testing the model were selected in the East-Central Iowa Drift Plain and the Southern Iowa Drift Plain. The East-Central Iowa Drift Plain has glacial deposits at or near the surface which is overlain by a layer of loess in the uplands (Prior 1991). The glacial deposits were left by a pre-Illinoian glaciation event over 500,000 years ago. Since that time, the landscape has been carved by stream erosion leaving many steep hills and valleys. One of the features of this physiographic region that could potentially interfere with the mound model is the small bedrock outcrops that are commonly found. The mound site candidate in Clinton County has not been field-checked since Ellison Orr visited it in 1935. The quality of Orr’s field maps are such that site locations usually can be narrowed down to a small area. While the exact location was not known for the site, testing the model in a 2-4 sq. km high-likelihood area is a practical test of how the model would work in normal presurvey planning.

The Southern Iowa Drift Plain is similar to the East-Central Iowa Drift Plain because of the similar glacial history. The only major difference between the two regions is the Southern Plain does not have bedrock near or at the surface in the form of outcrops. This region was anticipated as being the most “cooperative” to the mound model because the topography is generally large, rolling hills. The model was run in two areas, one along the North Skunk River valley in Keokuk County and the other in Lucas County. All other physiographic regions were excluded from the research because no BE DEMs were available or there were no well-documented, extant mound sites within the regions that had BE DEMs.

3.3 Research Methodology

The mound detection model was built in the ModelBuilder environment using many tools included with the Spatial Analyst extension. The model is reliant on the morphology of the conical mound. An ideal conical mound will have an aspect from 0 - 360° with a consistent, moderate slope different from the surrounding ground all the way around. The slope angle will not be consistent from edge to the top-center of the mound because the slope levels out as it reaches center, creating a gradual profile instead of a pointed one. The heights of mounds are within a reasonable range, excluding outliers which are from rare, large conical mounds. This metric was used along with slope and aspect to form the foundation of the model (Figure 19). The three major variables used in building the model are reclassified using a numerical system where each variable have values with a different number of digits. Height is single digits, slope is reclassified to the tens place (i.e. 10, 20, 30), and aspect variety is reclassified to integers in the hundreds. Added

together, the sum raster contains three-digit values where it is easy to determine what class of each variable has influence on detecting an actual mound and what values should be taken out of the preliminary results raster.

3.3.1 Defining parameters

BE DEMs are interpolated surfaces from points that have been classified by algorithms as bare-earth, so the metrics of mounds from field visits likely differ from what is expressed on the BE DEM. If they are substantially different, then creating a model for mound detection may have to use classification schemes and neighborhood sizes based on mound metrics acquired from the BE DEM and not from field survey because the model

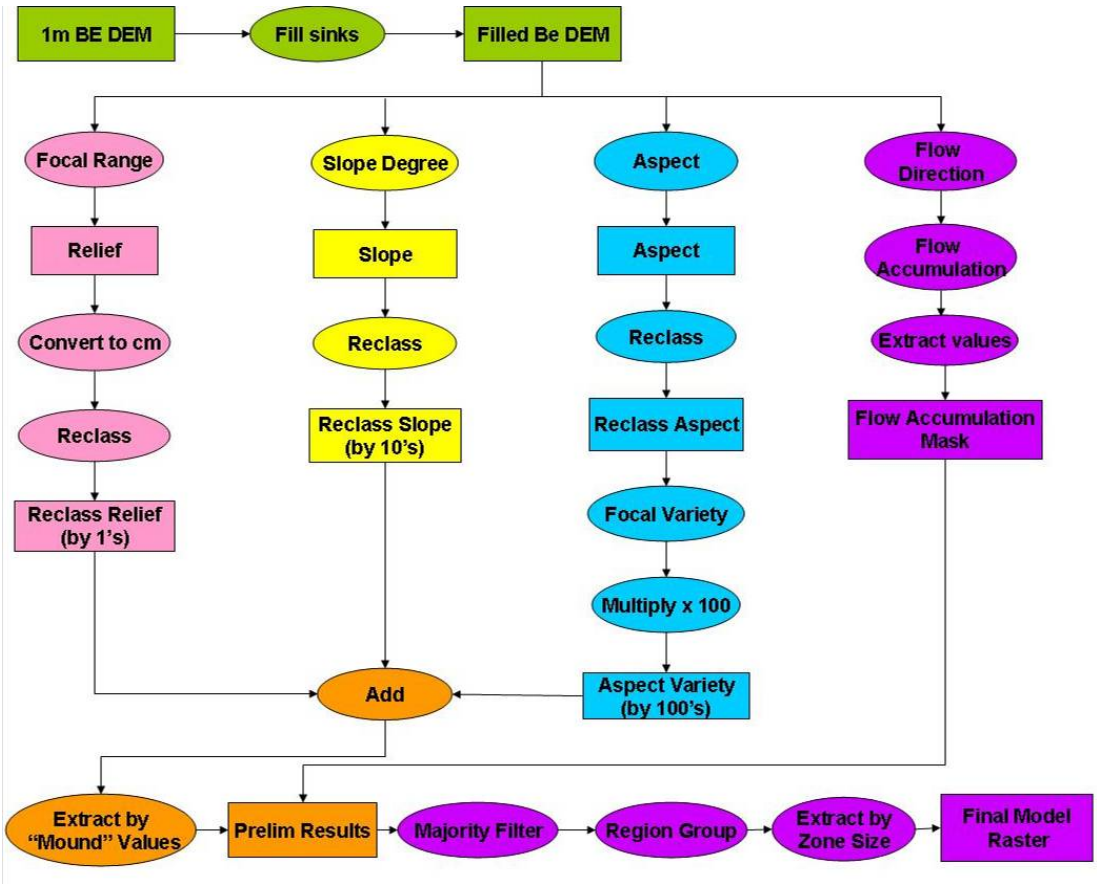

Figure 19. General framework of the mound detection model.

will be using metrics extracted from the BE DEM itself. The utility of field survey measurements is also important to other regions if they are to develop a similar mound detection model that fits the metrics of mounds in those regions.

Statistically exploring the differences between BE DEM and field measurements was precipitated based on professional, heuristic knowledge that field measurements can be subjective based on where the measurements were placed, how many measurements were taken for a single mound and method or precision of the measurement tool. Many times such details are not available in a report if a report is available at all. Field measurements can also differ because the edges of mounds are difficult to discern due to the gradual nature of the terminus to surrounding ground and heavy vegetation obscuring the view. Mounds are also exposed to looting, erosion, cultivation and excavations/backfilling which can change the measurements between mounds visits.

To empirically illustrate the extent survey measurements can differ between the same mounds at different times and by different people, a Wilcoxon matched-pairs signed rank test was conducted to compare diameter measurements between Ellison Orr's 1935-1939 surveys and Robert Petersen's 1983 survey (Table 1). Diameter measurements are less prone than height to change due to looting and partial excavation because those activities usually take place in the center of the mound. It would seem that if there is a chance of metrics matching between two surveys, it would be with diameter. Orr and Petersen's diameters of 30 conical mounds from Effigy Mounds National Monument were compared with the result that the measurements are not statistically the same with a very

small p-value of 0.0003 (Table 2). Some of the mounds had been subjected to looting and excavation/backfill with subsequent repair and restoration by the park between the two surveys; but other mounds that had not been disturbed or restored differed in diameter measurements by as much as 4 m. Orr's measurement precision of 0.5 ft (15 cm) compared to Petersen's 1-cm precision does not account for such large disparities in diameter measurements of undisturbed mounds.

Table 1. Mound diameter data from Orr and Petersen's surveys (Green *et al*. 2001).

Site	Mound Number	E. Orr 1930's Survey (m)	Petersen 1983 Survey (m)	Disturbance Between Surveys
13AM82	55	12.19	12.57	excavated center/restored
13AM82	56	7.62	5.49	looted/restored
13AM82	57	12.19	13.21	excavated/restored
13AM190	51	4.57	8.7	undisturbed
13AM190	50	4.57	8.36	undisturbed
13AM190	49	4.57	8.91	excavated/restored
13AM190	48	4.57	9	excavated/restored
13AM190	47	4.57	8.02	some restoration
13AM190	46	4.57	8.06	undisturbed
13AM190	45	4.57	7.9	partial excavation/restored
13AM190	44	4.57	7.9	partial excavation/restored
13AM190	43	4.57	7.03	partial excavation/restored
13AM190	42	4.57	7.56	partial excavation/restored
13AM190	41	10.67	7.78	partial excavation/restored
13AM190	40	4.57	6.7	some restoration
13AM190	37	4.57	5.1	restored
13AM190	36	6.1	5.8	restored
13AM190	35	13.71	13.4	restored
13AM190	34	10.67	11.82	some restoration
13AM190	33	15.24	16.85	excavated/restored
13AM190	38	6.1	6.73	partially excavated/restored
13AM190	39	4.57	5.75	partially excavated/some restoration
13AM206	17	9.14	9.15	partial excavation/restored
13AM207	18	13.72	14.5	partially excavated/backfilled/restored
13AM189	27	6.1	8.34	some restoration
13AM189	28	9.14	9.17	partially excavated/backfilled
13AM189	26	9.14	8.95	undisturbed
13AM189	25	9.14	9.92	restored
13AM189	24	9.14	8.82	restored
13AM189	23	6.1	7.31	undisturbed

Table 2. Results of Wilcoxon matched-pairs signed rank test for Orr survey mound diameter to Petersen survey mound diameter.

H_0: Ranked matched-pair differences are equal
H_A: Ranked matched-pair differences are not equal
W+ = 56.5
W- = 408.5
N = 30
p = 0.00003
Reject null hypothesis at 95% confidence level.

A Wilcoxon matched pairs signed rank test was then used to compare heights between the two surveys (Tables 3 and 4). The results failed to reject the null hypothesis that there is no difference in measurements at the 95% confidence level, although the small p-value of 0.05446 is weak. One of the pairs in the set differed by as much as 110 cm; none of the undisturbed mounds' paired measurements seem close either with differences from 54 to 77 cm. Like the diameter measurements, the disparity cannot be explained by difference in measurement precision.

The results imply that on a one-to-one comparison the field diameter measurements are not solid, heights are marginally reliable, and mound metrics, even in protected areas, are subject to change over a few decades. Although the measurements between each mound may be different, the set of diameter measurements taken as a whole may still have some value in determining an initial neighborhood size for focal statistics. The descriptive statistics of Orr and Petersen's diameter data are in enough agreement that an initial focal neighborhood can be determined for a 1-meter BE DEM (Table 5).

The descriptive data for height is not so clear-cut even though the pairs of measurements are not statistically different (Table 5). Using the range in Orr's dataset would create a much different threshold for low and high height values of a mound than Petersen's data. What needs to be considered is that many mound groups in Iowa that have documented measurements were reported by Ellison Orr 75 years ago and there have been no revisits since. Similar situations exist for other states regarding intensive mound surveys.

Table 3. Mound height data from Orr and Petersen's surveys (Green *et al*. 2001).

Site	Mound Number	E. Orr 1930's Survey (cm)	Peterson 1983 Survey (cm)	Disturbance Between Surveys
13AM82	55	61	105	excavated center/restored
13AM82	56	46	45	looted/restored
13AM82	57	61	115	excavated/restored
13AM190	51	99	45	undisturbed
13AM190	50	99	55	undisturbed
13AM190	49	99	55	excavated/restored
13AM190	48	99	55	excavated/restored
13AM190	47	99	65	some restoration
13AM190	46	99	45	undisturbed
13AM190	45	99	55	partial excavation/restored
13AM190	44	99	55	partial excavation/restored
13AM190	43	99	55	partial excavation/restored
13AM190	42	99	45	partial excavation/restored
13AM190	41	122	65	partial excavation/restored
13AM190	40	46	55	some restoration
13AM190	37	46	35	restored
13AM190	36	61	35	restored
13AM190	35	122	205	restored
13AM190	34	91	195	some restoration
13AM190	33	153	263	excavated/restored
13AM190	38	61	55	partially excavated/restored
13AM190	39	46	45	partially excavated/some restoration
13AM206	17	61	75	partial excavation/restored
13AM207	18	122	105	partially excavated/backfilled/restored
13AM189	27	61	45	some restoration
13AM189	28	91	65	partially excavated/backfilled
13AM189	26	122	45	undisturbed
13AM189	25	76	55	restored
13AM189	24	76	55	restored
13AM189	23	61	35	undisturbed

Table 4. Results of Wilcoxon matched-pairs signed rank test for Orr survey mound height to Petersen survey mound height.

H_0: Ranked matched-pair differences are equal
H_A: Ranked matched-pair differences are not equal
W+ = 326.5
W- = 138.5
N = 30
p = 0.05446
Fail to reject null hypothesis at 95% confidence level.

Table 5. Descriptive statistics of the Orr and Petersen survey datasets.

	Orr Survey Diameter (m)	Petersen Survey Diameter (m)	Orr Survey Height (cm)	Petersen Survey Height (cm)
MEDIAN	6.1	8.35	95	55
MEAN	7.52	8.96	85.87	74.27
MIN	4.57	5.1	46	35
MAX	15.24	16.85	153	263
s.d.	3.39	2.78	27.78	54.28

Relying solely on historic field surveys may not be ideal for creating a classification scheme for height measurements derived from modern BE DEMs because archaeological site taphonomic processes that have taken place since the 1930's or even earlier are not considered. More recent surveys are not entirely immune from scrutiny as Petersen's data for mounds 33, 34 and 35 are questionable (Table 3). The three mounds are "restored" to heights much taller than Orr's 1930's data while most of the other restored mounds are still shorter than the earlier survey's measurements. This may be a rare case where human disturbance actually increased a mound's height rather than depleted it.

Using metrics from BE DEM data to determine a classification scheme and focal neighborhood size may be preferable because the data is recent and the outer edges of the

mounds are easy to determine using profile graphs from the BE DEMs with vertical exaggeration applied. To see if there is a difference in more recent survey data and BE DEM data, height and diameter of conical mounds were sampled from the Slinde Mound Group and Effigy Mound National Monument that have measurement data from field visits within the last 25 years. A second set of measurements were taken from the BE DEM of the same mounds using several profile graphs for each mound as an aid in determining summits and horizontal extents of mounds.

A Wilcoxon matched-pairs signed rank test was used to determine if the differences in BE DEM and field diameter measurements are significant (Tables 6 and 7). The analysis concluded at the 95% confidence interval that there is a difference between mound diameter expressed on a BE DEM and field measurements. This is not unexpected considering the subjective nature of determining an edge in the field, especially with low-relief mounds in heavy vegetation. The other factor may be that even though using BE DEMs provide the luxury of viewing vertically exaggerated profiles, the profile graphs are interpolated curves that connect interpolated elevation values at each 1-meter horizontal interval. Rather than ruminate on which dataset to use based on a mound-to-mound comparison, descriptive statistics of the datasets as a whole were compared to see if both datasets would agree on a focal statistic neighborhood (Table 8). The descriptive statistics of the BE DEM dataset and recent field survey dataset are actually a closer match than between the datasets of Orr 1930's and Petersen 1983 field surveys. The mean diameter and standard deviation of both datasets would support the assertion that a 5 or 6 m radius circle neighborhood may be a good starting point in the modeling process

for focal statistics. An 8 or 9 m radius circle neighborhood, which would cover the large, outlier mounds, is too inclusive of surrounding microtopography for the mound model considering the large number of mounds in the sample is 10 m diameter or less.

Table 6. Height and diameter data from BE DEM and field surveys from 1983 and 1987 (Stanley and Stanley 1989, Green *et al.* 2001).

Site	Mound Number	BE DEM Diameter (m)	Field Diameter (m)	BE DEM Height (cm)	Field Height (cm)
13AM120	4	10	8	60	60
13AM120	5	9	8	30	30
13AM120	6	15	16	65	70
13AM120	9	9	8	45	40
13AM120	10	11	8	90	100
13AM120	11	11	12	60	60
13AM120	12	10	10	66	80
13AM120	13	11	9	52	50
13AM120	16	8	8	55	60
13AM120	17	10.5	10.5	108	100
13AM120	18	11	11	72	80
13AM120	2	5	5	34	40
13AM82	55	16.5	12.57	104	105
13AM82	56	10	5.49	95	45
13AM82	57	13	13.21	100	115
13AM82	61	11	10.8	58	95
13AM190	51	8	8.7	41	45
13AM190	50	8.7	8.36	57	55
13AM190	49	8	8.91	77	55
13AM190	48	7.4	9	71	55
13AM190	47	8	8.02	52	65
13AM190	46	9	8.06	44	45
13AM190	45	9	8	57	55
13AM190	44	8.4	7.9	60	55
13AM190	43	7	7.03	71	55
13AM190	40	8	6.7	45	55
13AM190	37	5.35	5.1	32	35
13AM190	36	7	5.8	47	35
13AM190	35	14	13.4	142	205
13AM190	34	13	11.82	150	195
13AM190	33	16	16.85	213	263
13AM190	38	6	6.73	45	55
13AM190	39	8	5.75	47	45
13AM206	17	10	9.15	74	75
13AM207	18	14.3	14.5	104	105
13AM189	27	9	8.34	67	45
13AM189	28	10	9.17	73	65

Table 7. Results of Wilcoxon matched-pairs signed rank test for BE DEM diameter to recent field survey diameter.

H_0: Ranked matched-pair differences are equal
H_A: Ranked matched-pair differences are not equal
W+ = 326.5
W- = 131.5
N = 32
p = 0.01358
Reject null hypothesis at 95% confidence level.

Table 8. Comparison of descriptive statistics for BE DEM and recent field survey.

	BE DEM Diameter (m)	Field Diameter (m)	BE DEM Height (cm)	Field Height (cm)
MEDIAN	9	8.36	60	55
MEAN	9.87	9.27	71.97	75.49
MIN	5	5	30	30
MAX	16.5	16.85	213	263
s.d.	2.79	2.91	36.57	49.62

Results of a Wilcoxon matched-pairs signed rank test between BE DEM height and recent field height measurements failed to reject the null hypothesis – the height measurements from the field and the BE DEM are not statistically different (Table 9). The high p-value of 0.42 indicates that rejecting the null leaves a high probability of committing a Type I error. Comparing the descriptive statistics of both datasets shows a clear agreement of the lower threshold that a mound height classification scheme might take (Table 8).

As with diameter, the maximum height value in both datasets is from a mound that is considered a rarity in Iowa. Large mounds like #33, which is at least 2 m (6.6 ft) high and 16 m (52 ft) in diameter, in Iowa were discovered in the mid to late 1800's and generally

Table 9. Results of Wilcoxon matched-pairs signed rank test for BE DEM height to recent field survey height.

H_0: Ranked matched-pair differences are equal
H_A: Ranked matched-pair differences are not equal
W+ = 249.5
W- = 345.5
N = 34
p = 0.4167
Failed to reject null hypothesis at 95% confidence level.

are well-documented and in protected areas or they were completely destroyed by excavations or intensive cultivation in the 1800's and early 1900's. It is highly unlikely that any more mounds this large are undiscovered. An upper limit of one standard deviation above the mean would be a more restrictive range which would be 109 cm from the BE DEM dataset and 125 cm from the recent field survey dataset. Because there is some gray area between BE DEM and field survey, a conservative upper limit for the "mound" class was created by using a rounded value of 110 cm. A second class including the datasets' values two standard deviations above the mean was created as a "possible mound" height and monitored throughout the model testing process to see if any values in that class range add more detected mound cells on real mounds without creating more false-positives. Large mounds would still be detected using a conservative height classification scheme because if the focal neighborhood is 10 m diameter, the large mound's relief within that window will likely be under 200 cm because the neighborhood will not cover the entire mound.

The demonstration of the efficacy of using survey data to establish parameters for a

mound detection model using a BE DEM concluded that using historical survey data may not be optimal, but using recent survey data is fine. The Orr 1930's dataset statistically differed with a more recent survey of the same mounds in diameter; and the heights failed to reject the null with a weak p-value so there is some gray area of whether these height pairs are considered a match. When comparing the descriptive statistics of Orr and Petersens' surveys to BE DEM and recent surveys, the BE DEM was in more agreement with the recent surveys than the Orr survey to the Petersen survey for both height and diameter. The differences in measurements of the same mounds between 1930's data and 1983 data can not be fully explained by taphonomic processes at work on the mounds because measurements of undisturbed mounds were different as well. Subjectivity in field measurement methodology cannot be ignored; even the time of year would have an effect on the amount of vegetation concealing the edges of mounds.

The model in this research uses measurements from the BE DEM itself in regard to aspect, slope and height; and the BE DEM mound heights are statistically no different than recent field surveys. In light of this, it is not unreasonable to conclude that deciding upon a classification scheme from a sample of mound heights taken from the BE DEM is just as effective as using more-recent field survey data and is preferable over old survey data. The agreement of diameter descriptive statistics at one-meter precision would also suggest that setting neighborhood sizes by BE DEM data is appropriate as well. It is common for large regions not to have recent mound surveys, or enough mound data to be considered a good sample, because funding is limited and is usually spent on extraordinary mound assemblages such as Effigy Mound National Monument or groups

getting nominated for the National Register of Historic Places such as Slinde. This exploration of BE DEM data demonstrates that obtaining samples for classification schemes and focal neighborhood sizes from BE DEMs is a viable option for areas with unreliable or sparse field data. The main drawback to this method is that in order to get diameters and heights from BE DEMs a profile tool available with the ArcGIS 3D Analyst extension was used, requiring an additional purchase of software beyond ArcGIS and Spatial Analyst extension. The zonal statistics tool in Spatial Analyst was not used to extract elevations because the edges of the mounds are difficult to see on a shaded relief image thus impeding the ability to place accurate zone boundaries around the mounds. The measurement tool was also not used to find diameter for the same reason.

3.3.2 Preparing the BE DEM

The interpolation process in creating a BE DEM inevitably causes spurious sinks (Maune *et al*. 2007). While assessing the data in the Slinde Mound Group area, patches of noisy areas were highly visible on an aspect image. A sink function revealed hundreds of small artificial sinks in a relatively small analysis extent (Figure 20). After extracting the BE DEM by the area of interest (AOI), the Fill function is the first function used before any more analysis is done (Figure 21). This removed some of the noise, but other noisy areas remain due to residual vegetation points creating small bumps or rough patches on the BE DEM.

3.3.3 Height variable

Height is determined by the difference between the minimum and maximum elevation

values (range) within a designated neighborhood (Figure 22). A circle neighborhood with 5 m radius was initially chosen because the mean and median for mound diameter taken from the BE DEMs are 9.87 m and 9 m respectively and recent field survey data also suggests that this is a good neighborhood size. This creates a window that would completely cover a 10 m mound and most area of larger mounds. Different filter sizes and shapes were tried, with 5 m radius circle being most selective of mounds without including too much non-mound area.

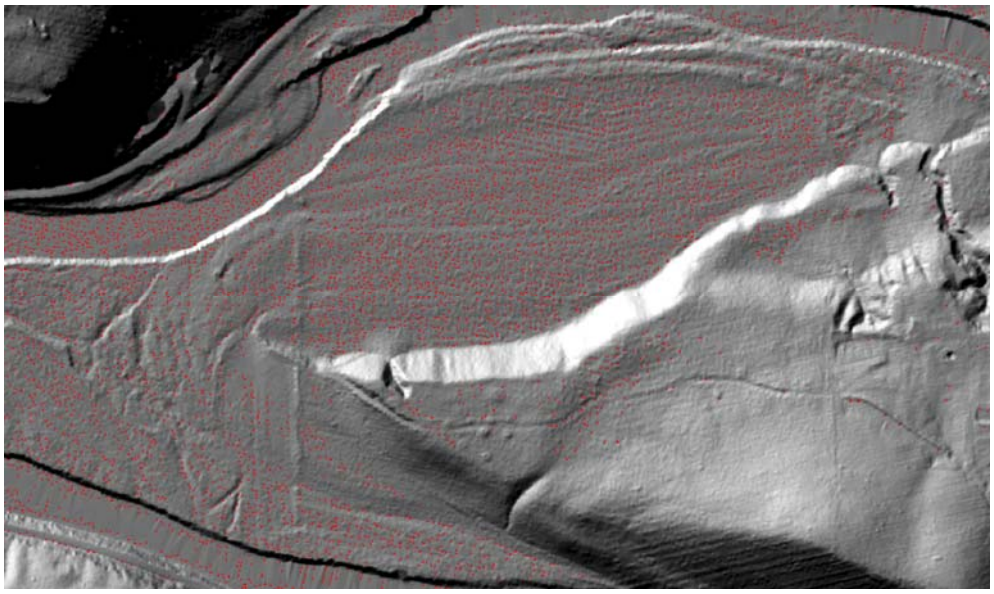

Figure 20. All the cells in red are detected sinks. These must be filled in order to have a cleaner final raster.

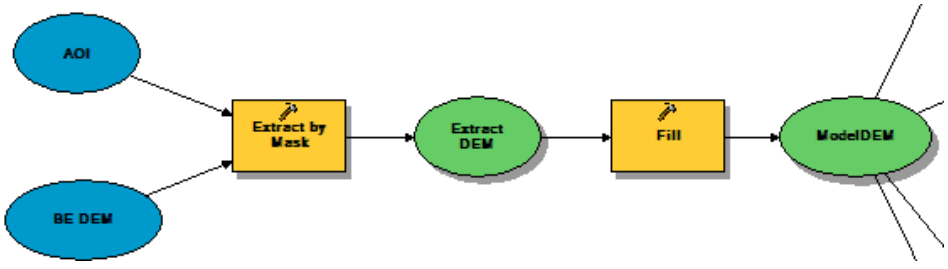

Figure 21. First segment in mound detection model clips BE DEM to area of interest (AOI) and fills spurious sinks.

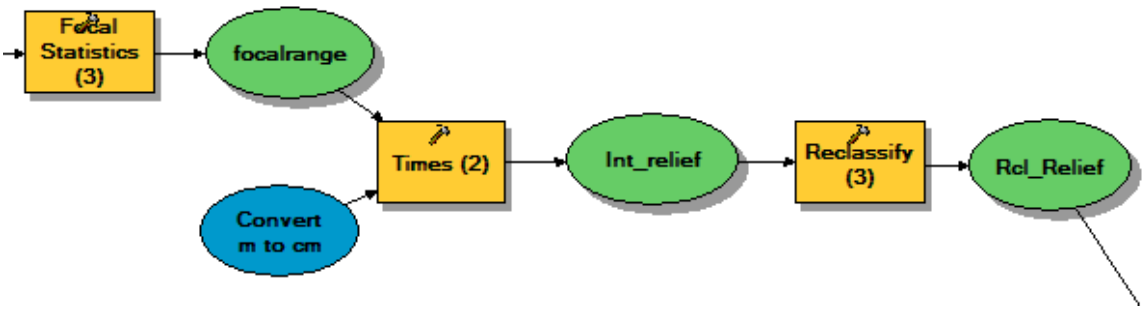

Figure 22. Relief segment in mound detection model.

In order to reclassify the values, the ranges were converted to integers by multiplying the focal range values by 100 (Figure 23). The height values were reclassified as follows:

0 – 30 cm = 0
30 – 110 cm = 2
110 – 200 cm = 1
200 – 1000 cm = 0

The upper limit of "old values", 1000 cm, was assigned arbitrarily as a large number so high relief in the analysis neighborhood would not be beyond the extent of the reclassification values. Ten meters was sufficient for all areas where the model was tested. The break-off value of 110 cm between class 1 and 2 is the height one standard deviation above the mean of BE DEM height values. This reclassification assignment is not firm, but more data is needed from detected mounds to determine what the upper limit of '2' values should be and what values to assign to 0. It is anticipated that the '1' class eventually will not be needed.

3.3.4 Slope variable

Slope for the model is calculated in degrees and reclassified according to a set of values that were queried directly from the slope raster (Figure 24). The slope of a mound is depicted as annuli, or "C"-shapes on the slope rasters created from the BE DEM;

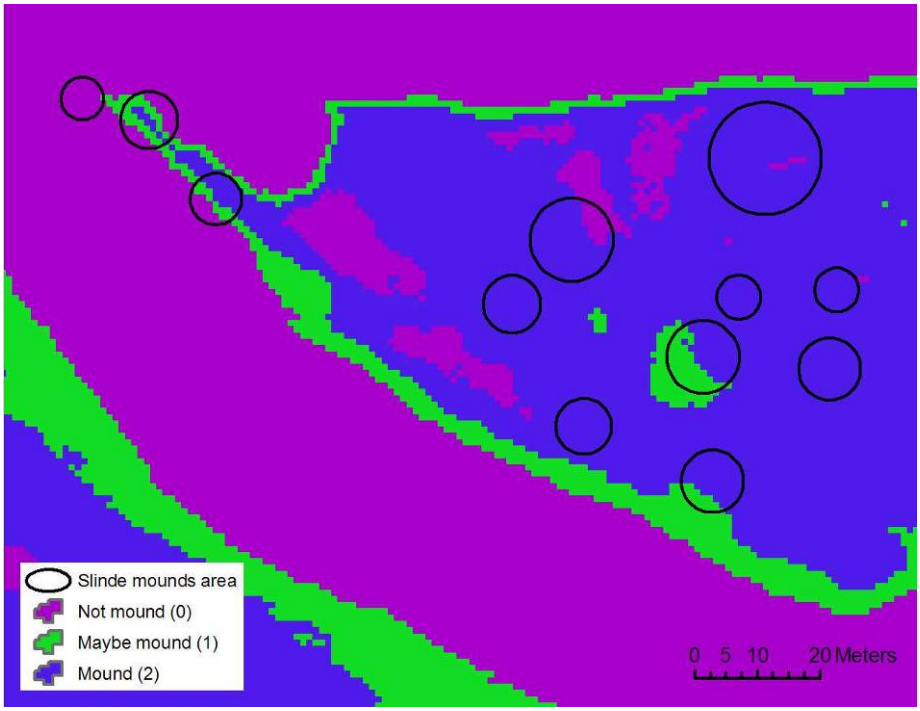

Figure 23. Reclassified relief over a portion of the Slinde Mound Group.

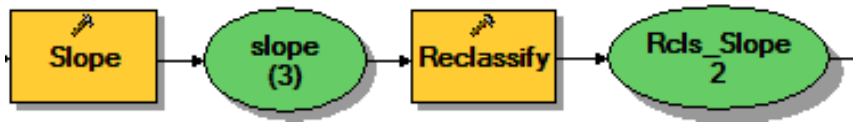

Figure 24. Slope segment of the mound detection model.

selecting the mound slope values differentiated from ground was not difficult (Figure 25). Slope values were reclassified as:

0 - 5° = 20
5 - 12° = 30
12 - 90° = 10

Like height, the range for value 20 will be monitored for appropriate break-off between values reclassified as 20 and 30 (Figure 26). If too many mounds are unmarked because they failed the slope test, then modifications to the classification regime may be required.

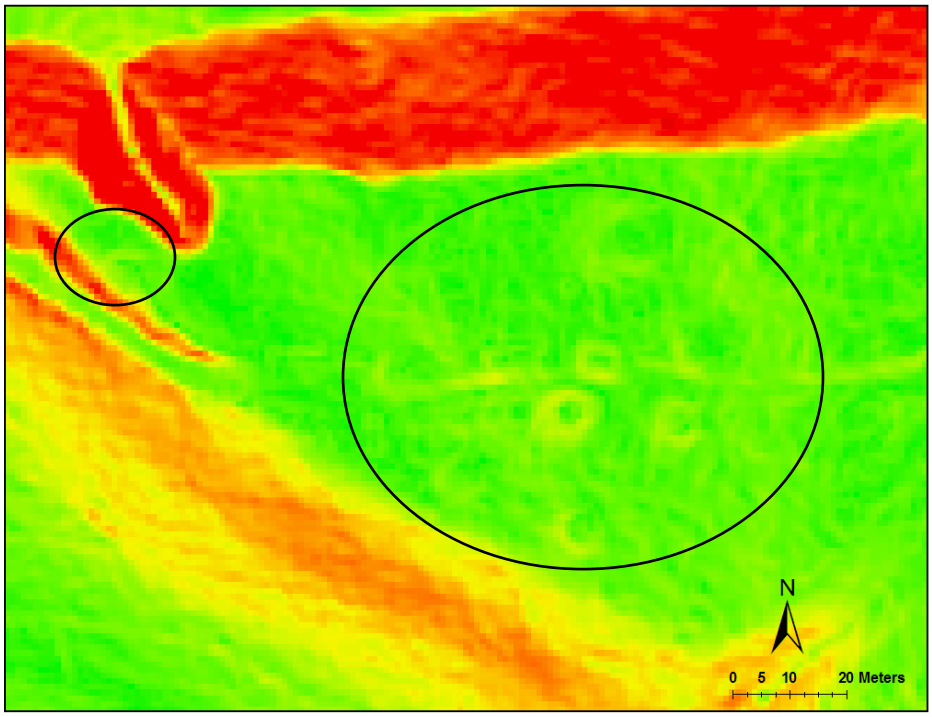

Figure 25. Local, steeper slopes from mounds generally are identifiable from the mound centers and surrounding ground in a slope raster.

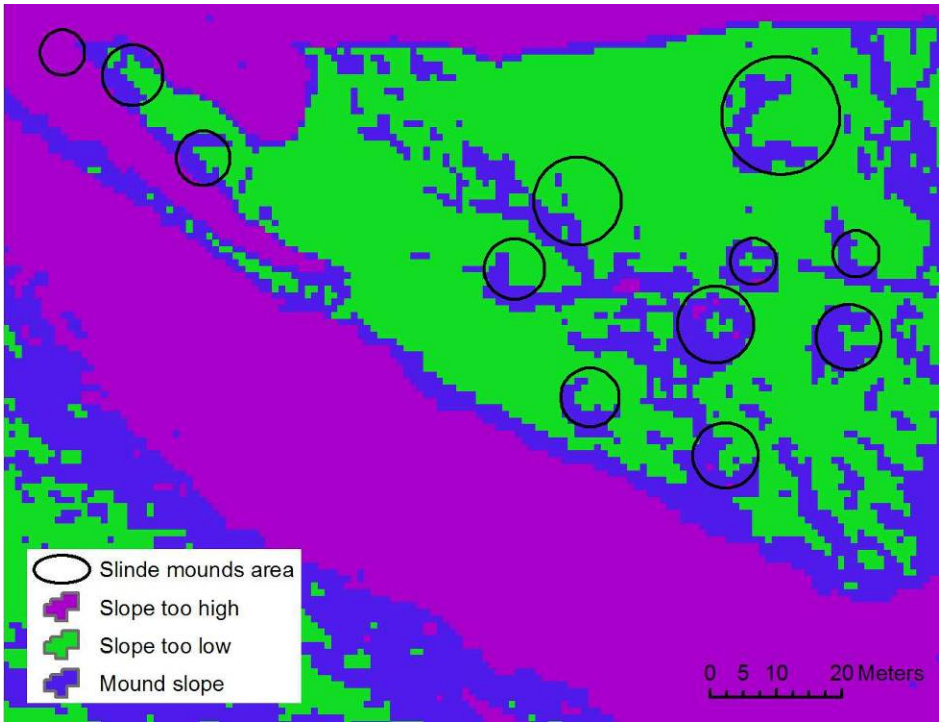

Figure 26. Reclassified slope over a portion of the Slinde Mound Group.

3.3.5 Aspect variable

The aspect raster was reclassified from degree values to 1 – 9; flat (-1) was assigned to 1, north (0 – 22.5° and 337.5 – 360°) assigned to 2, northeast values to 3 and so on clockwise (Figure 27). Then to highlight the mound's uniqueness of all aspects within a small area, variety was calculated with a 6 m radius circle neighborhood. The larger neighborhood for aspect was necessary for obtaining a good overlap between aspect variety and the mounds' slope. The resulting numbers 1 – 9 reflect the number of different reclassified aspect values that was found within the neighborhood. An ideal number for a mound would be 7 or 8; 9 would have included flat areas which are not indicative of a domed-shaped mound. The aspect variety file was then multiplied by 100 and the result was used in the final model calculation (Figure 28).

3.3.6 Flow accumulation and variable compilation

Flow accumulation is a function that uses elevation values to approximate the flow of water by producing a raster with values that are totals of upslope cells that are "draining" into each cell. If an elevation is higher than all of the neighboring elevations no water would accumulate in that high point, it would shed it off and the cell accumulation value at that high point would be zero. The next cell downslope would accumulate the cell upslope to it and have a value of 1 and so on. Mounds approximate a dome shape where the center of the mound is highest and radially slopes downward. A flow accumulation raster would assign the highest cell in the center with a value of zero because no other cells are draining into it. The edge of the mound would have a flow accumulation value of all the cells from the center to the edge as the mound surface slopes down- and

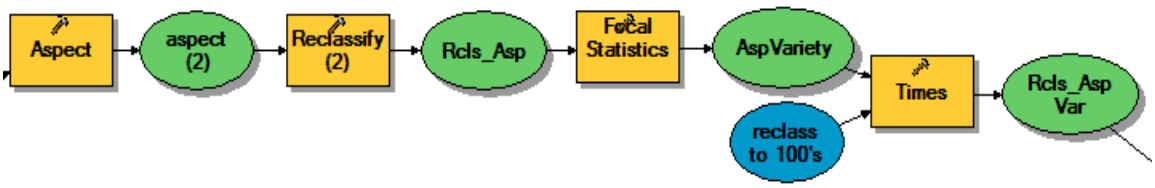

Figure 27. Aspect segment of the mound detection model.

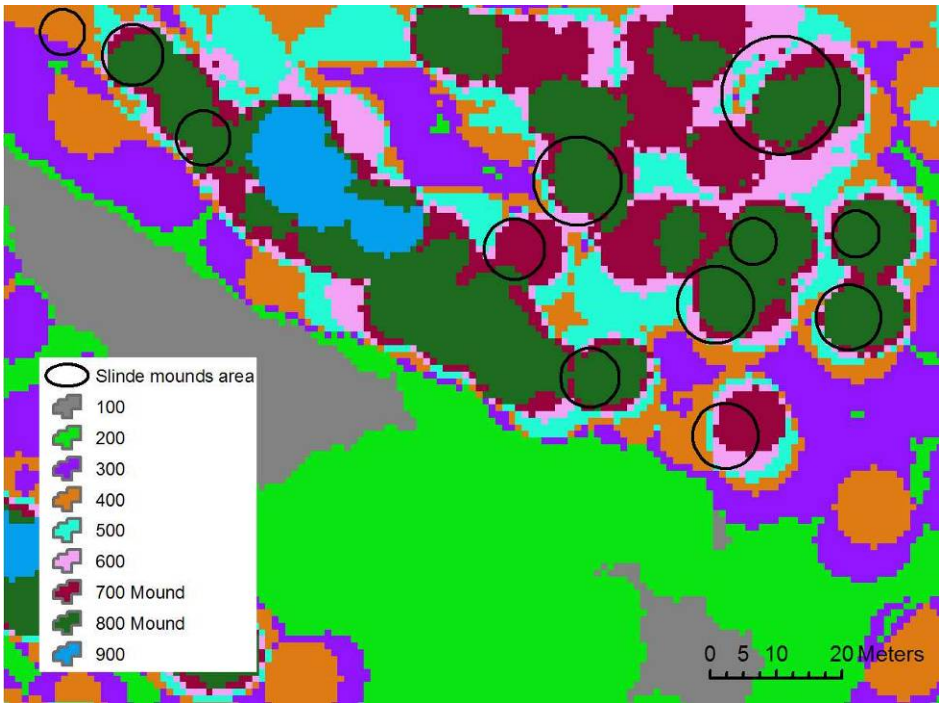

Figure 28. Reclassified aspect variety over a portion of the Slinde Mound Group.

outward. For example, a mound with 10 m diameter would have flow accumulation values of 0 – 5 along its radius from center to edge. After flow accumulation was calculated, the raster's values 0 – 5 seemed to represent mounds the best regardless of the turbation issues previously mentioned, but there were many areas within this range (Figures 29 and 30). The most effective way to use this variable was to mask out the cells in the model results that lie in flow accumulation areas greater than 5. This eliminates spurious "detected mound" cells that are in a bowl-like, microtopographic feature that

may have a pour point on one side but still have similar relief and aspect variety as a mound within the focal neighborhood in addition to similar slope.

To create the mound model results the three final variable files – reclassified slope, aspect variety and reclassified relief – were added resulting in a raster with 81 values (Figure 31). The values that were the most unique to the mounds, 832, 732, 831, and 731

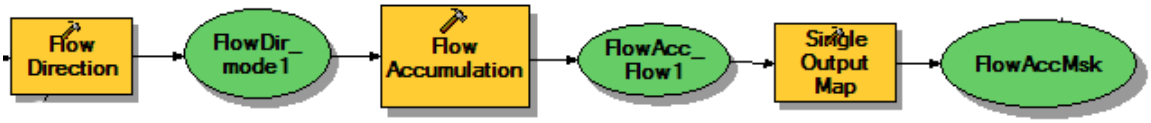

Figure 29. Flow accumulation mask segment of the mound detection model.

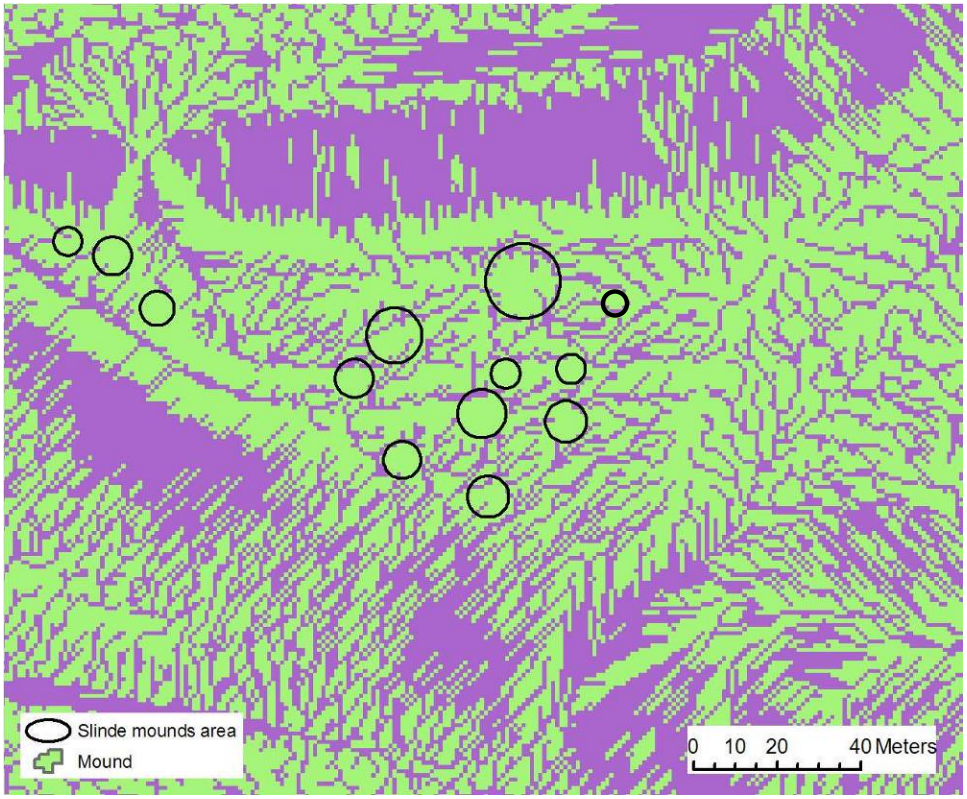

Figure 30. Green cells signify flow accumulation of 5 cells or less. Most cells within mound boundaries are in this category.

were extracted and used as the mound model raster with all other values changed to NoDATA (Figure 32). The flow accumulation mask was applied during this operation, masking out any cells where flow accumulation exceeds 5 cells.

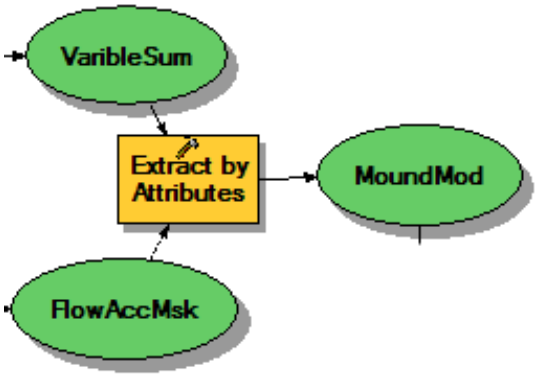

Figure 31. Mound value extraction segment of the mound detection model.

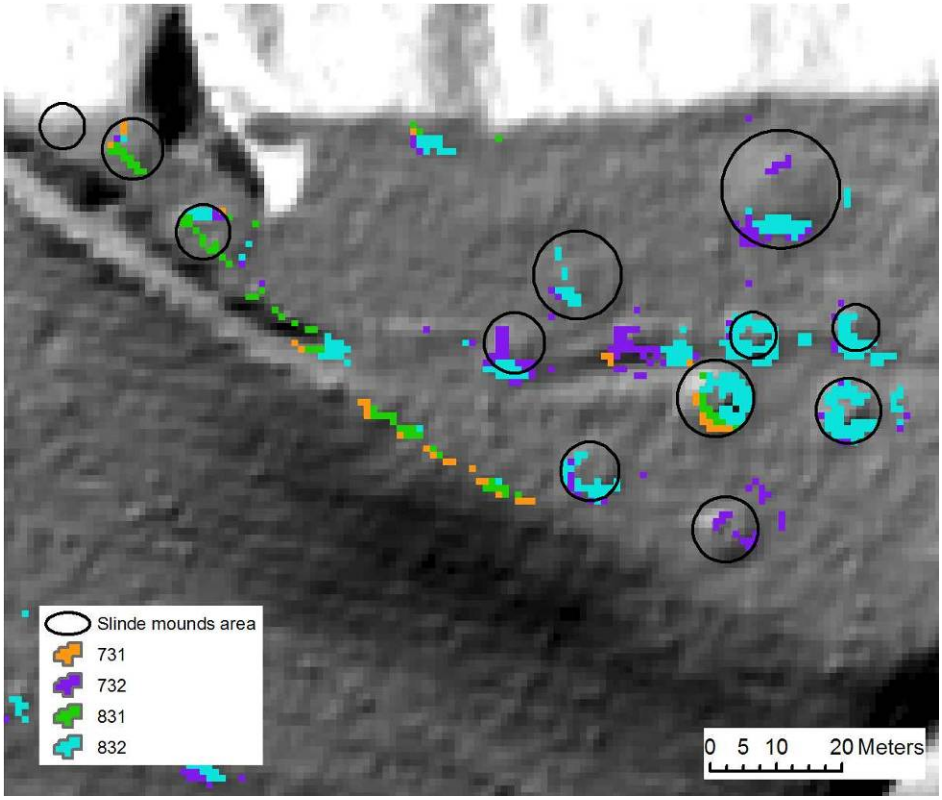

Figure 32. MoundMod raster over a portion of the Slinde Mound Group.

3.3.7 Model clean-up

Many false-positive cells remain in the MoundMod raster which require some method of semi-automated clean-up (Figure 33). The mound raster was reclassified into a single-valued raster, and then the Majority Filter tool was applied. The settings for the filter are to check the eight nearest neighbors of the cell in question (a 3 x 3 window) and the cell is replaced if five out of the eight neighbors have the same value, including NoData cells (Figure 34). The purpose of the Majority Filter is to remove thin strings of cells lining stream banks, bluffs and terrace edges and single cells scattered throughout the AOI. The second purpose is to fill in large zones of mound cells that may have sporadic NoData cells within the zones. Only one Majority Filter pass is appropriate because additional passes will start to whittle away at the "C" shaped cell groups marking a mound.

The result of the Majority Filter is then region grouped using four nearest neighbors; each resultant zone's cell count represents the area because the raster has 1 m cells. Zones with counts (area) too low to be included in the final model raster are excluded, leaving a raster with clustered "mound" cells. The low area threshold was set at 10 m^2; any region below ten cells is discarded with the Extract by Attributes tool. More data from model results on field-confirmed mounds is needed to determine an upper limit that will not erroneously delete a strongly-marked mound. The new raster is reclassified to a single value then converted to a polygon shapefile to facilitate manual clean-up and enhance visibility with thick polygon boundaries (Figure 35).

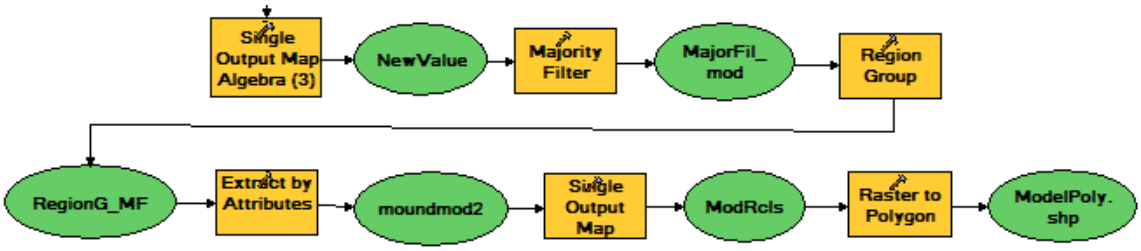

Figure 33. Clean-up segment of the mound detection model.

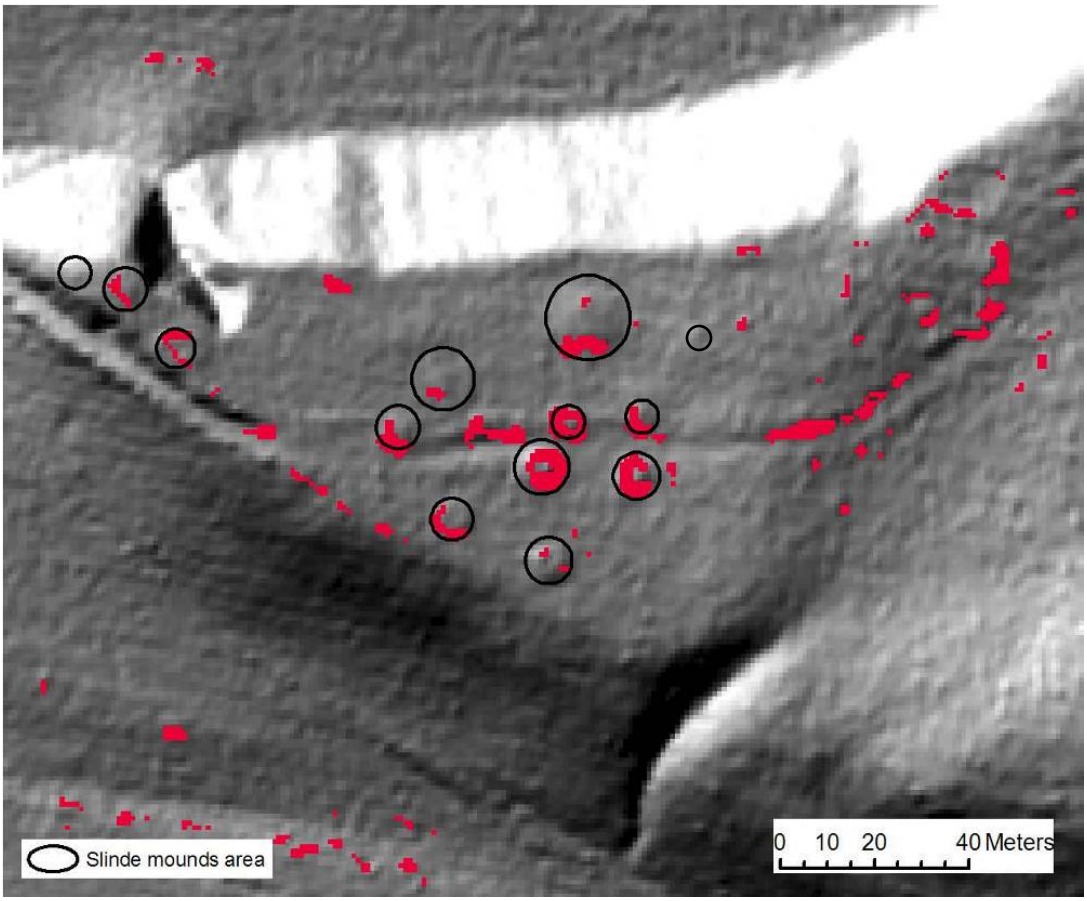

Figure 34. Majority Filter raster over a portion of the Slinde Mound Group.

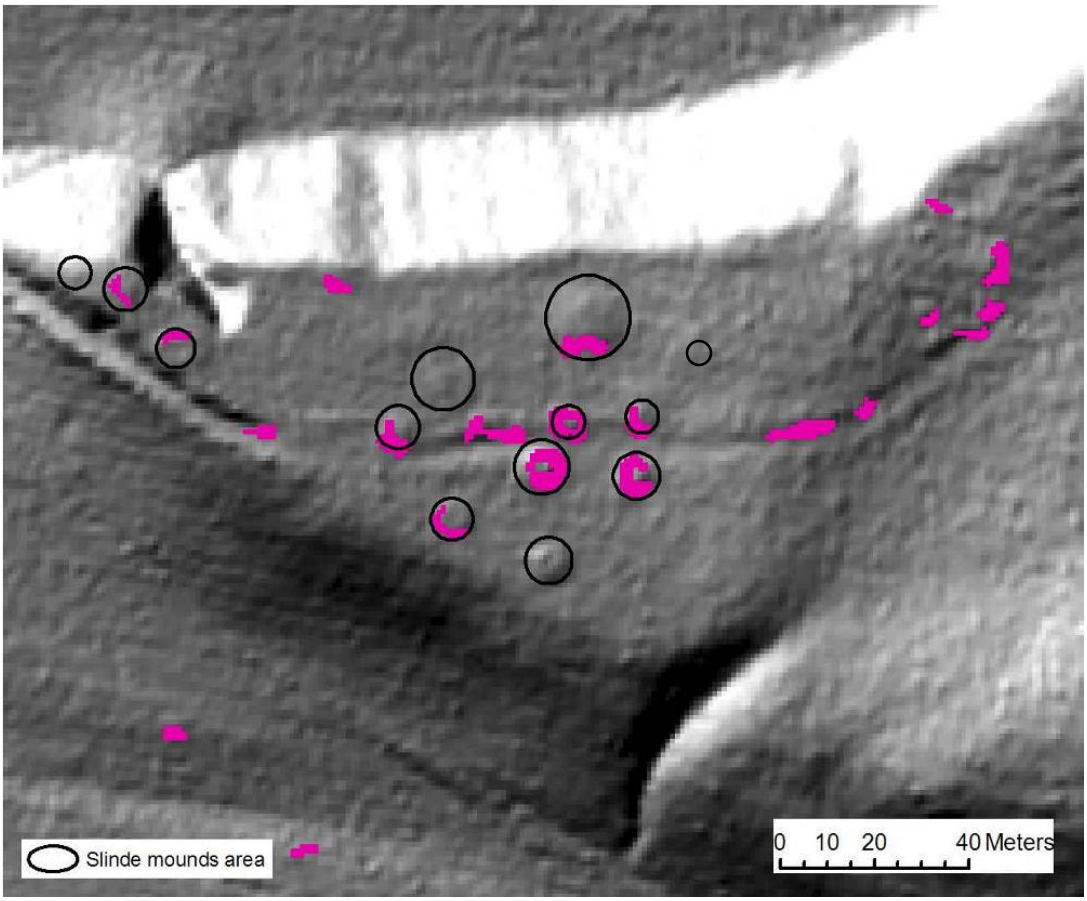

Figure 35. Final model raster over a portion of Slinde Mound Group after Region Group and Extract by Attributes tools were applied.

CHAPTER 4: ANALYSIS RESULTS

4.1 Slinde Mound Group Results

Several trials were run on Slinde using different focal neighborhood sizes and shapes, and testing different settings for Majority Filter and Region Group functions for the clean-up portion (Figure 36, Table 10). Each change in the process was assessed for how many true mounds were kept in the detection model versus how many spurious cells were eliminated. When each segment was to satisfaction, all the components were assembled together in ModelBuilder. After a model was developed that detected the most mounds with the least number of false-positive cells at the Slinde site, it was ran at the Effigy Mound area. Fine-tuning the model involved switching back and forth primarily between Slinde and Effigy Mound area, but each time a major change was made to the model the previous AOIs were retested. The running time at Slinde for the final, full model, from clipping the DEM to results converted to vector, was just under five minutes for an area of 4.93 km^2. After reviewing the model results, a road centerline buffer was used to remove erroneous positive mound polygons from the roadsides. The remaining model polygons represented only 0.4% of the total AOI; of the 0.4%, 2% are true mound positives (Figure 37).

Out of the 16 mounds mapped from the Stanley (1987) field visit of the Slinde Mound Group, 10 were marked in the final model results (Figure 38, Tables 11 and 12). Out of the six not detected, two were visible from a shaded relief image; the other four were only known for sure by using the field map. Another site (13AM129) in the Slinde AOI

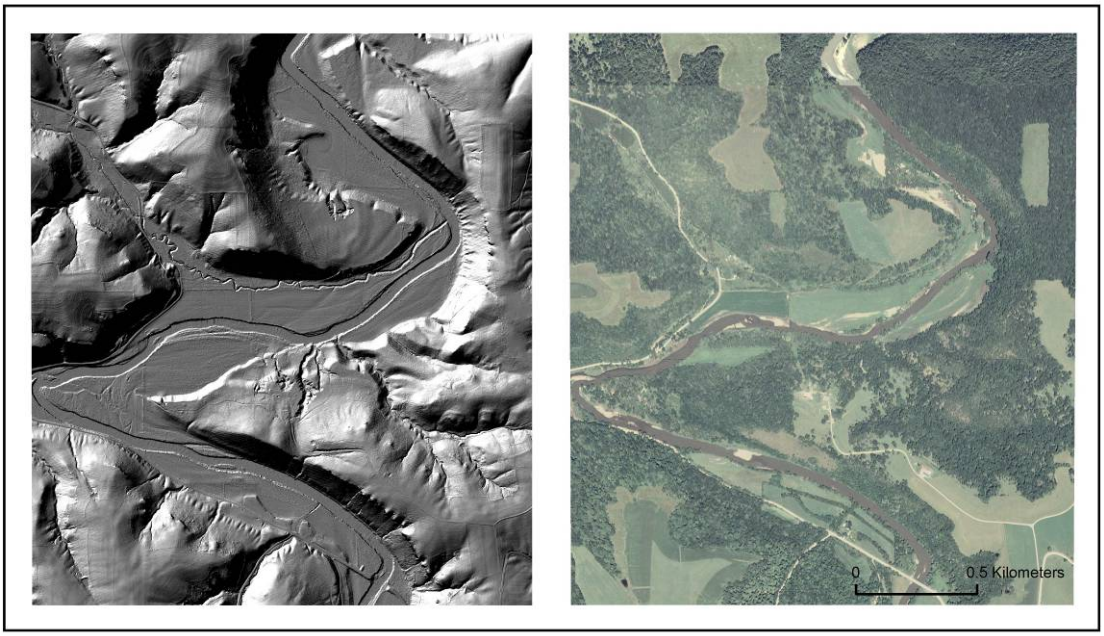

Figure 36. AOI of the Slinde Mound Group test. Left image is BE DEM shaded relief, right image is 2008 NAIP true color imagery to show vegetation cover.

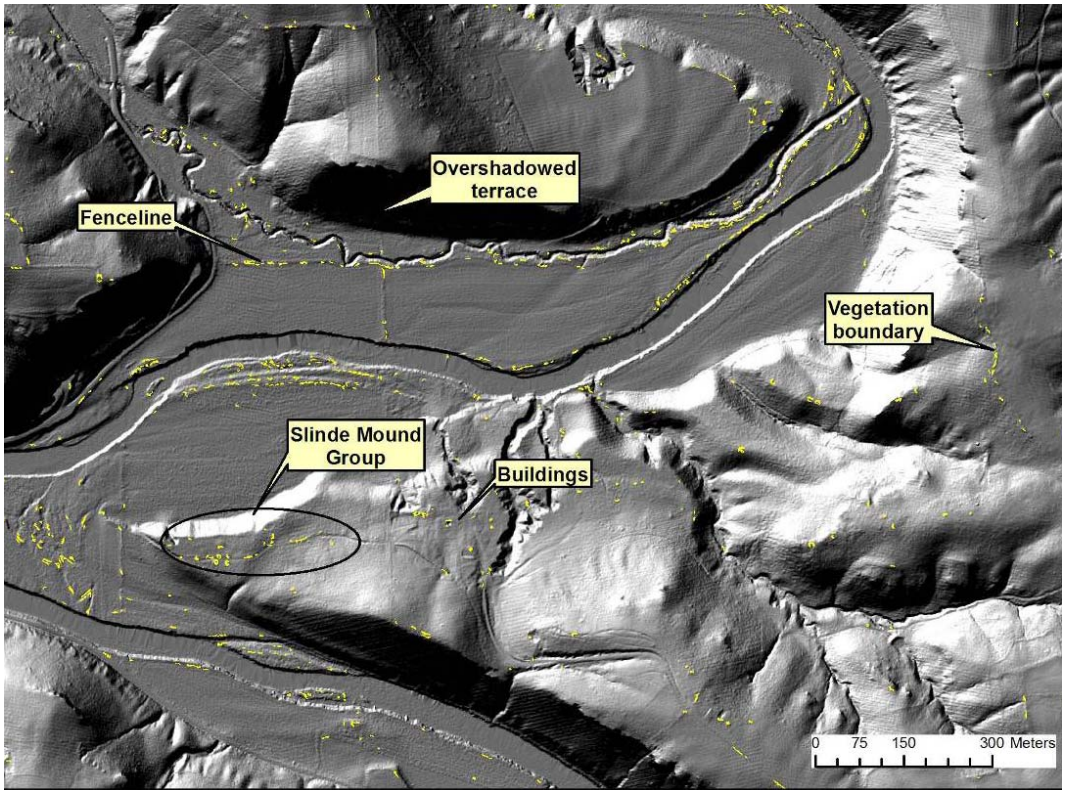

Figure 37. A portion of the Slinde test results, model positives shown in yellow.

Table 10. Trials of mound detection model development and results.

Trial	Test Comments	Conclusions	Cell/Mound Count
1 Slinde (incl. site north of group)	5 m radius focal neighborhood for height and aspect variety; upper cut-off for mound height (class 2) at 145 cm - two standard deviations above mean from BE DEM sample.	Height class 2 is too inclusive of non-mound features.	Common mound value = 832 and 732; total # positive cells in mound model results = 49,221 (1% of AOI); # mounds detected 13/17
2 Slinde	5 m radius focal neighborhood for height and aspect variety; upper cut-off for mound height (class 2) at 110 cm - one standard deviation above mean from BE DEM sample.	No difference in total pixels in detected mound raster, just decreased how many total pixels are class 2 vs class 1, no marked difference with detected mounds. Does height matter to the model at all?	Common value = 832 and 732; total # cells = 49,221 (1% of AOI); # mounds detected 13/17
3 Slinde	No height variable in model; aspect variety reclass to 10's, slope in 1's; extracted "mound" values 73, 83, 72 and 82.	What a disaster. Large number of false-positives, one mound actually dropped from detection. Height variable has great significance in decreasing # of cells in model results.	Common value = 82; total # of cells = 691,844 (14% of AOI); # mounds detected 12/17
4 Slinde	Noticed best slope value 30 expresses as annuli on raster where slope is steepest on mound which is away from near-flat centers; good slope has trouble with overlapping good height and aspect variety towards mound centers. Used 5 m majority filter with 2 m annulus to try to expand good slope rings into good height and aspect var. areas. Height and aspect settings same as trial 2.	Majority Filter w annulus neighborhood generalized the slope reclass raster but did not increase overlap with good height and good aspect var. Actually decreased the number of good slope cells on some mounds. Decreased total cell count but a lot of NoData values in majority-annulus filter slope raster. Increased zone size of mound model cells on some mounds.	Common value = 832; total # cells = 23,931 (.48% of AOI); # mounds detected 12/17
5 Slinde	Tried to shift good slope raster 5 m to force more overlap with good aspect var. and height.	Made groups of mound model cells over mounds thicker but also made strings of cells at stream banks and tree lines thicker too. Did not like that one side will not have 5 m swath in final model.	Common value 832 and 732; total # cells = 52,699 (1.07% of AOI) ; # mounds detected 12/17

Trial	Test Comments	Conclusions	Cell/Mound Count
6a Slinde	Buffered good slope zones greater than 10 cells by 2 m; tried extracting "good" zones by roundness (used roundness equation) to decrease long strings of stream bank and vegetation line false positives.	Buffer is too big will cause too many false positives just to get more overlap with aspect var.; roundness does not work, zones of true mound cells can be narrow too. Single cells are very "round". Raster format creates boundaries that are too jagged for equation to work properly. Finding a roundness threshold that will work everywhere is impossible.	total # cells = 36,817 (.75% of AOI)
6b Slinde	Introduced flow accumulation mask to model results in Trial 6a.	Flow accumulation mask works to get rid of false-positives.	total # cells = 30,952 (.63% of AOI)
7 Effigy	Used Trial 2 height classification and 5 m radius neighborhood for height and aspect var.; added flow accumulation mask to model; no extra processing to good slope.	Mounds of all types were detected - area tested conical, effigy, linear, compound; classification scheme works here and at Slinde.	Common value 832 and 732; total # cells = 30,137 (1.03% of AOI); mounds detected 50/53
8a Effigy	Begin to build clean-up segment of model; test Majority Filter Tool vs. Region Group and select all but smallest zones; first test region group on results of Trial 7.	RG with 8 neighbors, zone grouping within; result 5324 zones; Extract by Attributes zones w Count >7 (leaving out zones 9- and 10-cells big were eroding from the detected mounds. This method left much cleaner model and still detected mounds).	total # cells = 19,807 (.68% of AOI)
8b Effigy	Used filter to get rid of small zones of mound model cells using Majority Filter tool, all combinations of neighbors and replacement thresholds were compared; tested on results of Trial 7.	8 neighbors/HALF: 16,953 cells left - takes away from mounds too; 4/HALF: 20,236 cells, leaves many small spurious zones; 4 neighbors/ MAJORITY: 20,236 cells; 8/MAJORITY: 19,127 cells. Nearly identical results than region group/select method except more, small, spurious zones. Did fill in conical mound areas.	total # cells = 19,127 (.65% of AOI)
8c Effigy	Tried Region Group on 8b results to get rid of small, spurious zones; could increase zone size to leave behind because zones over mounds are larger from Majority Filter.	Did Region Group 8 neighbors, zone grouping within - 2394 regions; selected regions > 11 cells.	total # cells = 11,997 (.41% of AOI); mounds detected 50/53

Trial	Test Comments	Conclusions	Cell/Mound Count
8d Effigy	Noticed that much of the AOI is including wetland that will not have mounds, yet is very noisy in this area due to unfiltered marsh grasses/reeds. Took this portion out of AOI.	Changed AOI to realistic research area; included masking out roads buffered 20 m from centerline - takes out false-positives in road ditches/embankments.	total # cells = 6354 (.22% of new AOI); mounds detected 50/53
9 Effigy	Added Majority Filter, Region Group, Extract by Attributes processes to ModelBuilder and reran model; deleted "road" cells.	Same result as trial 8b - model functioning properly.	total # cells = 6354 (.22% of new AOI); mounds detected 50/53
10 Slinde	Tried new model that was used in Trial 9 on the Slinde Mound AOI.	Lost four mounds that have been detected before (Trial 2), but much cleaner model; mound model is ok before reduction processes. Majority Filter lost one mound; Region Group - Extract by Attributes lost 3 mounds that were detected before - mound zones too small?	total # cells = 16,409 (.33% of AOI); mounds detected 9/17
11a Slinde	Back to the issue of "fattening up" true mound zones; wo changing Extract by Attributes zone size threshold, increased aspect variety neighborhood to 6 m radius to increase overlap with slope.	Without changing Region Group - Extract by Attributes regained 2 of the dropped mounds in Trial 10. More cells covering mounds. Road false-positives not removed.	total # cells = 23,060 (.47% of AOI); mounds detected 11/17
12 Slinde	Change relief focal neighborhood to 6 m radius and kept aspect variety to 6 m - the more the merrier?	No, change to 6m filter for relief is bad - lost two mounds detected in Trial 11, did not add detected cells to mound areas.	total # cells = 20,773 (.42% of AOI), no road clean-up; mounds detected 9/17
11b Slinde	Back to Trial 11 parameters. Masked out road cells.	Before clean-up portion of model all but 4 mounds detected; Region Group, Extract by Attributes dropped 2 more (6- and 10-cell zones).	total # cells = 21,684 (.44% of AOI); mounds detected 11/17
13 Effigy	Apply 6 m radius neighborhood to aspect variety model to Effigy area (including clean-up portion).	Did not enhance already-detected conical mounds plus added more false-positives. BUT did pick up an effigy mound that was not in previous trials.	total # cells = 10,887 (.37% of AOI); mounds detected 51/53
14 Clinton	Apply 6 m aspect var filter model to 13CN6 area (including clean-up portion).	Selecting zones > 11 cells is too restrictive, dropped one possible mound that had zone of 11 cells.	

Trial	Test Comments	Conclusions	Cell/Mound Count
15 Clinton	Change Extract by Attributes from Region Group to zones > 9; reduce overall number of zones by using Region Group of 4 neighbors instead of 8.	This added mound back and could add a mound back at Slinde that had a zone of 10 cells; RG 4 neighbors resulted in fewer total cells than RG 8.	RG 8 total # cells = 1847; RG 4 total # cells = 1511 (.15% of AOI before road cell exclusion); mounds detected 2/6 visible; 2/9 mapped by Orr
16 Slinde	Does model revised at Clinton AOI work at Slinde? Region Group 4 neighbors; select zones > 9.	YES. Got cell count to same percentage as Trial 12, but got more mounds detected than Trial 12.	total # cells = 20,915 (.42% of AOI; after road clean-up .4%); mounds detected 11/17 total; 11/13 visible on image
17 Effigy	Does model revised at Clinton AOI work at Effigy? Region Group 4 neighbors; select zones > 9.	YES. Cell count was slightly increased from Trial 13 but still maintained same number of detected mounds.	total # cells = 11,755 (.4% of AOI, after road clean-up .35%); mounds detected 51/53
18 Keokuk	Applied Trial 17 model to large area in Keokuk Co. 180 km2.	Masked out historic floodplain where mounds will be buried or washed away; data such bad quality, could only do analysis of effectiveness to one site. Slope of two mounds barely outside the good slope classification did not get detected. Can't see third mound on shaded relief image.	total # cells = 478,905 (.27% of AOI); mounds detected 0/2 visible, 0/3 total
19 Lucas	Applied Trial 17 model to area in Lucas Co.	One recorded mound was not marked due to low slope. Many more cells could have been deleted with railroad buffer mask.	total # cells = 10,725 (.53% of AOI); mounds detected 1/2

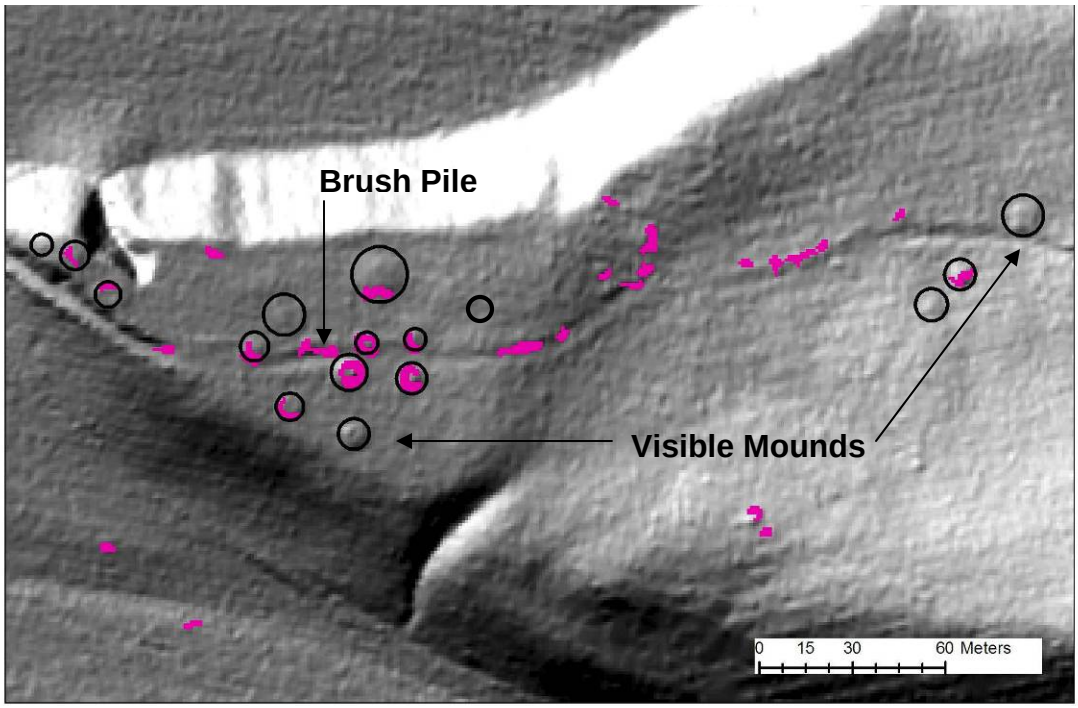

Figure 38. Mound model results for the Slinde Mound Group.

Table 11. Summary of mounds detected in the Slinde AOI.

Area of Interest	Number of Mounds Reported	Number Reported and Visible on Shaded Relief	Number Reported and not Visible on Shaded Relief	Total Visible and Detected by Model	% Visible Mounds Detected	Possible Unrecorded Mounds Detected
Slinde	17	13	4	11	85	1

Table 12. Summary of reported visible mounds by mound type detected in the Slinde AOI.

Area of Interest	Mound Type Reported and Visible				Visible and Detected by Model				% Visible and Detected by Model			
	Conical	Linear	Effigy	Compound	Conical	Linear	Effigy	Compound	Conical	Linear	Effigy	Compound
Slinde	12	1	0	0	10	1	0	0	83	100	NA	NA

1.6 km north of the Slinde Mound Group, recorded as a single linear mound, detected the bulbous end of the linear mound and a likely, unreported conical mound (Figure 39). Not considering the mounds too worn down to interpret from any shaded relief image, the model detected 11 out of 13 or 85% of the field-verified mounds in the Slinde AOI, including a linear mound.

Spurious cells were consistently along fencelines, roadsides, stream banks along natural levees, residual building footprints and sharp vegetation boundaries between pasture/field and trees (Figure 37). The model was successful in not marking small outcrops, most of the residual tree cells and colluvium below the bluffs. There were no positive cells in the terraces "overshadowed" by the bluffs above. Using two different shaded relief images of the same BE DEM, it was confirmed that there were really no mound-like features in

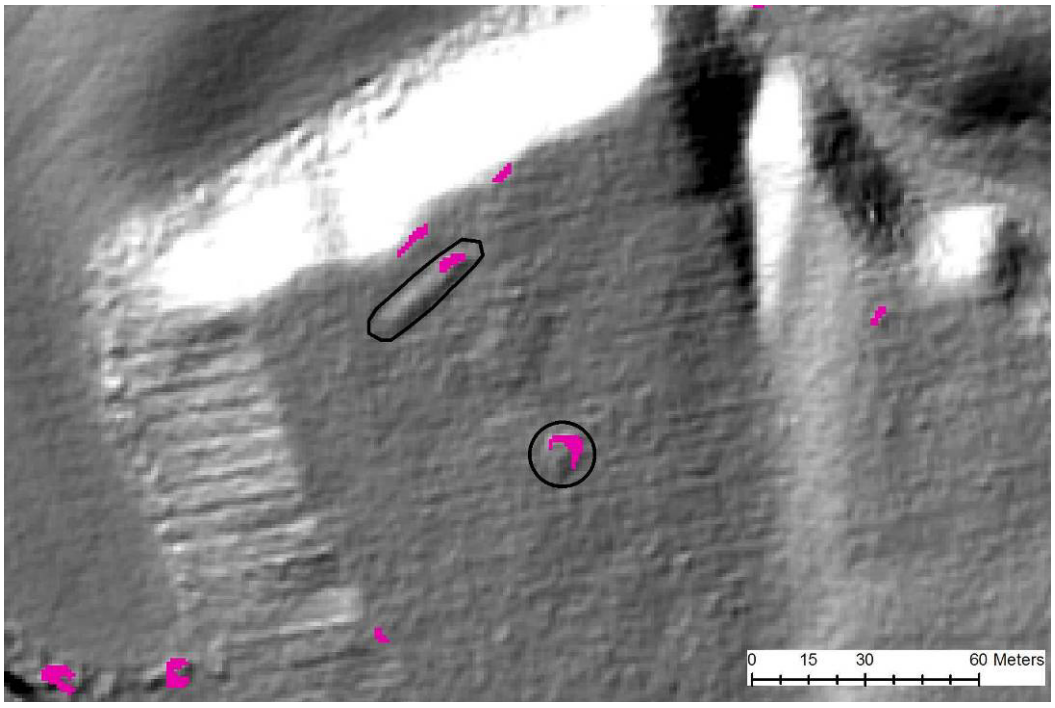

Figure 39. Mound model results for 13AM129; conical mound feature is not recorded.

these areas. According to S. Schermer, the UI-OSA Burials Director, an unmapped, detected mound feature in line with other mapped mounds along the farm path was field-confirmed as a brush pile (Figure 38; personal communication 30 Apr 2008).

The two mounds that were not detected but are clearly visible on the shaded relief were rejected by the model for different reasons. The mound with the main group was marked before clean-up with two small regions of five cells and one single cell. Origins of the small regions lie with the partial overlap of good aspect with good slope. Good slope goes only half-way around and becomes too low on the upslope side of the larger landscape. The mound was rejected by the model from the Extract by Attributes step where regions under 10 cells were deleted. The visible, undetected mound in the eastern portion of the group failed the aspect variety test and was never marked before clean-up. One of the mounds that required the field map to place was marked with a group of 10 cells, but majority filter took two cells away, then extracting regions greater than nine cells unmarked the mound altogether.

4.2 Effigy Mound National Monument Results

The set model used in the Slinde AOI was then applied to an area where several mound groups exist in Effigy Mound National Monument (Figure 40). Not only was the efficacy of the model tested on conical mounds, but also linear, effigy and compound mounds. The mound groups also differ from the Slinde Mound Group in that some of the mounds have been restored after being disfigured by excavation and backfilling, cultivation or looting. No changes were made to the final model ran on Slinde before it was applied to

the Effigy Monument groups.

After some false positives were eliminated using a 20 m road buffer, 0.35% of the AOI remained as detected mound polygons; of the 0.35%, 26% were from confirmed mounds. The linear, effigy and compound mounds were detected with as much success as the conicals (Figure 41, Tables 13 and 14). The model is robust enough to detect conical mounds of many sizes; recent field measurements range from 5.1 m diameter and 35 cm in height to 16.85 m diameter and 263 cm height. Linear mounds were generally marked on the ends. Two of the detected linear mounds have reported field heights of only 30 - 40 cm. Two sets of compound mounds, linears and conicals linked together, were heavily marked along the length of the features. The bear effigy mounds were marked around the head and rump areas. Altogether, 51 out of 53, or 96%, of the extant mounds were successfully detected. Of the two that were not, one is partially destroyed by an old logging road and the other is a linear mound that did not pass the aspect variety test (Green *et al.* 2001).

False-positive cells were on roadsides, some stream banks, rural dams, residual building footprints, vegetation boundaries and features from contour/terrace farming. An area where mass point vegetation filtering was not as complete left rough areas on the BE DEM where there is actually tall grass. This is where a large share of the false positives occurred (Figure 41).

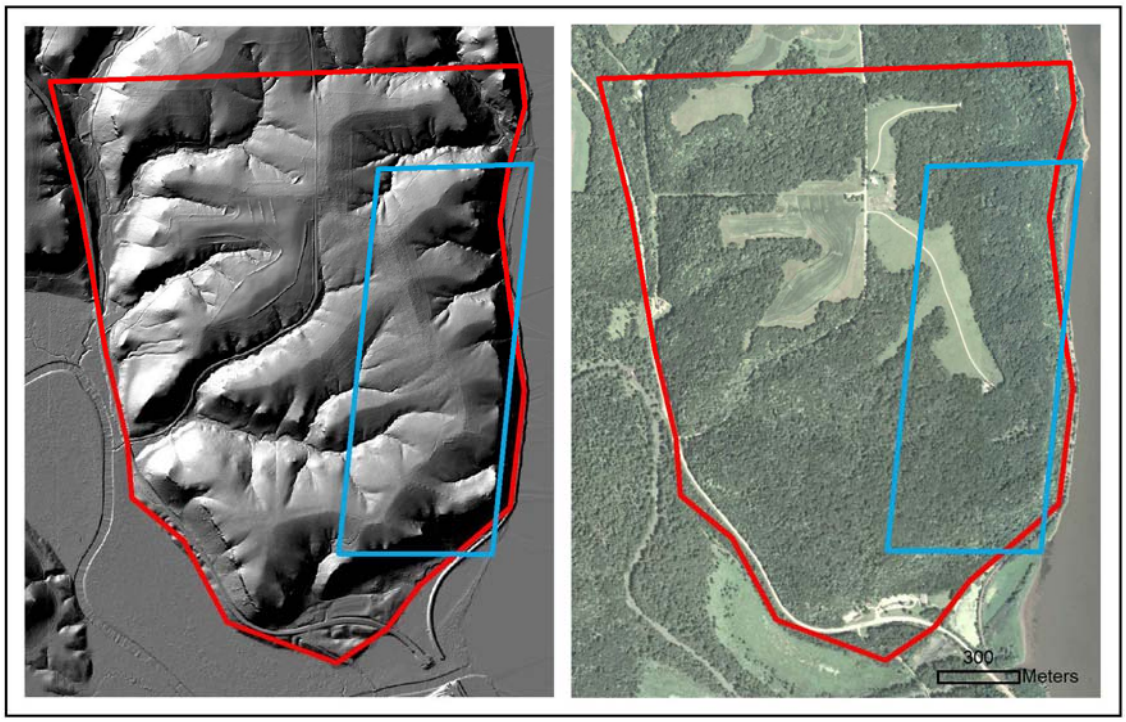

Figure 40. Effigy AOI delimited in red, Figure 41 area in blue. Left image is BE DEM shaded relief, right image is 2008 NAIP true color imagery to show vegetation cover.

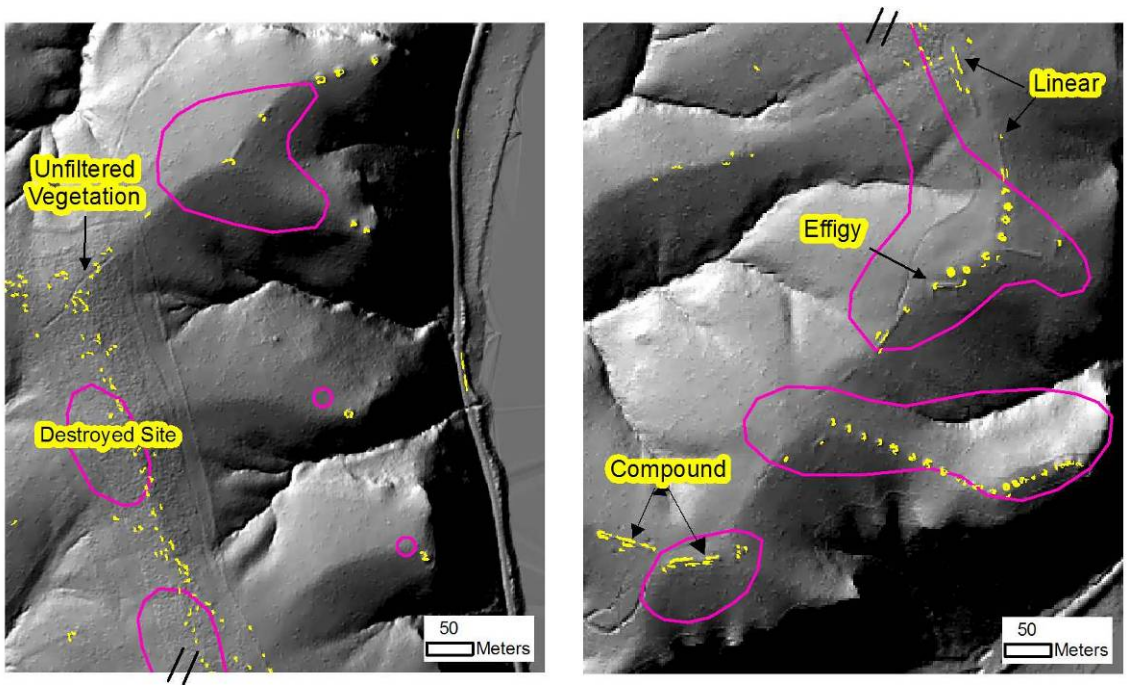

Figure 41. Results of mound detection model; UI-OSA site boundaries in pink are off from the true site locations. Image on left is north of image on right.

Table 13. Summary of mounds detected in the Effigy AOI.

Area of Interest	Number of Mounds Reported	Number Reported and Visible on Shaded Relief	Number Reported and not Visible on Shaded Relief	Total Visible and Detected by Model	% Visible Mounds Detected	Possible Unrecorded Mounds Detected
Effigy	53	53	0	51	96	0

Table 14. Summary of reported visible mounds by mound type detected in the Effigy AOI.

Area of Interest	Mound Type Reported and Visible				Visible and Detected by Model				% Visible and Detected by Model			
	Conical	Linear	Effigy	Compound	Conical	Linear	Effigy	Compound	Conical	Linear	Effigy	Compound
Effigy	38	10	3	2	37	9	3	2	97	90	100	100

4.3 Clinton County Results

The study in Clinton County shifted from using the model on mounds with clear documentation to a site where location was recorded by Ellison Orr, but have not been confirmed by modern field survey. The Lewis Fenger Mound Group (13CN6) was reported to the quarter section by Orr (1935) via a field map. At the time of his survey, the mound group was not in cultivation, only pasture. If the mounds stayed in pasture they are likely to be extant.

The AOI encompassed the tentative site location from the UI-OSA site shapefile, quarter section reported by Orr, steep, wooded ravines and natural sinkholes (Figure 42). The model processed the 1 km^2 area in 2.5 minutes. The resultant polygons after road buffer clean-up represented .15% of the total AOI. The low percentage was surprising because the shaded relief shows a rougher surface than the previous two AOIs in the wooded

Figure 42. Clinton County test. AOI delimited in red. Left image is BE DEM shaded relief, right is 2008 NAIP true color imagery to show vegetation cover.

areas. The unfiltered vegetation seems to have had little effect perhaps because the "trees" are very small bumps compared to the size of conical mounds the model was designed to detect. Large natural sinks and small outcrops also did not interfere with the model's performance.

False positives were at vegetation boundaries, farm paths, farmsteads and an occasional unfiltered tree (Figure 43). The area around the reported location of 13CN6 was checked and two positive polygons drew attention to a far corner of the 1-mile section (Figure 44, Tables 15 and 16). The polygons mark features that seem to be mounds; other mound-like features can be seen on the shaded relief image, but are not marked. According to Orr's (1935) measurements, six out of nine mounds were 30.5 cm (1 ft.) or less. All the

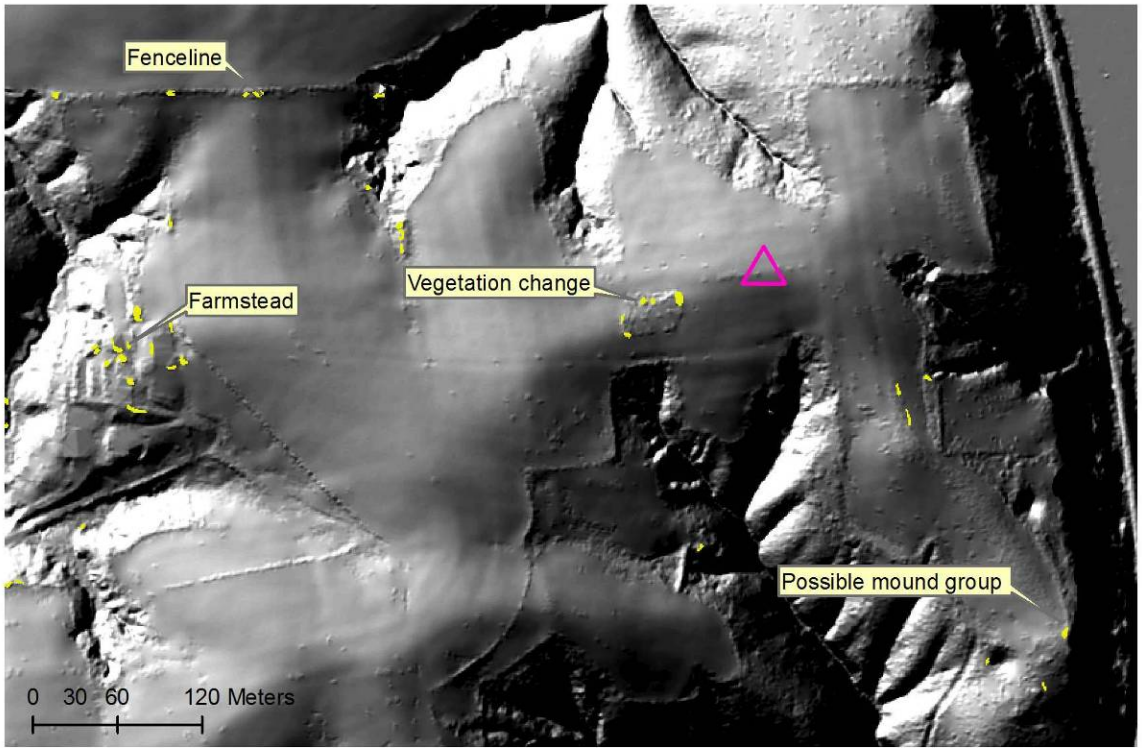

Figure 43. Results of Clinton County test in yellow. A marker from the UI-OSA site shapefile indicating a site with uncertain location is in pink.

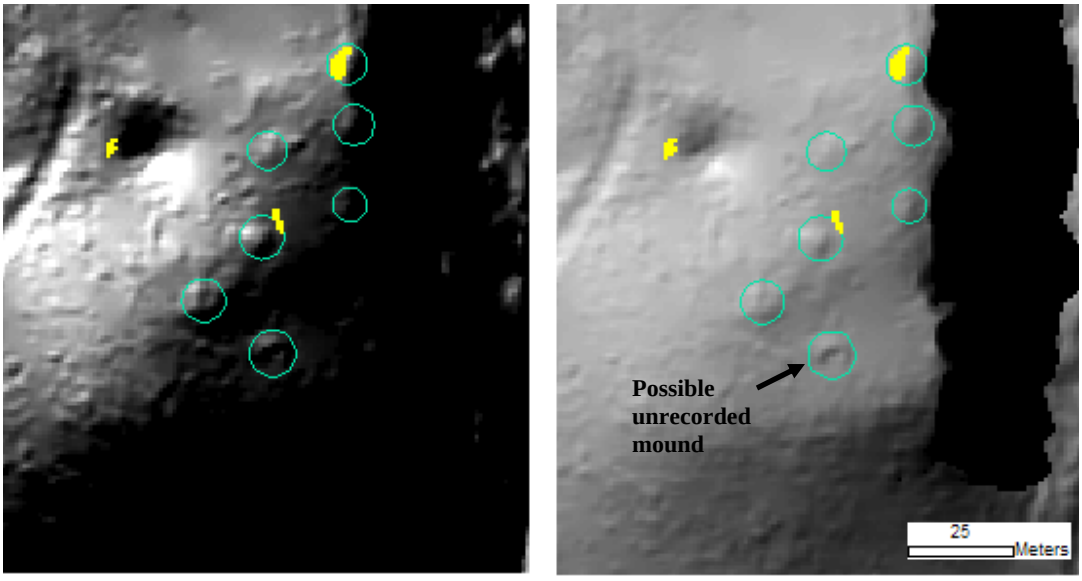

Figure 44. Shaded relief images using different stretch renderings display possible mound group 13CN6. Mound model results in yellow and possible mound features delimited in blue.

Table 15. Summary of mounds detected in the Clinton AOI.

Area of Interest	Number of Mounds Reported	Number Reported and Visible on Shaded Relief	Number Reported and not Visible on Shaded Relief	Total Visible and Detected by Model	% Visible Mounds Detected	Possible Unrecorded Mounds Detected
Clinton	9	6	3	2	33	0

Table 16. Summary of reported visible mounds by mound type detected in the Clinton AOI.

Area of Interest	Mound Type Reported and Visible				Visible and Detected by Model				% Visible and Detected by Model			
	Conical	Linear	Effigy	Compound	Conical	Linear	Effigy	Compound	Conical	Linear	Effigy	Compound
Clinton	5	1	0	0	2	0	0	0	40	0	NA	NA

mound-like features that had not been marked by the model did not pass the aspect variety test and one did not pass the height test. A side-by-side comparison of Orr's map with the mound-like features and surrounding landscape show a remarkable similarity, so these features cannot be excluded but need to be field verified (Figure 45).

Orr's mounds 2, 7, and 9 do not seem to appear on the shaded relief image and a mound-like feature that looks looted on the shaded relief image does not appear on Orr's map, but to consider this a mound is very tenuous until field-confirmed. Mounds 7 and 9 were only 24.5 cm (10") and mound 2 about 45 cm (18") in height according to Orr's survey map; the horizontal dimensions were also small. It is possible that they are still there, but not enough ground points were collected over the group, their points were filtered out or they were smoothed out in the point-to-DEM interpolation process. If the site is 13CN6, the marker in the site file is 350 m northwest of the true location. The legal location on the Orr map is also a little off; the potential site is in the extreme southeast corner of the

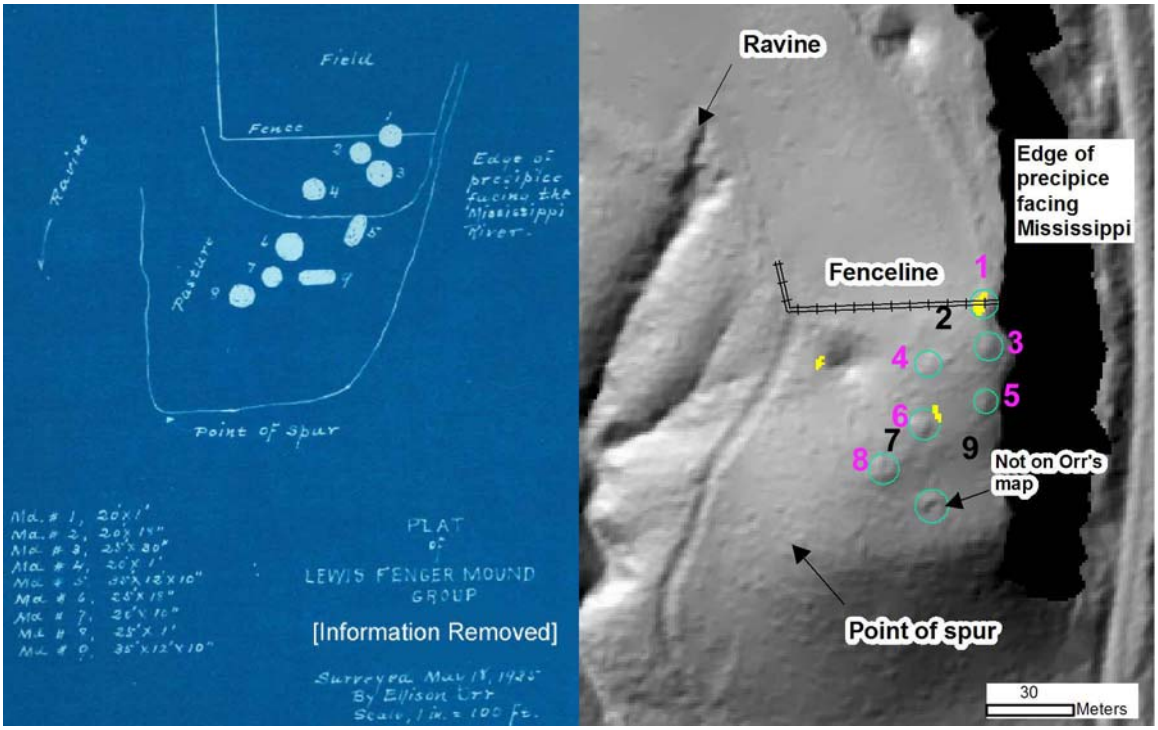

Figure 45. Side-by-side comparison of Orr's (1935) map and potential location of 13CN6. Pink numbers are Orr's mounds that are visible, black numbers indicate mounds not visible on shaded relief, used with permission.

reported section as well as the southwest, northeast and northwest corners of the three neighboring sections.

4.4 Keokuk County Results

The results of the mound detection model in the rough, wooded terrain of northeast Iowa were better than expected. With the expectation that the Southern Iowa Drift Plain would have a gentler topography and perhaps less vegetation, a large AOI of 180 km^2 was processed (Figure 46). The area included the forested North Skunk River valley in order to include sites with known and unknown locations. The model took eight hours to complete the processing.

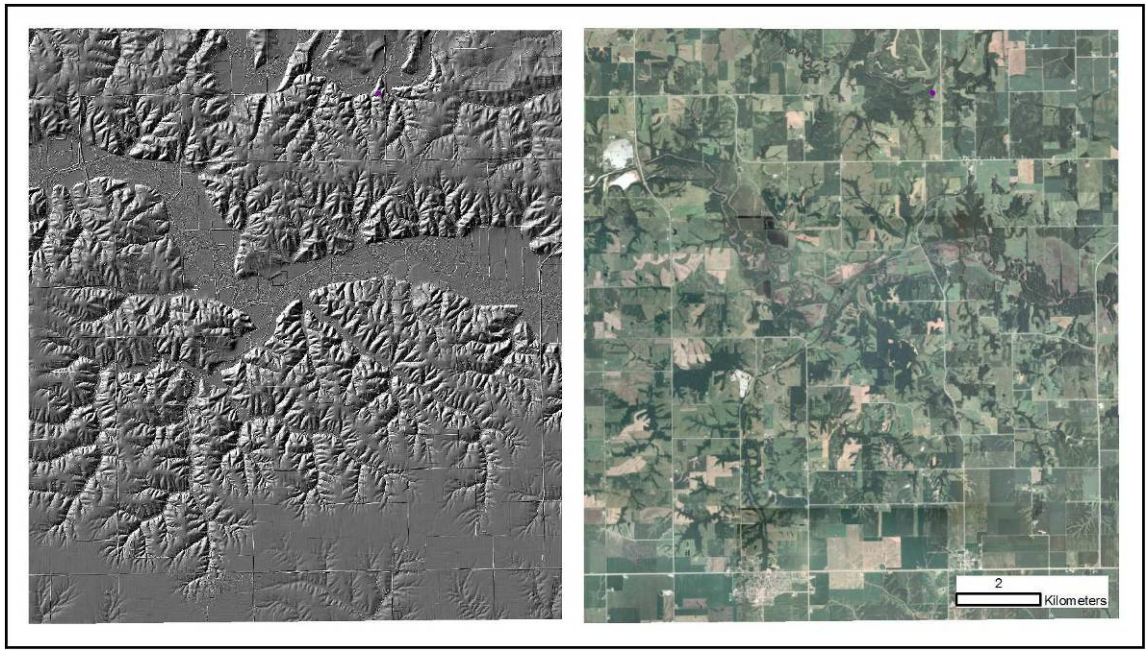

Figure 46. AOI of the Keokuk County test. Left image is BE DEM shaded relief, right is 2008 NAIP true color imagery to show vegetation cover.

The model results were cleaned using road centerline buffers and incorporated city boundaries. While examining the floodplain of the North Skunk River, it was apparent that detection in this area has little value because most of the soils' parent material is historic alluvium and there were many false positives. If there were prehistoric mounds in this area, they would have been destroyed by river avulsion or buried in a thick layer of alluvium. The model BE DEM elevations were sliced into equal intervals of 12 classes representing a range of 8 m per class. The two lowest classes were used to mask out the current floodplain, leaving higher terraces unaffected by this clean-up step. The final model had mound positives representing 0.27% of the total AOI. Some of the false positives were in predictable areas such as roadsides, fencelines, contour/terrace farming features, vegetation boundaries and farmstead buildings. Two sand and gravel quarries also were marked by some false positives. The flat landscape south of the valley, known

as table lands, was clear of false positives except for farmsteads, fencelines and stands of trees along drainages (Figure 47).

A disturbing trend of dense false positives was immediately noticed along all the small drainages and large creeks draining into the North Skunk River (Figure 47). These areas are no more rough or forested than the northeastern part of the state, yet there was a much higher occurrence of false positives. Closer examination of the BE DEM shaded relief revealed that there are data quality issues inconsistent with blocks in other parts of the state. Terraces and floodplains along streams should have a relatively flat surface; instead, many rugged facets represent the surface (Figure 48).

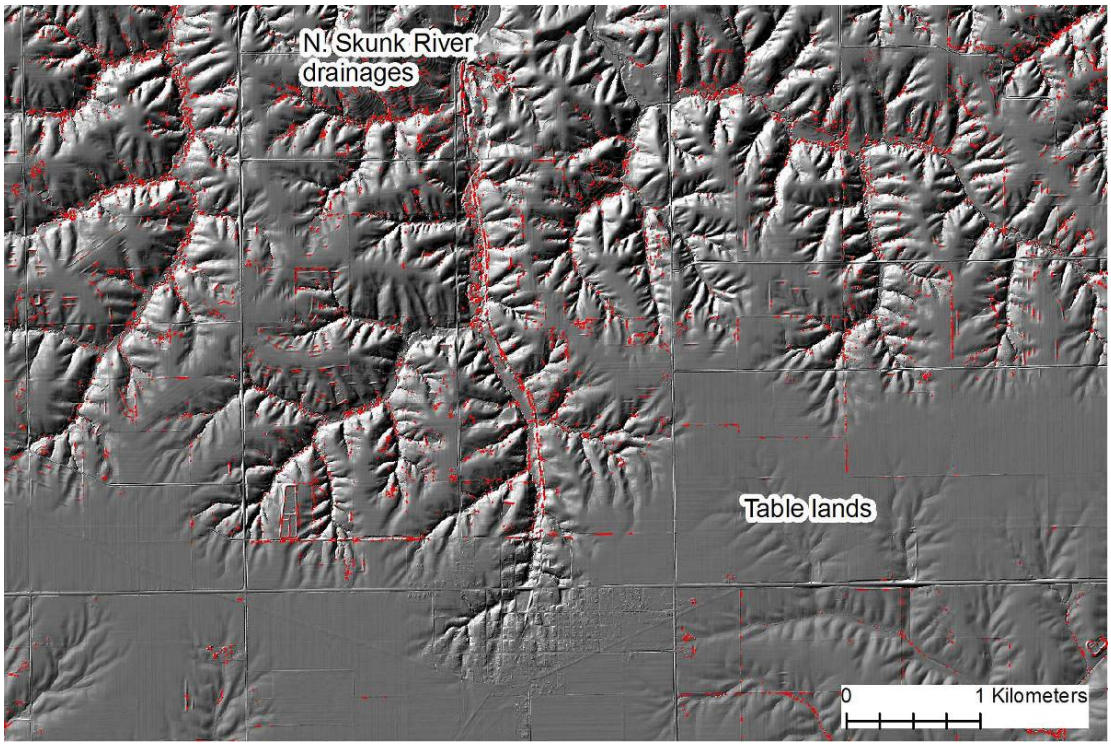

Figure 47. Mound model results in red along drainages and table lands.

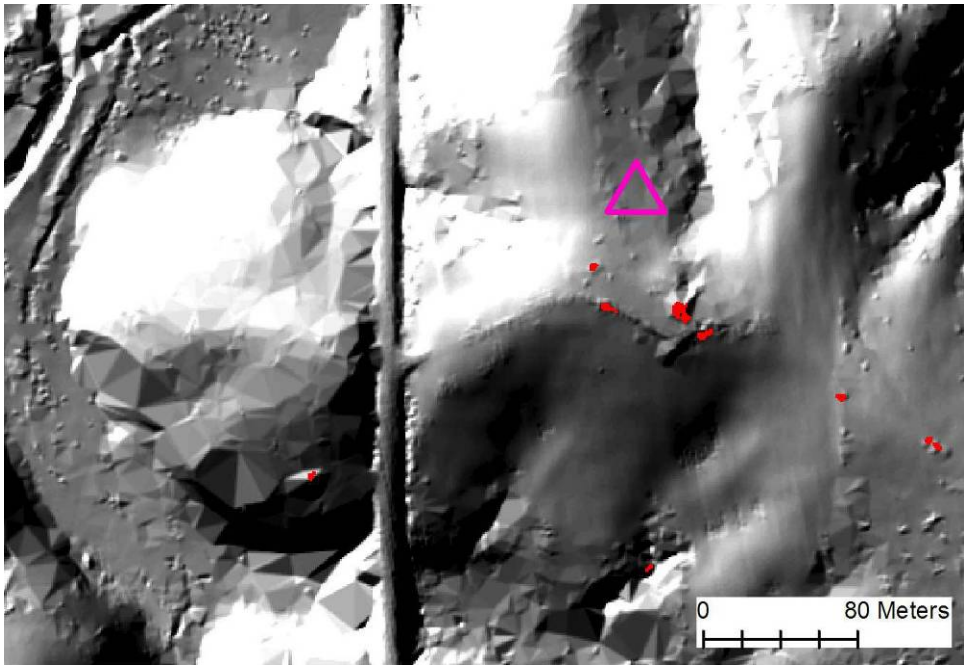

Figure 48. Faceted surface on ridge, slopes and terrace near uncertain location of site 13KK326.

The facets are likely caused by tree canopy elevation points interrupting the surrounding ground elevations causing the sudden jumps on the interpolated surface. Vegetation filtering was subpar in the entire AOI. Instead of small bumps where trees are filtered out, there is substantial relief where single trees or groves of trees exist (Figure 49).

The purpose of choosing the AOI was to test the model on seven mound sites with uncertain locations and one site with a known location. The site with known location (13KK19) was not marked positive for mounds (Figure 50, Tables 17 and 18). Two out of the three mounds reported in 1980 were barely interpretable from the shaded relief image. The third mound, even with good data on the site form (although no coordinates of the mound itself), could not be located from the shaded relief image. The two mounds that are visible on the shaded relief were not detected by the model because their slopes

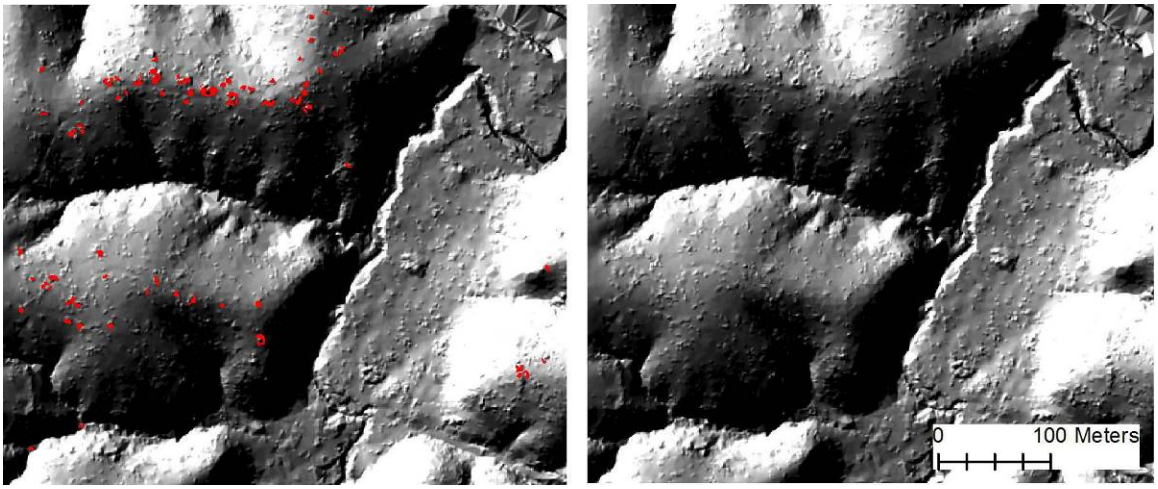

Figure 49. Example of poor vegetation filtering hindering efficacy of the model and image interpretation. Strong mound model positives (in red) in the shape of annuli at top of left image cannot be differentiated from unfiltered trees.

were too low; slopes around the mounds were 4.15 – 4.65°.

Interpreting the mound positives around the sites with uncertain location proved to be a frustrating experience due to the high amount of vegetation residuals and oddly-faceted surfaces. If the sites have survived since they were reported to Charles Keyes in 1928, they will be located in wooded areas or pasture and not areas that have been cultivated over the last 80 years. Unfortunately, the wooded areas are what suffered from poor-quality data.

A strong mound positive was located only a few meters from the marker for site number 13KK321 (Figure 51). Three other positives were 55 m west of the site marker. The closest positive looks like it could be a mound, the other three look more like a result of unfiltered tree points. One cannot be confident in the interpretation considering the erratic, neighboring microtopography. False positives were near site 13KK326 that are

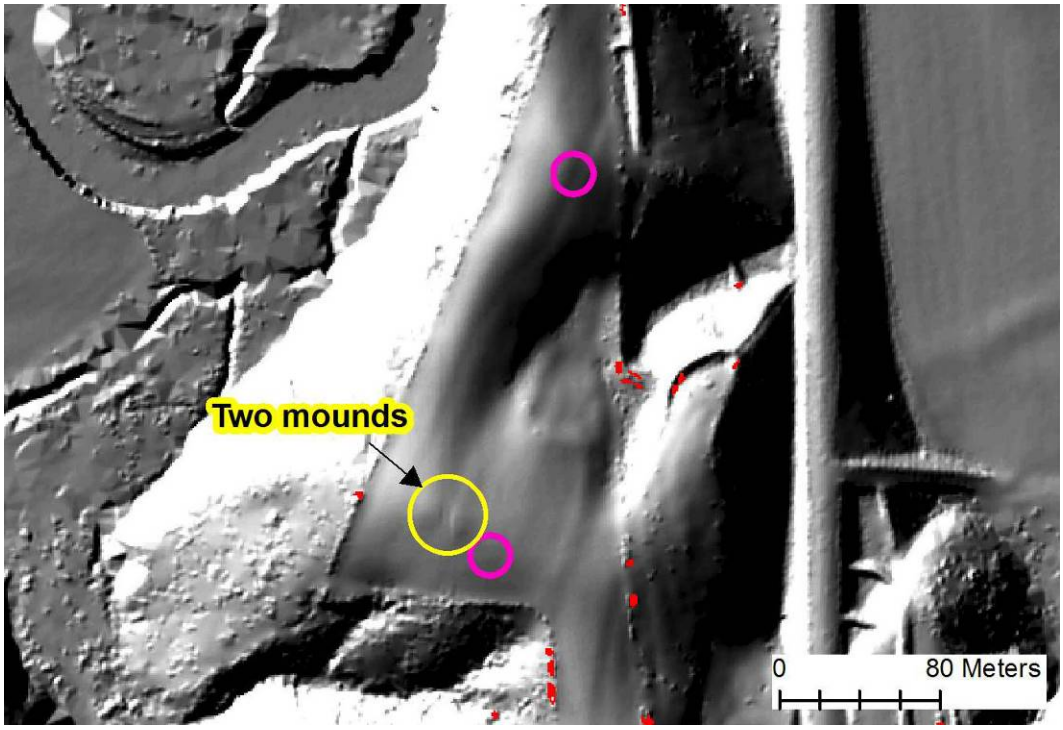

Figure 50. Site 13KK19 as recorded in the site boundary file in pink and two out of the three mounds interpreted from the image circled in yellow.

Table 17. Summary of mounds detected in the Keokuk AOI.

Area of Interest	Number of Mounds Reported	Number Reported and Visible on Shaded Relief	Number Reported and not Visible on Shaded Relief	Total Visible and Detected by Model	% Visible Mounds Detected	Possible Unrecorded Mounds Detected
Keokuk*	3	2	1	0	0	NA*

* Only site 13KK19 with certain location was used in the analysis due to the poor quality of the data hindering interpretation.

Table 18. Summary of reported visible mounds by mound type detected in the Keokuk AOI.

Area of Interest	Mound Type Reported and Visible				Visible and Detected by Model				% Visible and Detected by Model			
	Conical	Linear	Effigy	Compound	Conical	Linear	Effigy	Compound	Conical	Linear	Effigy	Compound
Keokuk	2	0	0	0	0	0	0	0	0	NA	NA	NA

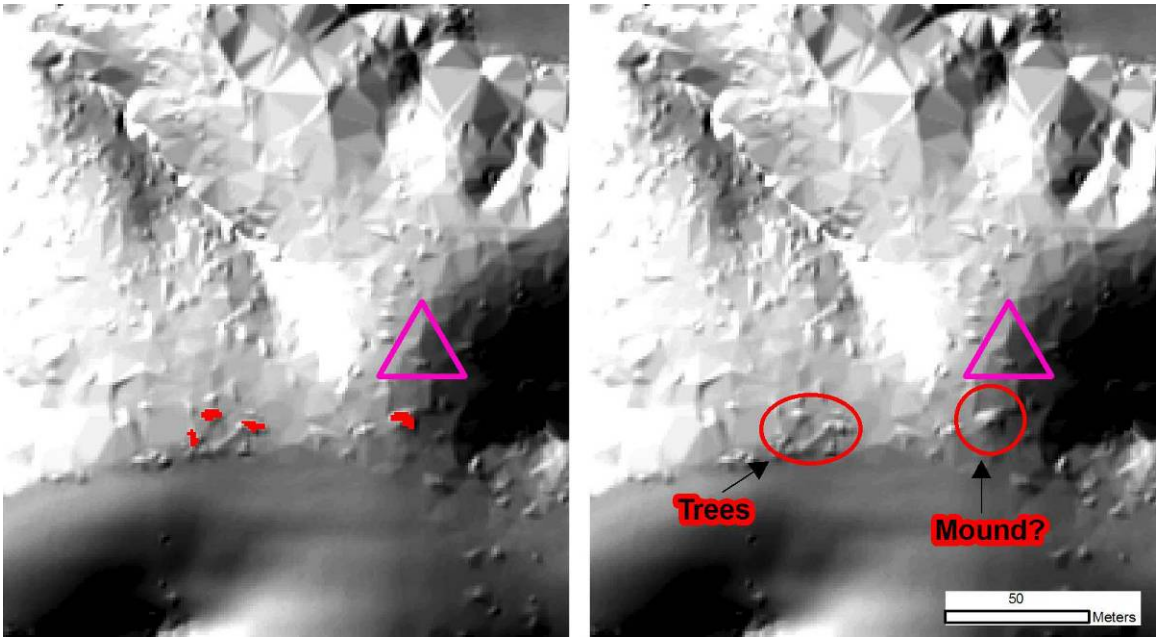

Figure 51. Uncertain location of 13KK321 marked in pink. Image on left shows mound model results; image on right shows difficulty in interpreting the BE DEM shaded relief image.

easily attributable to a farmstead. The most likely location for the site would be on a ridge spur just west of the site file polygon which had no mound model positives (Figure 48). The ridge is heavily forested and is not an exception to the rest of the low-quality data found in this block. These two site-checking scenarios were typical experiences of all seven sites with uncertain locations.

4.5 Lucas County Results

After the disappointing results in Keokuk County, a 4 km² area was chosen in Lucas County where quality of the block data was much better (Figure 52). The site (13LC17) in the test area was documented as having two mounds in 1984 and the model results detected one of the mounds (Figure 53, Tables 19 and 20; Perry 1984). Both mounds have a wide diameter of approximately 14 m but maximum height of only 55 cm on the

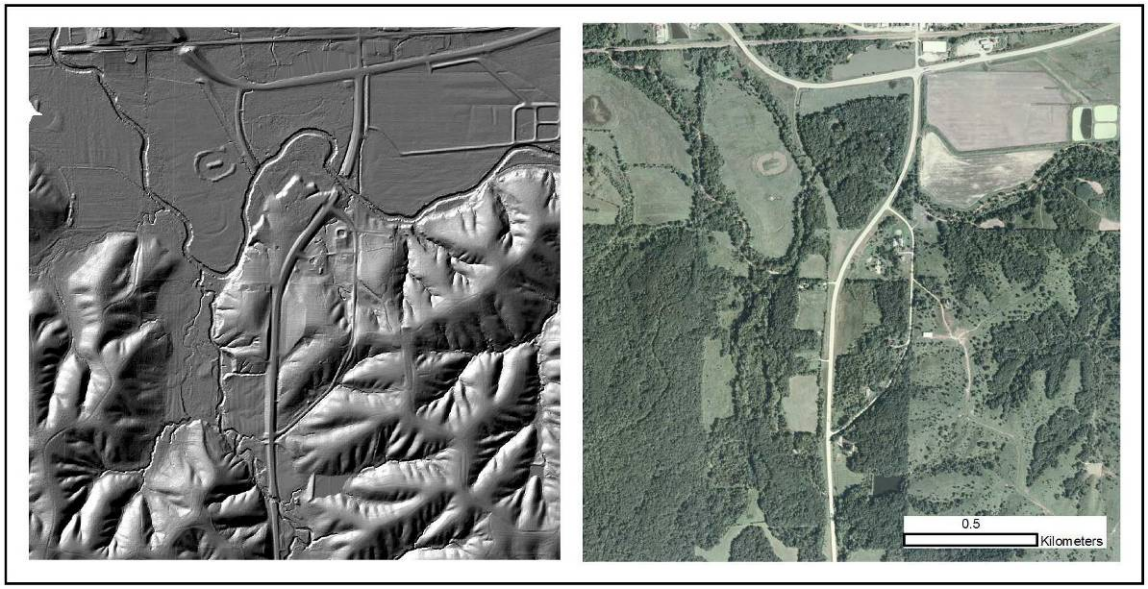

Figure 52. AOI of Lucas County test. Left image is BE DEM shaded relief, right image is 2008 NAIP true color imagery to show vegetation cover.

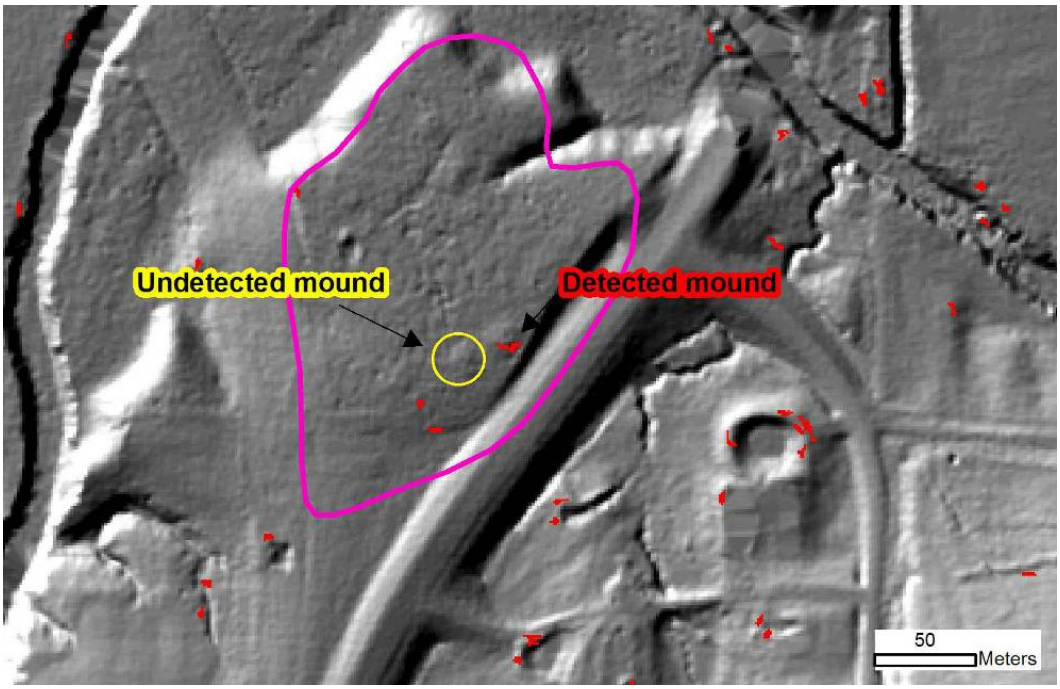

Figure 53. Mound model results at site 13LC17; UI-OSA site boundaries in pink.

Table 19. Summary of mounds detected in the Lucas AOI.

Area of Interest	Number of Mounds Reported	Number Reported and Visible on Shaded Relief	Number Reported and not Visible on Shaded Relief	Total Visible and Detected by Model	% Visible Mounds Detected	Possible Unrecorded Mounds Detected
Lucas	2	2	0	1	50	1

Table 20. Summary of reported visible mounds by mound type detected in the Lucas AOI.

Area of Interest	Mound Type Reported and Visible				Visible and Detected by Model				% Visible and Detected by Model			
	Conical	Linear	Effigy	Compound	Conical	Linear	Effigy	Compound	Conical	Linear	Effigy	Compound
Lucas	2	0	0	0	1	0	0	0	50	NA	NA	NA

BE DEM. The mound that was not detected was marked with a few sporadic cells that were subsequently removed during the clean-up segment of the model. The sparse marks on this mound were due to a very low slope around most of the mound reclassified to value 20. Slope values around the perimeter of the mound ranged from 2.6 – 4.9° and were very irregular.

False positives occurred in now-predictable areas: edge of stream banks, rural dams, roadsides, farmsteads and fencelines. All the model positives accounted for 0.27% of the total AOI. About .5 km southeast of the known site, a substantial, round positive mark drew attention to a likely unrecorded conical mound (Figure 54).

4.6 Summary and Discussion of Results

Tests at Slinde and Effigy Mound National Monument AOIs demonstrated that all the mound types in Iowa can be detected with the model. From all AOIs, excluding Clinton,

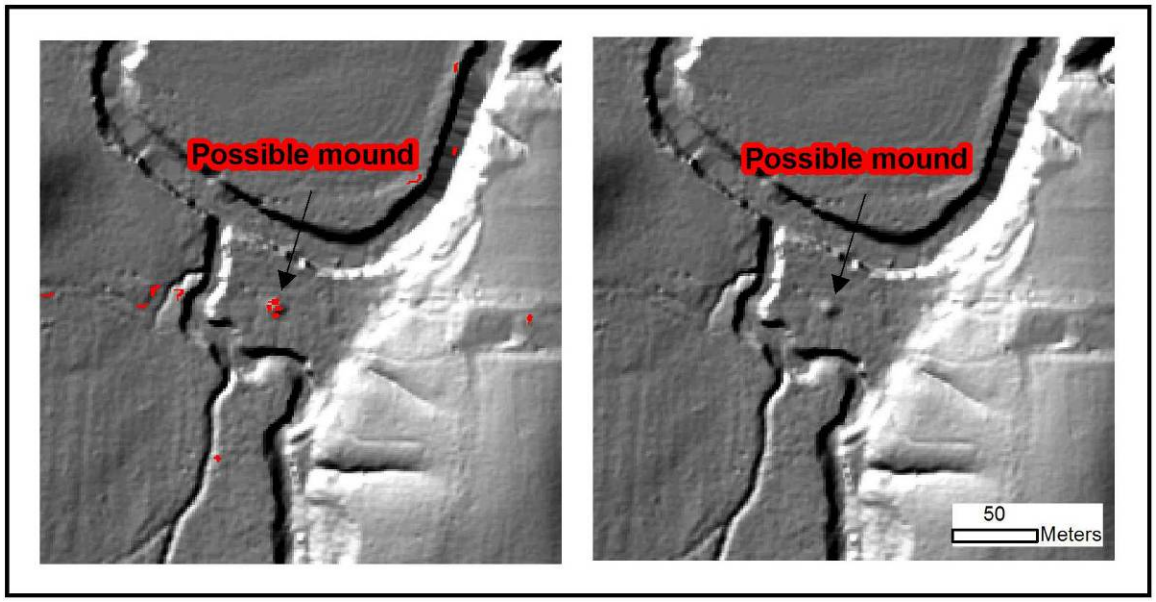

Figure 54. Possible unrecorded mound detected by model.

the model detected 63 out of 70 mounds, or 90%, that were recently field-verified and interpretable from shaded relief images (Tables 21 and 22). When the total includes the possible relocation of 13CN6 in the Clinton County AOI (which has not yet been field-verified as 13CN6) the rate is 86%. The mounds that were not detected by the model but visible on the shaded relief were omitted for various reasons (Table 23). Many of the rejections occur when the slope around the mound is too low. The ranges of low slope values vary and more tests on other well-documented mounds will be necessary to determine if a modified classification scheme will be needed for slope.

Most adjustments need to be focused on decreasing false positives. The percentage of AOI that are mound model positives seem to be low, but there are many individual polygons scattered across the AOIs. Fortunately, the causes for false positives are consistent and many involve man-made features that are easily identifiable on aerial

Table 21. Summary of mounds detected in the study. Clinton is not field-verified.

Area of Interest	Number of Mounds Reported	Number Reported and Visible on Shaded Relief	Number Reported and not Visible on Shaded Relief	Total Visible and Detected by Model	% Visible Mounds Detected	Possible Unrecorded Mounds Detected
Slinde	17	13	4	11	85	1
Effigy	53	53	0	51	96	0
Clinton	9	6	3	2	33	0
Keokuk	3	2	1	0	0	NA
Lucas	2	2	0	1	50	1
Total	84	76	8	65	86%	

Table 22. Summary of reported, visible mounds by mound type detected.

Area of Interest	Mound Type Reported and Visible				Visible and Detected by Model				% Visible and Detected by Model			
	Conical	Linear	Effigy	Compound	Conical	Linear	Effigy	Compound	Conical	Linear	Effigy	Compound
Slinde	12	1	0	0	10	1	0	0	83	100	NA	NA
Effigy	38	10	3	2	37	9	3	2	97	90	100	100
Clinton	5	1	0	0	2	0	0	0	40	0	NA	NA
Keokuk	2	0	0	0	0	0	0	0	0	NA	NA	NA
Lucas	2	0	0	0	1	0	0	0	50	NA	NA	NA
Total	59	12	3	2	50	10	3	2	85	83	100	100

Table 23. Reason model rejected known conical mounds that are visible on shaded relief.

Area	Mound	Reason for Rejection
Slinde	#12	Marked but deleted in clean-up; half of mound low slope (1.9 - 3.7°)
Slinde	#18	Failed aspect variety
Effigy	#56	Mound disfigured/destroyed beyond conical morphology
Clinton	13CN6 (4 mounds)	None passed aspect variety test; one has too low relief
Keokuk	13KK19 (2 mounds)	Both failed slope test - slopes too low (4.15 - 4.65°)
Lucas	13LC17 (1 mound)	Failed slope test - slope too low (2.6 - 4.9°)

photography. In the future, the IGS would like to create building footprints from the LiDAR DEMs that could be used to mask out the farmstead buildings. A buffered stream mask could also be created directly from the BE DEM to eliminate false positives along the stream banks. Some archaeologists may be opposed to this citing the few mounds that have been found along stream banks. The unconfirmed conical mound found in the Lucas County test demonstrates that the stream bank buffer should be narrow if one is used.

Landscape features of the different physiographic regions seemed not to have an affect on how the model functioned. Natural sinkholes, outcrops and steep slopes from deeply-entrenched streams did not disrupt the model or add many false positives. The quality of point cloud classification does have a large impact on the efficacy of using the model and the interpretability of the shaded relief images. It is recommended that in areas with low-quality data, such as the blocks covering Keokuk Co., running the model is inappropriate because image interpretation for mounds is nearly impossible. Communication with C. Kahle from IGS confirmed that they were aware of such problems and that subcontractors of Sanborn are not using consistent methodology for point cloud filtering (personal communication, 17 Feb 2009).

Another potential cause for the excessive residual vegetation points is the LiDAR scan angle off nadir; the wider the angle the larger the swath width. This expedites collection over large areas but the beam of light also intersects more tree canopy area before reaching the bare earth (Jensen 2007). It is plausible that the contract specs of 90% vegetation filtered was followed but the number of vegetation points increased

dramatically from a higher scan angle. Scan angle is stored in the .las files, so it can be verified if it was flown within contract specs. However, according to C. Kahle, no reflights or reprocessing will be done at this time and IGS might solve the problem of low-quality data in the future (personal communication, 17 Feb 2009).

CHAPTER 5: CONCLUSION

The objective of this research was to create a feature detection tool for conical mounds with the possibility of detecting linear and effigy mounds as well. The tool needs to be easily distributable to other archaeologists and functional with GIS software they are already familiar with. The model must also be easy to use to minimize the time spent on training and not intimidating to those with limited GIS experience. The results of the model are to be used as an image interpretation guide for the BE DEM shaded relief images. This is to help minimize time spent on prospection by: eliminating the need to "crawl" across the entire, zoomed-in image; reducing the usage of more than one shaded relief image from the same BE DEM to check all the overshadowed areas; and minimizing extra analysis such as measuring heights and widths for every little bump across the landscape. The model is also to help minimize human biases in interpretation that may occur from lack of experience, physical capabilities, boredom or fatigue.

For this research, a model was built in ArcGIS 9.2 in the ModelBuilder environment that succeeded in detecting 90% of all recent field-verified mounds that are viewable from a shaded relief image. Not only were conical mounds detected, but 15 out of 16 of all effigy, linear and compound types recently field-verified were detected. If mounds from site 13CN6, which has yet to be field-verified in recent times, are included in the analysis the model succeeded in detecting 86% of all mounds visible on a shaded relief image.

Most archaeologist in Iowa that use GIS use ArcGIS software; some may have to

purchase the Spatial Analyst extension in order to run the model. Other regions may have to purchase 3D Analyst to establish parameters if no reliable, recent field data are available. The model is easily transferable as a .tbx file that can be emailed as an attachment or downloaded from a website and added to ArcToolbox in a map document or template. The only interaction the user will have with the model is to assign the BE DEM and AOI in ModelBuilder that will be used and hit “Run Entire Model” in the Model drop-down menu. No extensive experience with raster manipulation or map algebra is necessary; the results are added to the map document as a vector file. The vector data model facilitates clean-up for GIS users that may have limited experience but can use common buffer and selection functions.

The model works well in rugged terrain as long as the BE DEM is of good-quality. It also does not mark items such as small outcrops or large rocks at the base of limestone bluffs that would cause one to pause and conduct extra analysis such as measurements. Viewing those features in ArcScene with vertical exaggeration may help in the interpretation process, but that would require the purchase of another ArcGIS software extension, 3D Analyst. Most of the false positives did not occur in areas that are overshadowed on the shaded relief, which cuts down interpretation time by not having to check those areas with multiple shaded relief images with different light source settings or stretch renderings.

Although the model detects mounds at a high rate, there are many false positives that need to be addressed. Features that create false positives are consistent and easily

identifiable on aerial photography. Aerial photography is used heavily by archaeologists as part of presurvey planning and creating maps for contract completion reports. Identifying the predominately man-made features that trigger false positives will not be an issue. Cleaning up the false positives does take some time, but not as much as searching the whole area and contemplating the morphology of every bumpy feature that is encountered.

However more should be done within the mound detection model to reduce the number of false positives the interpreter will have to filter through. The features that trigger the false positives are consistent, so the potential of eliminating many of them within the model is high. The IGS plans to make a building footprint file in the future which can be used to eliminate farmstead buildings, but it is not certain if or when such data will be available. With DSMs, that will also be available for public download, Hewett's (2005) building extraction model in ModelBuilder could be added as a segment to the mound detection model and used as a mask. Stream banks can be extracted by their steep slopes and sudden height change. Buffering stream banks by only a few meters and using the raster as a mask would be effective in eliminating many false positives in river valleys. The only caveat with the stream bank mask is the possibility of masking a mound; this may have to be a separate model to be used at the discretion of the archaeologist.

The biggest threat to this model working well is BE DEMs created from low-quality data. Using this model in areas like the blocks over Keokuk County is not appropriate because the model picks up too many trees and "facets" along drainages as mounds, and the

shaded relief image is not visually interpretable in areas where mounds are likely to exist. An unexpected benefit has come from this research in that the IGS received early feedback from this author as an end-user whose work has been affected by poor-quality data. The IGS will be taking the correspondence to Sanborn as “ammunition” to request better performance in data processing (C. Kahle personal communication, 17 Feb 2009). Almost half the state has not been collected so there is time for changes in processing and QA/QC practices to make a significant impact in the statewide dataset.

This research presents the possibility that regions with high mound density can be remotely surveyed for mound sites within a reasonable amount of time and a small budget. The results will aid in fine-tuning site boundaries and creating a second file of points that need to be field-verified before any public or private development can proceed in adherence to state and federal laws. A file of LiDAR-detected mound features will aid an already over-worked and under-funded State Historic Preservation Office in Section 106 review and state burial law compliance.

An Internet Map Service is currently in development by the UI-OSA that will provide information to government agencies at all levels the number of sites to the quarter section and surveyed areas without giving away exact boundaries to non-archaeologists. The number of LiDAR-detected sites in quarter sections would also aid planners in those agencies in making decisions on whether to design the project away from the area or hire an archaeologist early in the project. The Rock Island District of the U.S. Army Corps of Engineers has already expressed interest in applying the model to their one-mile swath of

LiDAR data along the Mississippi River in Iowa to aid in project planning and site avoidance.

The Wisconsin/Illinois side of the Mississippi also has a one-mile swath that the model can be applied to. Most of the LiDAR data currently being collected in other states follow the same specs as the data used in this research. While not all of the physiographic regions have been tested, the landscape seemed to have little effect on the performance of the model. Mound sizes can be different regionally so modifications to focal neighborhood size and reclassification schemes may need to be adjusted. ModelBuilder is very flexible in changing these items and running several trials for comparison on what works best.

Field verification of detected mounds that are unrecorded or have uncertain locations will solidify the utility of the model. It is likely that some “conical mounds” encountered on a shaded relief are modern piles of soil, brush or feed lot manure. Feed lots are simple to detect on aerial imagery and will likely be discounted as being part of a farmstead. Brush and soil piles can only be confirmed with field visits. With older, grass-covered dirt piles, subsurface soil testing is often necessary to declare the feature prehistoric. LiDAR cannot replace field survey but will be an invaluable tool for mound prospection and perhaps other prehistoric site types that left an endurable mark on the earth.

REFERENCES

Alex, L.M., 2000. *Iowa's archaeological past.* Iowa City: University of Iowa Press.

Altaweel, M., 2005. The use of ASTER satellite imagery in archaeological contexts. *Archaeological Prospection,* 12 (3), 151-166.

Anfinson, S.F., 1984. Cultural and natural aspects of mound distribution in Minnesota. *The Minnesota Archaeologist,* 43 (1), 3-30.

Applied Imagery, 2009. *Qiuck Terrain Modeler™ application notes: transportation* [online]. Available from: http://www.appliedimagery.com/Quick%20Terrain%20Modeler%20Application%20Notes%20-%20Transportation.pdf [Accessed 13 January 2009].

Barnes, I., 2003. Aerial remote-sensing techniques used in the management of archaeological monuments on the British Army's Salisbury Plain Training Area, Wiltshire, UK. *Archaeological Prospection,* 10 (2), 83-90.

Barlindhaug, S., Holm-Olsen, M.I., and Tømmervik, H., 2007. Monitoring archaeological sites in a changing landscape – using multitemporal satellite remote sensing as an 'early warning' method for detecting regrowth processes. *Archaeological Prospection,* 14 (4), 231-244.

Bewley, R. H., 2003. Aerial survey for archaeology. *Photogrammetric Record,* 18 (104), 273-292.

Bubenzer, O. and Riemer, H., 2007. Holocene climatic change and human settlement between the central Sahara and the Nile Valley: archaeological and geomorphological results. *Geoarchaeology: An International Journal,* 22 (6), 607-620.

Challis, K., 2006. Airborne laser altimetry in alluviated landscapes. *Archaeological Prospection,* 13 (2), 103-127.

Cunningham, R., Gisclair, D. and Craig, J., 2004. *The Louisiana statewide Lidar project,* [online]. Available from: ftp://ftp-fc.sc.egov.usda.gov/NCGC/products/elevation/la-lidar-project.pdf [Accessed 19 October 2007].

Dalan, R.A. and Bevan, B.W., 2002. Geophysical indicators of culturally emplaced soils and sediments. *Geoarchaeology: An International Journal,* 17 (8), 779-810.

de Sherbinin, A., Balk, D., Yager, K., Jaiteh, M., Pozzi, F., Giri, C. and Wannebo, A., 2002. *Social science applications of remote sensing, a CIESIN thematic guide* [online]. Palisades, Center for International Earth Science Information Network of Columbia University. Available from: http://sedac.ciesin.columbia.edu/tg/guide_main.jsp [Accessed 11 January 2009].

Devereux, B.J., Amable, G.S., Crow, P. and Cliff, A.D., 2005. The potential of airborne Lidar for detection of archaeological features under woodland canopies. *Antiquity*, 79 (305), 648-660.

Dobbs, C.A., 1999. *A brief history of archaeology in Minnesota* [online]. The Institute for Minnesota Archaeology. Available from: http://www.fromsitetostory.org/sources/papers/mnhistory/mnhistory.asp [Accessed 11 January 2008].

Environment Agency, 2007. *LiDAR coverage map*, [online]. Available from: http://www.environment-agency.gov.uk/commondata/103196/219863?referrer=/science/monitoring/131047 [Accessed 25 October 2007].

Florida State Emergency Response Team, 2007. *FloridaDisaster.org*, [online]. Available from: http://www.floridadisaster.org/gis/lidar [Accessed 19 October 2007].

Fowler, M.J.F., 2002. Satellite remote sensing and archaeology: a comparative study of satellite imagery of the environs of Figsbury Ring, Wiltshire. *Archaeological Prospection*, 9 (2), 55-69.

Fowler, R.A., Samberg, A., Flood, M.J., and Greaves, T.J., 2007. Topographic and terrestrial Lidar. *In*: D.F. Maune, ed. *Digital elevation model technologies and applications: the DEM users manual, 2nd edition*. Bethesda, MD: American Society for Photogrammetry and Remote Sensing, 199 - 248.

Gallagher, J.M. and Josephs, R.L., 2008. Using LiDAR to detect cultural resources in a forested environment: an example from Isle Royale National Park, Michigan, USA. *Archaeological Prospection*, 15 (3), 187 - 206.

Green, W., Zimmerman, L.J., Lillie, R.M., Makes Strong Move, D. and Sly-Terpstra, D., 2001. *Effigy Mounds National Monument cultural affiliation report*. Research papers. Office of the State Archaeologist, University of Iowa, Iowa City.

Gritzner, J.H., 2006. Identifying wetland depressions in bare-ground LIDAR for hydrologic modeling. In *26th annual ESRI international user conference proceedings.* San Diego, CA 7-11 August 2006. Available from: http://www10.giscafe.com/link/display_detail.php?link_id=13624 [Accessed 30 November 2007].

Harmon, J. M., Leone, M. P., Prince, S. D. and Snyder, M., 2006. Lidar for archaeological landscape analysis: a case study of two eighteenth-century Maryland plantation sites. *American Antiquity*, 71 (4), 649-670.

Henry, R.J. and Gonzalez, L.A., 2005. *Use of LIDAR in wetland delineation on West Galveston Island, Texas* [online]. Houston, USGS National Biological Information Infrastructure. Available from: http://cswgcin.harc.edu/ecoregion/gulfofmexico/nearshore/wetlands/index.html [Accessed 12 January 2009].

Hewett, M., 2005. Automating feature extraction with the ArcGIS Spatial Analyst extension. In *25th annual ESRI international user conference proceedings.* San Diego, CA 25-29 July 2005. Available from: http://www10.giscafe.com/link/display_detail.php?link_id=13624 [Accessed 30 November 2007].

Hopkinson, C., Chasmer, L.E., Zsigovics, G., Creed, I.F., Sitar, M., Treitz, P. and Maher, R.V., 2004. Errors in LiDAR ground elevation and wetland vegetation height estimates. In *Proceedings of the ISPRS working group VIII/2 'Laser-scanners for forest and landscape assessment'*. Freiburg, Germany 03-06 October 2004. Available from: http://www.isprs.org/commission8/workshop_laser_forest [Accessed 12 January 2009].

Humme, A., Lindenbergh, R. and Sueur, C., 2006. Revealing Celtic fields from Lidar data using kriging based filtering. In *The proceedings of ISPRS Commission V symposium: image engineering and vision metrology.* Dresden, Germany 25-27 September 2006. Available from: www.isprs.org/commission5/proceedings06/paper/1241_Dresden06.pdf [Accessed 10 September 2007].

Iowa Department of Natural Resources, 2007. *LiDAR interactive mapping,* [online]. Available from: http://www.iowadnr.gov/mapping/lidar [Accessed 19 October 2007].

Iowa Department of Natural Resources, 2009. *Iowa LiDAR project-collection status,* [online]. Available from: http://www.iowadnr.com/mapping/lidar/files/schedule.pdf [Accessed 18 February 2009].

Jensen, J.R., 2007. *Remote Sensing of the Environment: an earth resource perspective.* 2nd ed. Upper Saddle River, NJ: Pearson Prentice Hall.

Lorenzo, H. and Arias, P., 2005. A methodology for rapid archaeological site documentation using ground penetrating radar and terrestrial photogrammetry. *Geoarchaeology: An International Journal,* 20 (5), 521-535.

Mass, H., and Vosselman, G., 1999. Two algorithms for extracting building model from raw laser altimetry data. *ISPRS Journal of Photogrammetry and Remote Sensing*, 54 (2-3), 153-163.

Maune, D.F., 2007. DEM user applications. *In*: D.F. Maune, ed. *Digital elevation model technologies and applications: the DEM users manual, 2nd edition*. Bethesda, MD: American Society for Photogrammetry and Remote Sensing, 391 – 421.

Maune, D.F., Kopp, S.M., Crawford, C.A., and Zervas, C.E., 2007. Introduction. *In*: D.F. Maune, ed. *Digital elevation model technologies and applications: the DEM users manual, 2nd edition*. Bethesda, MD: American Society for Photogrammetry and Remote Sensing, 1 – 35.

Minnesota Department of Natural Resources, 2009. *Project overview*, [online]. Available from: http://www.dnr.state.mn.us/mis/gis/semn_lidar/index.html [Accessed 13 January 2009].

Mutlu, M., Popescu, S.C., and Zhao, K., 2008. Sensitivity analysis of fire behavior modeling with LIDAR-derived surface fuel maps. *Forest Ecology and Management*, 256 (3), 289-294.

North Carolina Flood Mapping Program, 2007. *Public documents,* [online]. Available from: http://www.ncfloodmaps.com/pubdocs [Accessed 19 October 2007].

O'Bright, J.Y., 1989. *The perpetual march: an administrative history of Effigy Mounds National Monument.* Omaha: National Park Service.

Ohio Office of Information Technology, 2007. *Ohio's statewide imagery program*, [online]. Available from: http://oit.ohio.gov/Sdd/ESS/Ogrip/ImageryProgram.aspx [Accessed 19 October 2007].

Opitz, D.W., Rao, R., and Blundell, J. S., 2006. Automated 3-D feature extraction from terrestrial and airborne Lidar. In *ISPRS Commission IV: bridging remote sensing and GIS, 1st international conference on object-based image analysis.* Salzburg University, Austria 4-5 July 2006. Available from: http://www.commission4.isprs.org/obia06/papers.htm [Accessed 30 November 2007].

Oregon Lidar Consortium, 2008. *LiDAR collection and mapping*, [online]. Available from: http://www.oregongeology.org/sub/projects/olc/default.htm [Accessed 5 January 2009].

Orr, E., 1935. *Report of surveys and excavations of mound groups along the Mississippi River bluffs and terraces from McGregor to Clinton, Iowa, under Project 1047 of the Iowa Planning board, by Party under Dr. Charles R. Keyes, Apr. 8 to Aug. 10, 1935.* [electronic document]. Office of the State Archaeologist, University of Iowa, Iowa City.

Pennsylvania Department of Conservation and Natural Resources, 2006. *PAMAP elevation data,* [online]. Available from: http://www.dcnr.state.pa.us/topogeo/pamap/elevation.aspx [Accessed 19 October 2007].

Perry, M., 1984. *BRF-65-2(3) Lucas County Primary Roads.* Project completion report. Office of the State Archaeologist, University of Iowa, Iowa City.

Pidgeon, W., 1852. *Traditions of De-Coo-Dah and antiquarian researches.* New York: Horace Thayer.

Pollefeys, M., Koch, R., Vergauwen, M., and van Gool, L., 2000. Automated reconstruction of 3D scenes from sequences of images. *ISPRS Journal of Photogrammetry & Remote Sensing,* 55 (4), 251-267.

Prior, J.C., 1991. *Landforms of Iowa*. Iowa City: University of Iowa Press.

Renslow, M., Greenfield, P., and Guay, T., 2000. *Evaluation of multi-return LIDAR for forestry applications* [online]. US Department of Agriculture Forest Service – Engineering. Available from: http://www.ndep.gov/USDAFS_LIDAR.pdf [Accessed 12 January 2009].

Romain, W.F. and Burks, J., 2008. *LiDAR imaging of the Great Hopewell Road* [online]. Available from: http://www.ohioarchaeology.org/joomla/index.php?option=com_content&task=view&id=231&Itemid=32 [Accessed 13 January 2009].

Sarris, A., Dunn, R.K., Rife, J.L., Papadopoulos, N., Kokkinou, E., and Mundigler, C., 2007. Geological and geophysical investigations in the Roman cemetery at Kenchreai (Korinthia), Greece. *Archaeological Prospection,* 14 (1), 1-23.

Sithole, G. and Vosselman, G., 2004. Experimental comparison of filter algorithms for bare-earth extraction from airborne laser scanning point clouds. *ISPRS Journal of Photogrammetry & Remote Sensing,* 59 (1), 85-101.

Sever, T. and Wagner, D.W., 1991. Analysis of prehistoric roadways in Chaco Canyon using remotely sensed digital data. *In*: C.D. Trombold, ed. *Ancient road networks and settlement hierarchies in the New World.* Cambridge University Press, 42-52.

Stanley, L.A. and Stanley, D.G., 1989. *National Register of Historic Places registration form: Slinde Mound Group*. Iowa City: University of Iowa Office of the State Archaeologist.

Spatial Resources, 2009. *Airborne Lidar surveys electric transmission lines,* [online]. Available from: http://www.spatialresources.com/id70.html [Accessed 12 January 2009].

Tao, V.C. and Hu, Y., 2002. Assessment of airborne Lidar and imaging technology for pipeline mapping and safety applications. In *Integrated remote sensing at the global, regional and local scale, ISPRS commission I mid-term symposium in conjunction with Pecora 15/land satellite information IV conference proceedings*, Denver, CO, 10-15 November 2002. Available from: http://www.isprs.org/commission1/proceedings02/paper/00009.pdf [Accessed 12 January 2009].

United States Army Corps of Engineers, 1999. *US Army Corps of Engineers wetlands delineation manual* [online]. Available from: http://www.wetlands.com/regs/tlpge02e.htm [Accessed 12 January 2009].

United States Department of Agriculture – Natural Resources Conservation Service Wyoming, 2005. *Wyoming statewide LIDAR effort* [online]. Available from: http://www.wy.nrcs.usda.gov/wygis/lidar.html [Accessed 19 October 2007].

van Zijverden, W. K. and Laan, W. N. H., 2003. Landscape reconstructions and predictive modeling in archaeological research, using a LIDAR based DEM and digital boring databases. In *Archeologie und computer, workshop 7.* Vienna, Austria 2003. Available from: http://www.archeologie.leidenuniv.nl/content_docs/research/vanzijverden_laan_2005_landscape__reconstructions.pdf [Accessed 10 September 2007].

Visual Learning Systems, Inc., 2005. The LIDAR Analyst™ extension for ArcGIS™: automated feature extraction software for airborne LIDAR datasets, white paper. Available online at: http://gi.leica-geosystems.com/documents/pdf/VLS_LIDARAnalyst_WhitePaper2.pdf (accessed 30 November 2007).

Votteler, T.H., Muir, T.A., 1999. Wetland management and research: wetland protection legislation. In *United States Geological Survey Water Supply Paper 2425* [online]. Available from: http://water.usgs.gov/nwsum/WSP2425/legislation.html [Accessed 12 January 2009].

Weidner, U., Förstner, W., 1995. Towards automatic building extraction from high resolution digital models. *ISPRS Journal of Photogrammetry & Remote Sensing,* 50 (4), 34-49.

Wilkinson, K.N., Beck, A.R., and Philip, G., 2006. Satellite imagery as a resource in the prospection for archaeological sites in central Syria. *Geoarchaeology: An International Journal*, 21 (7), 735-750.

Young, J., 2007. Sanborn Mapping Company Lidar project in Iowa. In *GeoTREE Lidar Workshop.* University of Northern Iowa, Cedar Falls 7-8 August 2007. Notes from public presentation.